5-1-1994

Genetic, Structural, and Two-Dimensional Protein Electrophoretic Characterization of Normal and dek23 Mutant Embryogenesis in Maize (Zea mays L.)

Guy E. Farish

GENETIC, STRUCTURAL, AND TWO-DIMENSIONAL PROTEIN ELECTROPHORETIC CHARACTERIZATION OF NORMAL AND *dek23* MUTANT EMBRYOGENESIS IN MAIZE (*Zea mays* L.)

by

Guy E. Farish
Bachelor of Science, University of Minnesota-Duluth, 1985
Master of Science, University of North Dakota, 1988

A Dissertation

Submitted to the Graduate Faculty

of the

University of North Dakota

in partial fulfillment of the requirements

for the degree of

Doctor of Philosophy

Grand Forks, North Dakota
May
1994

This dissertation, submitted by Guy E. Farish in partial fulfillment of the requirements for the Degree of Doctor of Philosophy from the University of North Dakota, has been read by the Faculty Advisory Committee under whom the work has been done and is hereby approved.

William F. Sheridan
(Chairperson)

Maria Vandegrift

Roger M. Greene

Owen R. Larson

Barry Mitchell

This dissertation meets the standards for appearance, conforms to the style and format requirements of the Graduate School of the University of North Dakota, and is hereby approved.

Harvey Knull
Dean of the Graduate School
May 2-94

PERMISSION

Title Genetic, Structural, and Two-dimensional Protein Electrophoretic Characterization of Normal and *dek23* Mutant Embryogenesis in Maize (*Zea mays* L.)

Department Biology

Degree Doctor of Philosophy

In presenting this dissertation in partial fulfillment of the requirements for a graduate degree from the University of North Dakota, I agree that the library of this University shall make it freely available for inspection. I further agree that permission for extensive copying for scholarly purposes may be granted by the professor who supervised my dissertation work or, in his absence, by the chairperson of the department or the dean of the Graduate School. It is understood that any copying or publication or other use of this dissertation or part thereof for financial gain shall not be allowed without my written permission. It is also understood that due recognition shall be given to me and to the University of North Dakota in any scholarly use which may be made of any material in my dissertation.

Signature Suzy Farris

Date 4/28/94

TABLE OF CONTENTS

LIST OF FIGURES

LIST OF FIGURES CONTINUED

LIST OF FIGURES CONTINUED

LIST OF FIGURES CONTINUED

LIST OF TABLES

ACKNOWLEDGEMENTS

I would like to thank my Major Professor, Dr. William F. Sheridan, for his support and encouragement during my graduate studies. Other people have played important roles in my efforts, including Brian Walsh and Josh Wieland, two students who worked closely with me in the lab. I must also thank Jan Clark and Bing-Quan Huang who have given freely of their expertise and advise, and Don Auger, from whom I've learned much about cooperation and ingenuity. Last of all I thank my wife Beth. I could not have completed this phase of my life without her support and enthusiasm.

ABSTRACT

Embryogenesis in maize (*Zea mays* L.) is a genetically regulated process that gives rise to a large embryo with shoot and root apical meristems, a large scutellum, and five or six leaf primordia. An embryo-lethal *defective kernel* mutation *dek23*, located on chromosome arm *2L*, affects the formation of the shoot apical meristem, coleoptilar ring, and leaf primordia in mutant embryos. Comparison of mutant and normal embryo development at the structural and biochemical levels should give insight into the role of the *dek23* normal gene product in normal development. Fresh dissection, light microscopy, and transmission electron microscopy of normal and mutant embryos at different developmental stages reveal a divergence between mutant and normal embryo morphology at nine days after pollination (dap). Mutant embryos are developmentally delayed and the cells of the shoot apical meristem region contain enlarged vacuoles and abnormal nuclei and subsequently become

necrotic. Two-dimensional polyacrylamide gel protein profiles of normal embryos from the transition stage (nine dap) through stage 5/6 (40 dap) were obtained and used as standards for comparison to mutant embryo protein profiles at five different developmental stages. Normal embryo protein profiles exhibited a set of 16 landmark spots found at all stages. Two early embryonic proteins were found in embryos up to stage 1. Three stage specific proteins were observed at the coleoptilar stage, as well as a set of spots that increased in intensity until stage 3 and then decreased. Accumulation of globulin storage proteins was clearly evident. Mutant embryo profiles were generally similar to normal profiles of an earlier chronological age. Two landmark spots found in normal profiles were absent or diminished in mutant profiles. One early embryonic protein identified in normal profiles was also absent from mutant profiles, and may provide a marker for identifying mutant embryos before morphological differences are evident. Mutant embryos failed to accumulate any globulins. The *dek23* locus was mapped 22 centimorgans distal to *w3*. Reduced sexual transmission of the mutant allele through the pollen and unequal distribution of mutant kernels on a self

pollinated ear indicate that the *dek23* gene is active in the male gametophyte.

CHAPTER I: INTRODUCTION

Embryogenesis in flowering plants has long been the focus of investigation (Maheshwari 1950; Raghavan 1986; Meinke 1991). Maize (*Zea mays* L.) in particular has been the subject of much study (Randolph 1936; Kiesselbach 1949; Abbe and Stein 1954; Sheridan 1988; Sheridan and Clark 1994). Early development is thought to be under control of a sequentially regulated genetic program (Sheridan and Neuffer 1981; 1982; Neuffer et al. 1986). Expression of this program results in a well-developed embryo possessing the basic structure and vegetative organ primordia of the mature plant (Sheridan and Clark 1994).

Mutational analysis provides a means to identify and characterize particular genes in that are involved in normal embryogenesis. Comparison of normal and mutant embryogenesis can reveal the effect of a single mutation, and from this comparison we can infer the probable function of the normal gene product. Genes for structural proteins and enzymes can be distinguished from genes that exert a

regulatory effect by their control of the activity of cascades or sequences of other genes. The regulatory genes can have dramatic effects on embryogeny and other developmental processes by controlling the rate and timing of transcription of several genes; they may give insight into evolutionary relationships among species.

In maize, two main types of mutation have been isolated that are useful in genetically dissecting the role of genes in embryogeny. The *defective kernel* (*dek*) mutations affect both embryo and endosperm development (Neuffer and Sheridan 1980), and the *embryo specific* (*emb*) mutations, alter embryo development but do not affect the endosperm phenotype (Clark and Sheridan 1991; Sheridan and Clark 1993), both types are embryo-lethal mutations. The *emb* mutations have recently become the focus of intensive study, due to the difficulty in identifying and maintaining them. A set of 51 *emb* mutations has been isolated from Robertson's *Mutator* (*Mu*) transposable element stocks (Clark and Sheridan 1991; Sheridan and Clark 1993). It is likely that these mutations are tagged with a *Mu* element that will aid in the cloning of these loci. Many *dek* mutations have been characterized genetically, morphologically, and

physiologically (Neuffer and Sheridan 1980; Neuffer et al. 1986; Clark and Sheridan 1986; Sheridan and Thorstenson 1986; Clark and Sheridan 1988). Scanlon et al. (1994) have described a set of 63 new *defective kernel* mutations presumably induced by one of the *Mu* transposable elements. Several of the genes tagged by the *Mu* element have been cloned.

This study reports on further investigations of one of the original ethyl methane sulfonate (EMS) induced *dek* mutations, *dek23*. Homozygous *dek23* kernels can be detected on a self-pollinated ear at about 12 days after pollination (dap) when grown under field or greenhouse conditions in North Dakota. The endosperm is reduced and the kernel has a defective crown phenotype at maturity (Neuffer and Sheridan 1980). The *dek23* allele behaves as a Mendelian recessive, but displays aberrant segregation ratios on ears, indicating it may be expressed in the gametophyte. This emphasizes the pleiotropic nature of *dek* loci; their normal gene products affect the development of the embryo, endosperm, and in some cases, are required for normal gametophyte function.

Previous studies of *dek23* reveal that the mutant allele affects embryo development at the time of shoot apical

meristem formation (Clark and Sheridan 1986). Mutant embryos are unable to form a normal shoot apical meristem or normal leaf primordia. At maturity the scutellum is smaller and more pointed than is normal, and necrosis often appears near the shoot apex region. An apparently normal root meristem is formed and persists until kernel maturity; this indicates a very specific effect of the mutation on shoot but not root meristem organization. Another mutation called *dks8* has a similar phenotype. Mutant *dks8* embryos lack a shoot apex, but they have a normal root meristem, scutellum, and endosperm (Sollinger and Rivin 1993). Our lab has shown *dks8* to be non-allelic to *dek23* (data not shown). The separate control of shoot and root meristem in the embryo suggests a regulatory role for the *dek23* locus.

This study seeks answers to several questions about both normal and *dek23* mutant embryogenesis. These questions and the methodology used in an attempt to answer them are presented here.

1.) Does the *dek23* mutant allele have an observable effect at the cellular or subcellular level? A more detailed histological examination than has previously been undertaken can identify cellular and ultrastructural

differences between normal and mutant embryos. The failure of shoot meristem formation and subsequent necrosis may be preceded by an alteration in organelle morphology or abundance, or other structural changes visible only at the ultrastructural level.

2.) Does the *dek23* mutation cause loss of gene function, or a lowered activity or amount of gene product? Dosage analysis of the mutant *dek23* allele may provide insight into the nature of the genetic lesion. If the normal gene product is completely absent, the allele is classified as an amorph; if the gene product is present at reduced levels or if it functions at a reduced capacity it is termed hypomorph (Muller 1932).

3.) Why are *dek23* mutant kernels on a self-pollinated ear present at less than the expected frequency of 25% and why are they not evenly distributed on the ear? The analysis of progeny produced by reciprocal crosses with a normal stock can identify whether a reduction in male or female transmission of the *dek23* mutant allele is the cause for the mutant kernels being present at lower than the expected frequency of 25% on self-pollinated ears, and their distribution on the ear not being uniform. This analysis

can reveal the expression of the gene in the male or female gametophyte, and define the mechanism that limits transmission of the mutant allele.

4.) Where is the *dek23* gene located with respect to other genes on chromosome arm *2L*? Genetic mapping of the *dek23* locus identifies the precise position of the gene on chromosome arm *2L*. This information will assist future efforts to tag and clone the gene. Targeted mutagenesis of this region of the genome is possible using the transposable element *Activator* (*Ac*) and translocation or inversion stocks that bring the *Ac* into close proximity with this region. Experiments that use the translocation stocks carrying *Ac* have a much higher potential for success than do experiments that depend on transposition of an *Ac* element from another chromosome or from further away on the same chromosome (Auger and Sheridan 1994).

5.) Does the *dek23* mutant allele have an observable effect on the protein profile of embryos at different developmental stages? Analysis of the proteins produced during normal embryogenesis may provide a picture of the molecular processes underlying the morphogenetic changes occurring during embryogeny. The protein products of the

hundreds of genes expressed during embryogenesis can be visualized by two-dimensional polyacrylamide gel electrophoresis (2-D PAGE). These protein profiles, obtained by sampling different stages of normal embryo development, will provide a baseline for comparison to mutant embryo profiles. Changes in these patterns of proteins can be attributed ultimately to the disruption of a single gene.

References

Abbe, E.C., and O.L. Stein, 1954 The growth of the shoot apex in maize: embryogeny. Am. J. Bot. 41:285-293.

Auger, D.A., and W.F. Sheridan, 1994 Using cytogenetics to enhance transposon tagging with *Ac* throughout the maize genome. pp. 234-239. In: *The Maize Handbook*. Edited by M. Freeling and V. Walbot. Springer-Verlag, New York.

Clark, J.K., and W.F. Sheridan, 1986 Developmental profiles of the maize embryo-lethal mutants *dek22* and *dek23*. J. Hered. 77:83-92.

Clark, J.K., and W.F. Sheridan, 1988 Characterization of the two maize embryo-lethal defective kernel mutants *rgh*-1210* and *fl*-1253B*: effects on embryo and gametophyte development. Genetics 120:279-290.

Clark, J.K. and W.F. Sheridan, 1991 Isolation and characterization of 51 embryo-specific mutations of maize. The Plant Cell 3:935-951.

Kiesselbach, T.A., 1949 *The Structure and Reproduction of Corn*. Univ. Nebr. Agric. Exp. Stn. Bull. 161:96pp., Lincoln, NB.

Maheshwari, P., 1950 *An Introduction to the Embryology of Angiosperms*. McGraw-Hill, New York.

Meinke, D.W., 1991 Genetic analysis of plant development. Pp. 437-490. In: *Plant Physiology, A Treatise*. Volume 10 Growth and development. Academic Press, New York.

Muller, H.J., 1932 Further studies on the nature and causes of gene mutations. Proc. Int. Cong. Genet. 6th 1:213-255.

Neuffer, M.G., and W.F. Sheridan, 1980 Defective kernel mutants of maize. I. Genetic and lethality studies. Genetics 95:929-944.

Neuffer, M.G., M.T. Chang, J.K. Clark, and W.F. Sheridan, 1986 The genetic control of maize kernel development. Pp. 35-50. In: *Regulation of Carbon and Nitrogen Reduction and Utilization in Maize*. Edited by J.C. Shannon, D.P. Knievel and C.D. Boyer. American Society of Plant Physiologists, Rockville, MD.

Raghavan, V., 1986 *Embryogenesis in Angiosperms*. Cambridge University Press, Cambridge.

Randolph, L.F., 1936 Developmental morphology of the caryopsis in maize. J. Agric. Res. 53:881-916.

Scanlon, M.J., P.S. Stinard, M.G. James, A.M. Myers, and D.S. Robertson, 1994 Genetic analysis of sixty-three mutations affecting maize kernel development isolated from *Mutator* stocks. Genetics 136:281-294.

Sheridan, W.F., 1988 Maize developmental genetics: genes of morphogenesis. Ann. Rev. Genet. 22:353-385.

Sheridan, W.F. and J.K Clark, 1993 Mutational analysis of morphogenesis of the maize embryo. The Plant Journal 3:347-358.

Sheridan, W.F., and J.K. Clark, 1994 Fertilization and embryogeny in maize. Pp. 3-10. In: *The Maize Handbook*. Edited by M. Freeling and V. Walbot. Springer-Verlag, New York.

Sheridan, W. F., and M.G. Neuffer, 1981 Maize mutants altered in embryo development. Pp. 137-156. In: *Levels of genetic control in development*. Edited by S. Subtelney and U. Abbot. New York, Alan R. Liss Inc.

Sheridan, W.F., and M.G. Neuffer, 1982 Maize developmental mutants. Embryos unable to form leaf primordia. J. Hered. 73:318-329.

Sheridan, W.F., and Y.R. Thorstenson, 1986 Developmental profiles of three embryo-lethal maize mutants lacking leaf primordia: *ptd*-1130, cp*-1418,* and *bno*-747B*. Dev. Genet. 7:35-49.

Sollinger J.D., and C. Rivin, 1993 dks8, a mutation specifically eliminating shoot formation during embryogenesis. Maize Genet. Coop. Newslett. 67:34-35.

CHAPTER II: EFFECTS OF THE *defective kernel* MUTATION *dek23* ON THE MORPHOLOGY AND ULTRASTRUCTURE OF DEVELOPING MAIZE (*Zea mays* L.) EMBRYOS.

Introduction

Normal maize embryogenesis has been described in detail at the morphological and histological level. The sequence of developmental events taking place that give rise to a large embryo with shoot and root apical meristems, a large scutellum, and five or six leaf primordia (Randolph 1936; Kiesselbach 1949; Abbe and Stein 1954) has been defined. Mutations, either spontaneously occurring or induced, provide tools to study the genetic control of developmental events. The normal function of the genes affected by the mutations and the role of the gene in embryogenesis may be inferred from the analysis (Suzuki et al. 1981).

A large number of mutants can be produced by treating seeds or pollen with chemical mutagens, or by exposing them to X-rays (Neuffer 1982). Initial characterization at the morphological level should identify mutants with defects in so-called "housekeeping" genes. Mutations of this type

affect embryogenesis because of a defect in metabolic processes (e.g. ribosome assembly). They are likely to prevent any embryonic development or allow development for a variable length of time, resulting in a variable mutant embryo phenotype.

Mutants that are defective in some developmental process should not prevent embryo development entirely; they should result in embryos that are permanently and uniformly blocked at a particular stage of development, or within a narrow range of stages (Sheridan and Neuffer 1982). A number of mutants blocked at several different stages of embryonic development are desirable so that the sequence and timing of gene action can be observed.

Defective Kernel Mutants of Maize: Mutant kernels with a severely collapsed endosperm and abnormal embryos were first described by Jones (1920). These recessive mutants, along with several additional mutants, were described in detail by Mangelsdorf (1923; 1926). The mutant embryos were blocked over a range of stages, from the transition or coleoptilar stages of Abbe and Stein (1954) to late in development, thus indicating that these mutations were defects in the sequential program of development.

Germless (*gm*) mutants, which have a phenotypically normal endosperm but appear to lack an embryo at maturity, have also been described (Demerec 1923; Wentz 1930; Sass and Sprague 1950). Recent studies on mutants of this type, now called *embryo-specific* (*emb*) mutants, have identified 51 putatively transposon-induced mutations (Clark and Sheridan 1991; Sheridan and Clark 1993). These mutants display a wider range of embryo phenotypes than the previously described mutants. Some *emb* mutant embryos are blocked early in development at the proembryo stage, others reach an abnormal stage 4 or 5.

In other recent studies Neuffer and Sheridan (1980) and Sheridan and Neuffer (1980) describe 194 *defective kernel* (*dek*) mutants selected from a collection of 2457 recessive mutants produced by EMS mutagenesis of pollen (Neuffer and Coe 1978). Two types of *dek* mutants have been distinguished, both of which are defective in embryo and endosperm development. One group is defined as nutritional-type mutants (Neuffer and Sheridan 1980; Sheridan and Neuffer 1980). Immature mutant embryos of this type are able to germinate precociously when cultured on nutrient containing media (Sheridan and Neuffer 1981; 1982). Among

the 108 of these mutants, Sheridan and Neuffer (1981; 1982) found four proline auxotrophs that are allelic to the *pro-1* mutant of Gavazzi et al. (1975).

The second class of *dek* mutants are developmental-type mutants. This group consists of 35 mutants, of which 15 are unable to form leaf primordia. A few form some leaf primordia, but are unable to germinate when cultured as immature embryos and do not germinate at kernel maturity (Sheridan and Neuffer 1981; 1982; Neuffer et al. 1986). These mutants also are blocked at various stages of embryo development.

Developmental profiles have been generated by serial sectioning for several *dek* mutants. Those blocked very early in embryogenesis are *dek22* and *dek31*. Mutant *dek22* embryos are blocked at what appears to be a normal transition phase (Clark and Sheridan 1986); mutant *dek31* embryos are blocked at an abnormal transition phase and subsequently undergo cell enlargement and necrosis (Sheridan and Thorstenson 1986). Mutant *dek23* embryos are blocked slightly later in embryo development, at an abnormal coleoptilar stage; the embryos form a root apical meristem but no shoot apex (Clark and Sheridan 1986). The mutant

cp-1418* forms normal appearing coleoptilar stage embryos that enlarge somewhat and form root primordia, but no leaf primordia (Sheridan and Thorstenson 1986). The mutant *bno*-747B* also forms a normal appearing coleoptilar stage embryo that subsequently enlarges but does not develop any further (Sheridan and Thorstenson 1986).

Scanlon et al. (1994) have described a set of 63 new *defective kernel* mutations presumably induced by Robertson's *Mutator* (*Mu*) transposable elements. Several of these mutations have been cloned and characterized molecularly.

Embryo-Endosperm Interaction: One of the advantages of maize as a system for studying the role of genes in embryogenesis is the extensively differentiated large embryo and endosperm. This system is well suited for analysis of genes that affect only embryo development, only endosperm development, or development of both types of tissues. Since endosperm may serve as a nutritive tissue for the developing embryo, it is possible that a defective endosperm may indirectly affect the development of a genetically normal embryo (Sheridan and Neuffer 1981; 1983). Conversely, a defective embryo might possibly affect the development of the endosperm.

Use of B-A translocation stocks (Beckett 1994) has allowed manipulations of embryo and endosperm genotype. Sheridan and Neuffer (1981; 1982) found that interaction between embryo and endosperm is not the fundamental cause of defective kernel phenotype in most mutants. They found that a mutant endosperm usually does not inhibit development of a normal embryo, although it may have an effect on seedling survival. They also noted that normal endosperm usually will not rescue a mutant embryo, nor will a mutant embryo seriously affect development of a genetically normal endosperm. Based on these findings they concluded that the developmental paths of both the embryo and the endosperm are largely independent; it is their own genetic constitution that determines their developmental fate (Sheridan and Neuffer 1981; 1982).

Normal Embryogenesis in Maize: The development of the maize embryo has been meticulously studied in a variety of materials and locations (Randolph 1936; Kiesselbach 1949; Abbe and Stein 1954; Sass 1977). Maize embryos follow a consistent pattern of development, passing through a series of characteristic stages (Figure 1), the timing of which may

be influenced by environmental factors and individual genotypic variations.

Randolph (1936) provided a detailed histological description of fertilization and embryogenesis of material grown in Ithaca, New York. Kiesselbach (1949) also used histological techniques to describe material grown in Lincoln, Nebraska. Both investigators used primarily chronological schemes for identifying and classifying stages of embryo development.

Abbe and Stein (1954) observed that there is no precise correlation between morphological stage and calendar age. They proposed a system of staging based on newly appearing morphological structures. Sass (1977) used histological techniques to describe maize embryogenesis, and Sheridan and Neuffer (1981) summarized embryo development in materials grown in Columbia, Missouri. Sheridan and Clark (1994) have described three phases of embryogeny which characterize the changes in overall organization of the embryo. These phases include phase 1, setting apart of the embryo proper and suspensor, phase 2, establishment of the meristems and embryonic axis, and phase 3, elaboration of embryonic structures. The work of Sheridan and Neuffer (1981) and

Sheridan and Clark (1994) is the basis for the following description; the stages are those set forth by Abbe and Stein (1954).

Phase 1 begins with fertilization of the mature egg, which occurs about 15 to 24 hours post-pollination, depending on the temperature and length of silks. The first division of the zygote occurs 10 to 12 hours after fertilization, creating a two-celled proembryo. Cell division continues somewhat asymmetrically, being more rapid in the upper region and slower in the lower region of the proembryo. This results in a club-shaped proembryo with smaller, more densely packed cells in the upper region and larger cells in the lower region.

The transition stage is characterized by the first evidence of differentiation in the embryo. Phase 2 begins about midway through this stage. An epidermal layer forms on the proembryo. The upper region, the future embryo proper, becomes a nearly spherical mass of small dense cells, while the lower region continues to elongate into the suspensor. It is at this phase that the embryo passes from being radially symmetrical to asymmetrical. A wedge of closely packed cells becomes apparent internally beneath the

surface where the shoot apical meristem will form. The embryo and suspensor together are about 1.0 to 1.5 mm long.

The coleoptilar stage is marked by several changes. The embryo proper lengthens and enlarges at its base, becoming triangular in face view. It flattens on the side that will become the embryo face and a group of cells begin to bulge out of the embryo face and become recognizable as the shoot apical meristem. Around it another bulge forms, that eventually encircles the shoot apex. This tissue is the coleoptilar ring and is the morphological marker that lends its name to this stage. Also evident in Toluidine Blue O stained longitudinal sections is a darkly staining internal region marking the site of the future root apical meristem. The suspensor has elongated to its maximum extent, about 1.0 mm, and the embryo proper is 0.5 to 1.0 mm long.

Stage 1 begins with the formation of the first leaf primordium on the lower face of the shoot apical meristem. The coleoptile has enlarged to partly cover the shoot apex and first leaf primordium. The scutellum has enlarged and flattened somewhat and is more prominent than the suspensor. The embryo proper is now over 1.0 mm long. Phase 3 begins

at this point, after the formation of the first leaf primordium.

Stage 2 is characterized by the formation of the second leaf primordium on the upper face of the shoot apical meristem, opposite to the first leaf primordium. The scutellum has lengthened and a groove has formed that partially engulfs the embryonic axis. The coleoptile now completely envelopes the shoot apical meristem and leaf primordia, except for a small opening at the top, the coleoptilar pore. The suspensor has become relatively inconspicuous and the embryo plus suspensor is about 2.5 mm long.

Stage 3 is characterized by the formation of the third leaf primordium, opposite to the second. The scutellum continues to broaden and now appears ovoid in face view. The lips of the scutellar groove envelope more of the embryonic axis than at stage 2. A root primordium is now evident in longitudinal section and a protective covering, the coleorhiza, completes the lower portion of the embryonic axis. The suspensor is no longer readily visible and the whole embryo is about 3.0 mm long.

Stage 4 begins with the formation of the fourth leaf primordium, located according to the alternating pattern of the first three leaf primordia. These first leaf primordia have enlarged and folded over the shoot apical meristem. The embryonic axis is almost completely covered by the infolding of the lips of the scutellar groove. A constriction, the forming mesocotyl, can be seen just below the shoot apex. The embryo is 5.0 to 6.0 mm long.

Stage 5 embryos are similar to stage 4 embryos with the addition of a fifth leaf primordium. The embryo is slightly larger in all parts than at stage 4 with an overall length approximately 6.0 mm long. A seminal root primordium can be seen emerging from the mesocotyl. Many embryos enter dormancy at this stage. Environmental factors and genotype determine whether they will continue on to the next stage.

Stage 6 is characterized by the formation of the sixth leaf primordium. The embryo is now considered a mature embryo, although many embryos remain in stage 5 at kernel maturity. The embryo is 6.0 to 8.0 mm long. When examined in longitudinal section extensive vascular tissue is observed to extend the length of the embryonic axis and branch up and down into the scutellum.

Normal Endosperm Development: The primary endosperm nucleus first divides two to four hours after fertilization. Mitotic divisions without cytokinesis continue until three to four days post-pollination when cell walls are formed and the endosperm cellularizes (Sass 1977). The endosperm continues to enlarge and starch grain deposition begins about 12 dap (Sass 1977; Wilson 1978). The endosperm continues to synthesize starch and other storage products such as the protein zein (Salamini and Soave 1982) until 40 to 50 dap, after which the endosperm matures and dries (Wilson 1978).

Fine structure of maize embryos has also been described (Diboll 1964; Schel et al. 1984; Van Lammeren 1986). These works reveal an orderly pattern of development at the ultrastructural level. Many of the events that establish the polarity, set apart the embryo proper, and determine meristem position take place very early in the development of the young embryo (Sheridan 1988; Sheridan and Clark 1994). Mutations that affect these processes will likely exert their initial effect at these very early stages, before gross morphological changes can be observed. Alteration in fine structure in mutants may provide insight

into the role of the normal gene product during embryogeny (Sheridan and Clark 1987). Secondary effects such as degeneration and necrosis are also revealed earlier by ultrastructural examination.

In order to reveal the nature of the defect during embryogenesis caused by the *dek23* mutation (Clark and Sheridan 1986), mutant and normal embryos were examined and compared by three different methods. Mutant and normal embryos from the same ear were examined to ascertain the time at which mutant and normal embryos could be distinguished ultrastructurally, and the extent of the morphological abnormality of the mutant embryos at each developmental stage.

Light microscopy of semi-thin plastic sections was used to assess the effect of the *dek23* mutation at the cellular level. Abnormality of the shoot apical meristem region (sam) is one phenotypic trait of mutant *dek23* embryos (Clark and Sheridan 1986), and light microscopy may indicate the exact time that this abnormality becomes apparent. The initial organization of the shoot apical meristem (sam) occurs during the transition stage when outward morphological differences are not yet apparent between

mutant and normal embryos (Randolph 1936). Light microscopy was also useful for orientation for subsequent transmission electron microscopy analyses.

Transmission electron microscopy (TEM) was performed on the same material used for light microscopy to observe the difference between mutant and normal sam cells at the organellar level. Mutant *dek23* embryos often undergo necrosis at the sam region, and TEM may reveal the mechanism or steps that lead to the degeneration of cells in this region. Differences between mutant and normal sam cells may also provide clues about the role of the normal *dek23* gene product in embryogenesis and its effect on subcellular components.

This investigation was intended to answer questions pertaining to 1.) the timing of mutant embryo divergence from normal embryos, 2.) the ultimate developmental stage reached by mutant embryos, and 3.) the cellular and ultrastructural basis of the abnormality. Answers to these questions should reveal the timing and role of the normal *dek23* gene product and its effect on controlling cell fate in the shoot apical meristem region.

Materials and Methods

Fresh dissection: Kernels from a self-pollinated ear segregating for *dek23* were grown in the greenhouse. Plants were self-pollinated and a portion of the ears from several different plants harvested (for dissection) at different ages. Kernels for a given developmental stage were taken from the same region of the ear to control for variability in maturity along the long axis of the ear.

Kernels were classified as mutant or normal based on endosperm phenotype when possible. At early stages the two types of kernels were indistinguishable and they were collected blindly then dissected under a stereomicroscope. At least twelve kernels were dissected at each developmental stage. A photographic record of three normal kernels and four to eight mutant kernels for each stage was kept using Kodak Gold 100 color print film.

Plastic sectioning: Several different sources of seed with varying genetic backgrounds and rates of maturity were used. Kernels were harvested from greenhouse or field grown material, the embryos were dissected free and fixed in 2% glutaraldehyde in 0.05 M potassium phosphate buffer pH 6.8 for four hours. Potassium phosphate buffer was made by

titrating 0.2 M potassium phosphate monobasic (KH_2PO_4) with 0.2 M potassium phosphate dibasic (K_2HPO_4) to reach pH 6.8. This solution was then diluted to 0.05 M.

Embryos were rinsed with 0.05 M potassium phosphate buffer four times for two minutes each, and post-fixed in 4% osmium tetroxide (OsO_4) in the same buffer overnight. Embryos were again rinsed in buffer several times and then dehydrated through an ethyl alcohol series and infiltrated and embedded in Spurr's resin (Spurr 1969) by the schedule listed in Table 1. Some embryos were infiltrated and embedded in Epon/Araldite resin instead of Spurr's. For each developmental stage, eight to twelve embryos were examined. Embedded embryos were sectioned at 1 μm using glass knives on a Reichert-Jung Ultracut E Ultramicrotome. Sections were stained with 1% Toluidine Blue O in 1% sodium borate and photographed on a Leitz Labrolux S compound microscope equipped with a photoautomat and automatic camera. Kodak T-Max 100 black and white print film was used.

Transmission electron microscopy: Embryos used in thick plastic sectioning were trimmed and sectioned at

70-80 nm using a diamond knife. Sections were collected on 2 x 1 cm slotted grids coated with formvar/carbon. Grids were stained for 30-45 minutes in saturated aqueous uranyl acetate, rinsed for 30 minutes in distilled water, and stained with modified Sato's lead stain for 30-45 minutes. Sato's lead stain contains 6.8 mM anhydrous lead citrate $Pb(C_6H_5O_7)_2$, 11.1 mM lead nitrate $Pb(NO_3)$, 7.9 mM lead acetate $Pb(CH_3COO)_2 \cdot 3H_2O$, 68 mM sodium citrate $Na_3(C_6H_5O_7) \cdot 2H_2O$ in 0.2 N NaOH. Grids were viewed on a JEOL JEM-100S transmission electron microscope at 80kV and photographed on Kodak 4489 transmission electron microscopy film.

Table 1. Dehydration and embedding protocol.

Solution	Time
25% ethanol	5 minutes
30% ethanol	5 minutes
35% ethanol	5 minutes
40% ethanol	5 minutes
45% ethanol	5 minutes
50% ethanol	5 minutes
55% ethanol	5 minutes
60% ethanol	5 minutes
65% ethanol	5 minutes
70% ethanol	5 minutes
75% ethanol	5 minutes
80% ethanol	5 minutes
85% ethanol	5 minutes
90% ethanol	5 minutes
95% ethanol	5 minutes
100% ethanol	5 minutes x 3
1:3 propylene oxide:ethanol	30 minutes
3:1 propylene oxide:ethanol	30 minutes
100% propylene oxide	30 minutes x 2
1:3 Spurr's resin:propylene oxide	12 hours
1:1 Spurr's resin:propylene oxide	12 hours
3:1 Spurr's resin:propylene oxide	12 hours
100% Spurr's resin	24 hours x 2
Embed and polymerize at 70° C.	36 hours

Results

Fresh dissection: Fresh dissection of kernels revealed a divergence in embryo phenotype before any reliable difference in endosperm phenotype or kernel size could be detected (Figure 2). In 9 dap greenhouse-grown material, mutant and normal kernels could not be reliably distinguished, but a difference in size of mutant embryos as compared to normal embryos was evident; that is mutant embryos were smaller than normal embryos, but no detectable abnormality was observed. Normal embryos were at the transition stage and presumed mutant embryos were at an early transition stage.

At 10 dap, mutant and normal kernels could be distinguished and the divergence between mutant and normal embryos was greater. Normal embryos were at the coleoptilar stage, while mutant embryos were at the late transition stage (Figure 2). Mutant embryos were normal in morphology for that stage and merely lagged behind normal embryos of the same chronological age.

By 20 dap, the divergence between mutant and normal embryos was large. Normal embryos were at stage 3, while mutant embryos were at an abnormal coleoptilar stage (Figure

3). Mutant embryos had developed a small characteristically pointed scutellum and some had a rudimentary shoot apex. No necrosis was evident. Mutant kernels were noticeably smaller than normal kernels; the endosperm did not completely fill the surrounding pericarp.

By 25 dap, normal embryos had reached stage 4 while mutant embryos remained at abnormal coleoptilar stage (Figure 3). Mutant embryos had enlarged slightly from 20 dap but little or no elaboration of the shoot apex was apparent.

At 60 dap (kernel maturity) normal embryos were at stage 6. Mutant embryos had not enlarged from 25 dap, although some changes were visible at the shoot apex region (Figure 4). A distinct coleoptilar ring was visible on several mutant embryos, and a few embryos developed large bulges or lobes in the region of the coleoptile (Figure 4).

Light microscopy: One micron plastic sectioning of mutant and normal embryos revealed an early divergence in phenotype. In 9 dap greenhouse grown material of this genetic background, normal embryos were at a coleoptilar stage, while mutant embryos remained in transition stage (Figure 5). This seed source was different than that used

for fresh dissections. No apparent abnormality was observed in mutant embryos other than the developmental delay.

In 13 dap greenhouse grown material, normal embryos had reached coleoptilar stage. A prominent upper lobe of coleoptilar tissue had formed as well as the lower bulge, in some embryos the shoot apical meristem was evident between them. Mutant embryos were developmentally delayed as compared to normal embryos; the mutant embryos had reached a very early coleoptilar stage (Figure 5). No upper lobe of coleoptilar tissue had formed with only slight thickenings where the upper and lower coleoptilar bulges should appear. The scutellum was also somewhat flatter and the suspensor thicker and more persistent than on normal embryos of the same developmental stage.

Material collected for 14 dap and older was field grown while younger embryos were harvested from greenhouse grown plants. In 14 dap field grown material, normal embryos had reached stage 2. The use of an artificial light source, growing plants in pots in an artificial soil mixture, and frequent use of pesticides in the greenhouse may have affected the plants adversely and may account for the

differences observed between greenhouse grown normal embryos at 13 dap and 14 dap field grown material.

All mutant embryos examined at 14 dap had reached an abnormal early stage 1. Several embryos had differentiated a complete coleoptilar ring, shoot apical meristem, and a first leaf primordium (Figure 6). A well-defined root apical meristem was also visible in some embryos. The scutellum was somewhat flattened and pointed, and the abaxial side was irregular.

At 17 dap normal embryos were at stage 2 (data not shown) and mutant embryos were at an abnormal stage 1 or late coleoptilar stage (Figure 7). All mutant embryos examined at the previous developmental stage had formed a shoot apical meristem, so it can be inferred that they failed to maintain organization of a distinct coleoptilar ring, shoot apical meristem, and leaf primordia. Some irregular lobes were present in the shoot apex region, but the darkened areas indicated the onset of necrosis. The scutellum had elongated and become distinctly pointed and flattened. Some dark patches near its top may also be regions of tissue degeneration.

At 22 dap normal embryos were at stage 3-4 (data not shown) and mutant embryos were at an abnormal flattened scutellum stage (Figure 8). At least one mutant embryo had differentiated an irregular coleoptilar ring and formed a shoot apical meristem (Figure 8). Other embryos showed no evidence of lobes with only a sunken region in the scutellum forming above and behind the location of the potential shoot apex.

Transmission electron microscopy: Electron micrographs of 9 dap normal and mutant embryos revealed differences in amount of vacuolization of cells. Mutant embryos (Figure 10) appeared to have somewhat larger vacuoles, and their nuclear membranes seemed more convoluted than normal cells (Figure 9).

Normal embryonic cells at 14 dap had accumulated numerous lipid droplets and plastids containing starch grains (Figure 11). Mutant cells contained larger, more numerous vacuoles, but fewer lipid droplets and rough endoplasmic reticulum (Figures 12 and 13). Nuclei were large and lobed and plastids were enlarged but contained no starch (Figure 12).

In 17 dap normal embryonic cells, a difference between cells of the first leaf primordium and cells of the shoot apical meristem were apparent (Figure 14). Meristem cells contained many more mitochondria and lipid droplets and had fewer vacuoles than cells of the leaf primordium.

Mutant embryos at 17 dap already showed evidence of cell degeneration and necrosis (Figure 15). Vacuoles were fairly large, and some contained organelles and other cellular debris, indicating degeneration was occurring. Abundant plastids with distorted membranes were also present and nuclei were highly lobed (Figure 16).

At 22 dap, mutant embryos displayed patches or regions of necrotic cells. Large vacuoles containing organelles were visible (Figure 17) and some degenerating cells had ruptured (Figure 18). Surrounding cells showed signs of degeneration also as electron dense cytoplasm shrank away from cell walls (Figure 19). A summary of observations made by light microscopy and TEM on normal and mutant *dek23* embryos is presented in Table 2.

Table 2. A comparison of light microscopy and TEM observations

	Normal embryos	Mutant *dek23* embryos
Light microscopy	9 dap- embryos at coleoptilar stage	9 dap- developmental delay apparent, embryos at late transition stage, no apparent abnormality
	14 dap- embryos at stage 2	14 dap- embryos at abnormal stage 1, scutellum flattened
	17 dap- embryos at stage 2	17 dap- embryos at abnormal stage 1, necrosis and loss of sam organization
	22 dap- embryos at stage 3-4	22 dap- embryos at flattened scutellum stage
TEM	9 dap- sam cells have small vacuoles	9 dap- sam cells have large vacuoles and convoluted nuclear membrane
	14 dap- abundant lipid droplets, plastids contain starch granules, small nucleus and vacuoles	14 dap- large vacuoles, few lipid droplets, no starch in plastids, large nuclei with convoluted membranes
	17 dap- numerous lipid droplets, few vacuoles, small nuclei	17 dap- large vacuoles, few lipid droplets, nuclei with convoluted membranes, necrosis
		22 dap- necrosis spreading, large vacuoles containing organelles

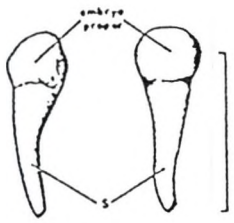

TRANSITION PHASE

A

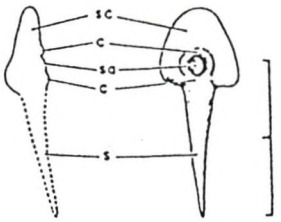

COLEOPTILAR STAGE

B

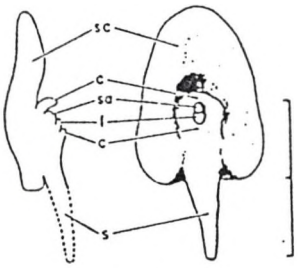

STAGE 1

C

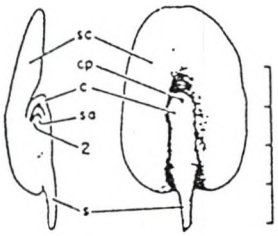

STAGE 2

D

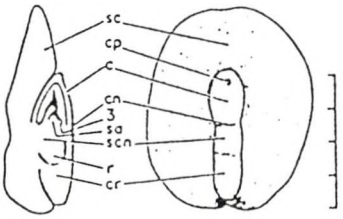

STAGE 3

E

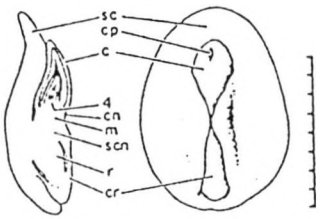

STAGE 4

F

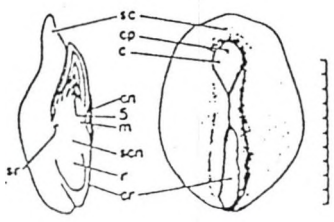

STAGE 5

G

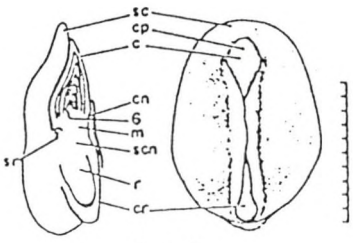

STAGE 6

H

EXPLANATION OF SYMBOLS

1,2,3,4,5,6 - leaf primordia in order of appearance
c - coleoptile
cn - coleoptilar node
cp - coleoptilar pore
cr - coleorhiza
m - mesocotyl
r - primary root primordium
s - suspensor
sa - shoot apex
sc - scutellum
scn - scutellar node
sr - seminal root primordium

SCALE: each division is 0.5 mm.

Figure 2. Fresh dissections of 9 and 10 dap greenhouse grown kernels.

A and E. Normal 9 dap kernel with transition stage embryo.

B and F. Mutant 9 dap kernel with early transition stage embryo lagging behind normal embryo.

C and G. Normal 10 dap kernel with coleoptilar stage embryo.

D and H. Mutant 10 dap kernel with late transition stage embryo, lagging well behind normal embryos on the same ear.

Scale bars = 1 mm.

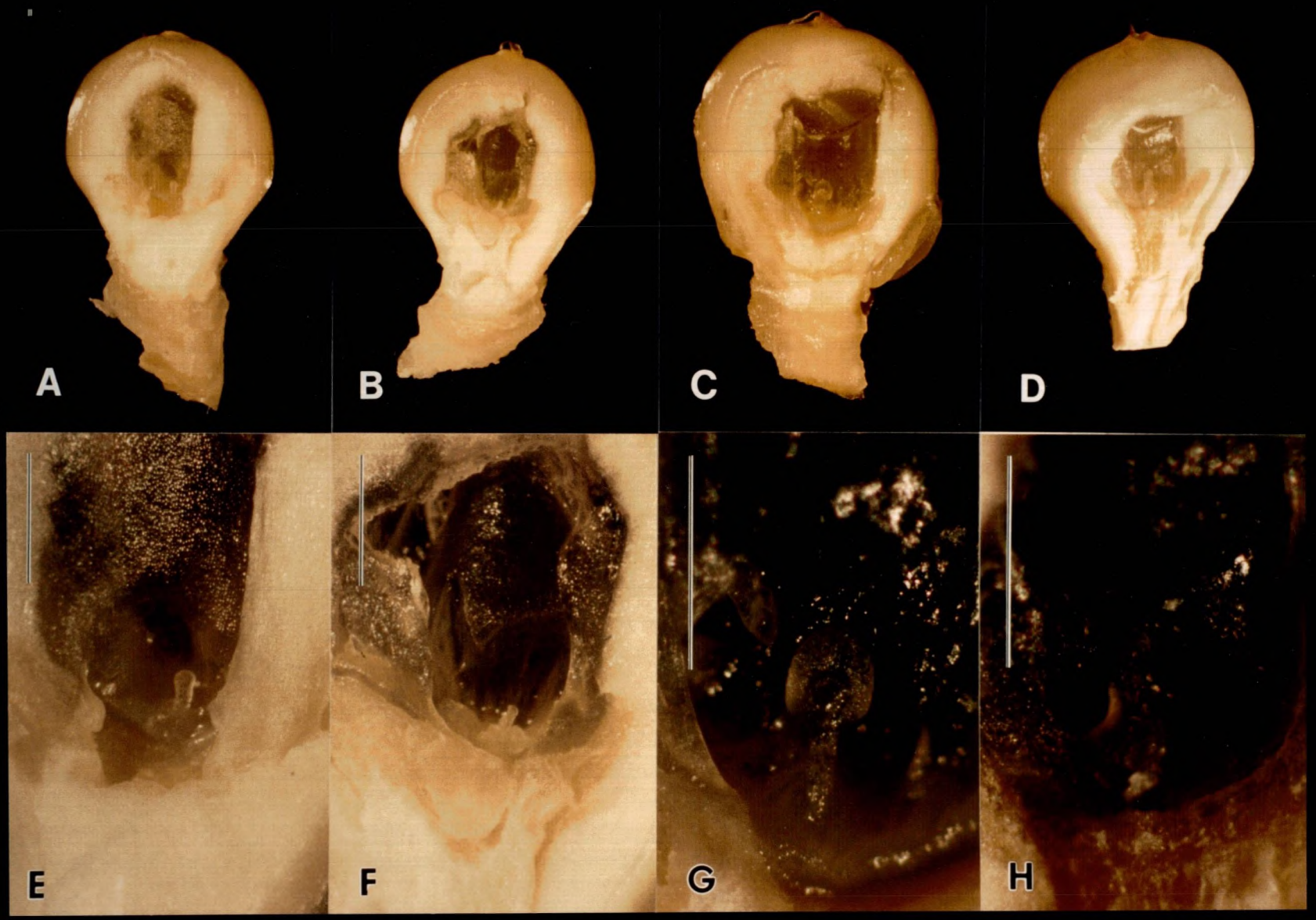
A
B
C
D
E
F
G
H

Figure 3. Fresh dissections of 20 and 25 dap greenhouse grown kernels.

A. Normal 20 dap kernel with stage 3 embryo.

B-D. Mutant 20 dap kernels with abnormal coleoptilar stage embryos. Mutant embryos had formed a small pointed scutellum and rudimentary shoot apex, but no apparent leaf primordia.

E. Normal 25 dap kernel with stage 4 embryo.

F-H. Mutant 25 dap kernel with abnormal flattened scutellum stage embryos. Mutant embryos had enlarged somewhat and the scutellum flattened, but no further development of the shoot region was apparent. Scale bar = 1 mm.

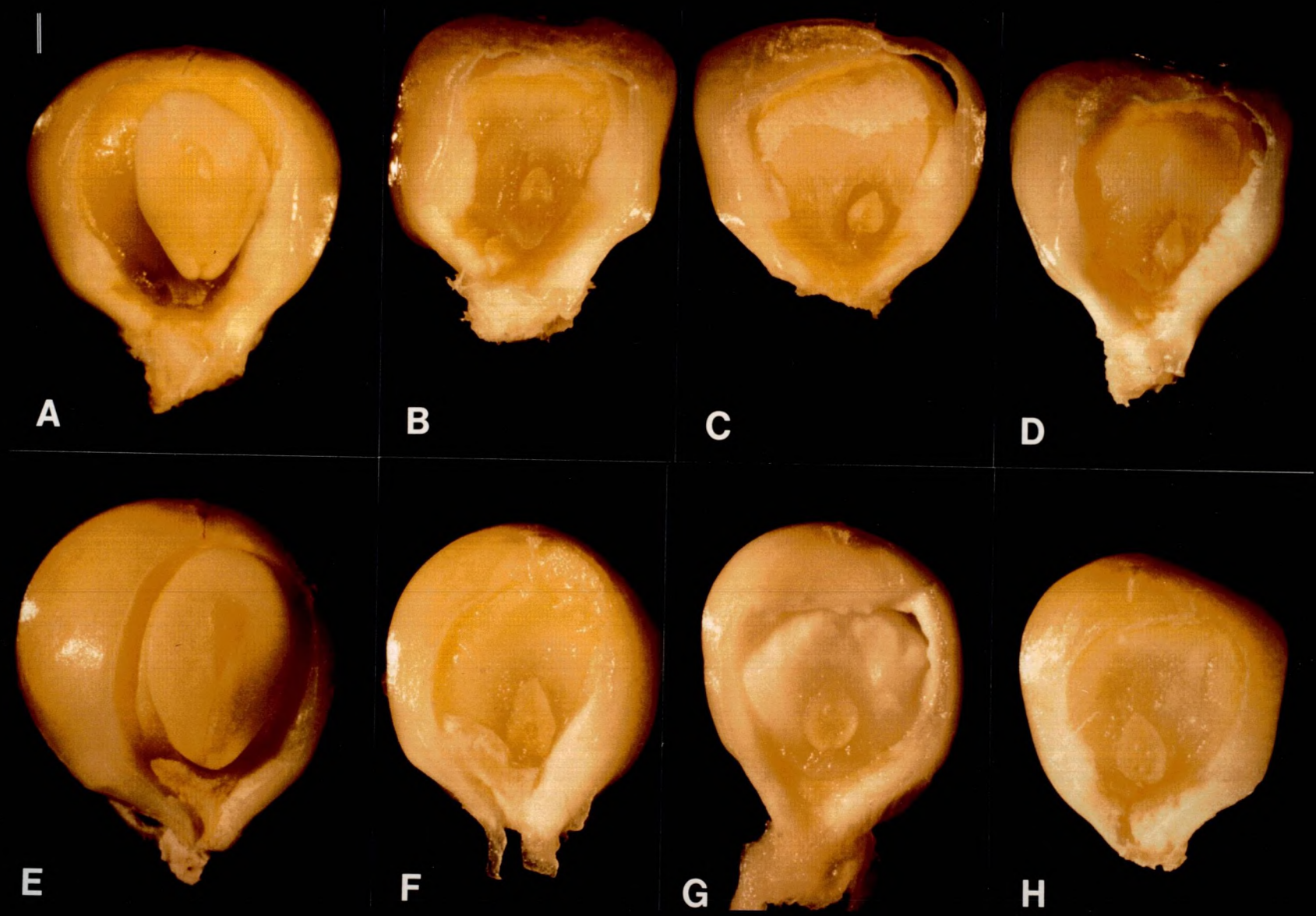
A
B
C
D
E
F
G
H

Figure 4. Fresh dissections of 60 dap greenhouse grown kernels.

A. Normal 60 dap kernel with stage 6 embryo.

B-D. Mutant 60 dap kernels with abnormal degenerative stage embryos. Mutant embryos had not enlarged significantly from 25 dap embryos (see Figure 3) but some proliferation of tissue was apparent in the shoot apex area. Some necrosis was also evident in B. Scale bar = 1 mm.

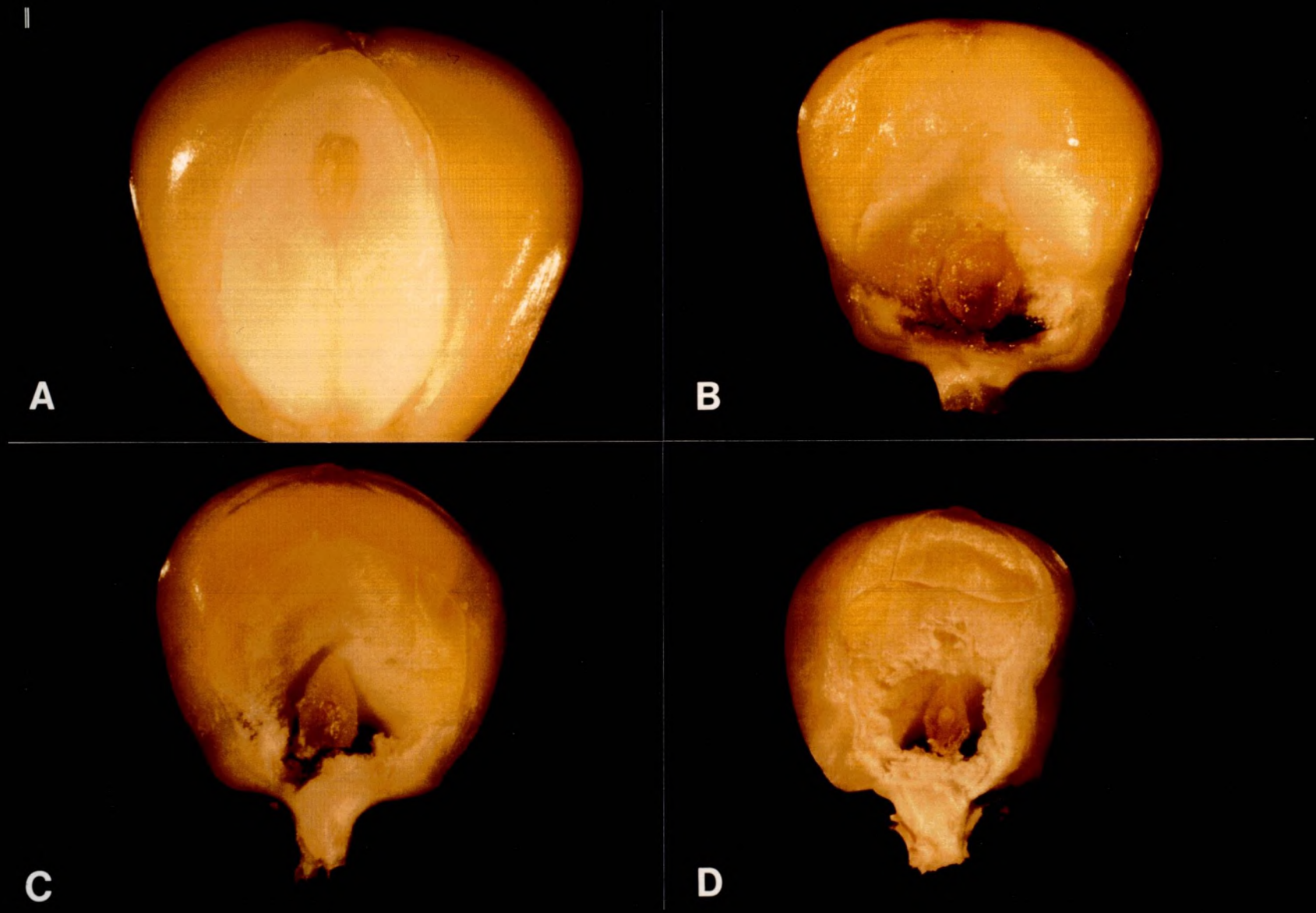
A
B
C
D

Figure 5. Plastic sections (1 μm thick) of 9 and 13 dap embryos from greenhouse grown material.

A-C. Normal 9 dap embryos at early coleoptilar stage.

D-F. Mutant 9 dap embryos at late to early transition stage respectively. Mutant embryos already lagged behind normal embryos by a discernable margin at this age.

G-I. Normal 13 dap embryos at late to early coleoptilar stage respectively.

J. Mutant 13 dap embryo at very early coleoptilar stage. Note the flattened scutellum and thick suspensor as compared to normal embryos. Abbreviations: cr = coleoptilar ring or ridge, sam = shoot apical meristem, sc = scutellum, su = suspensor. Scale bar = 0.25 mm.

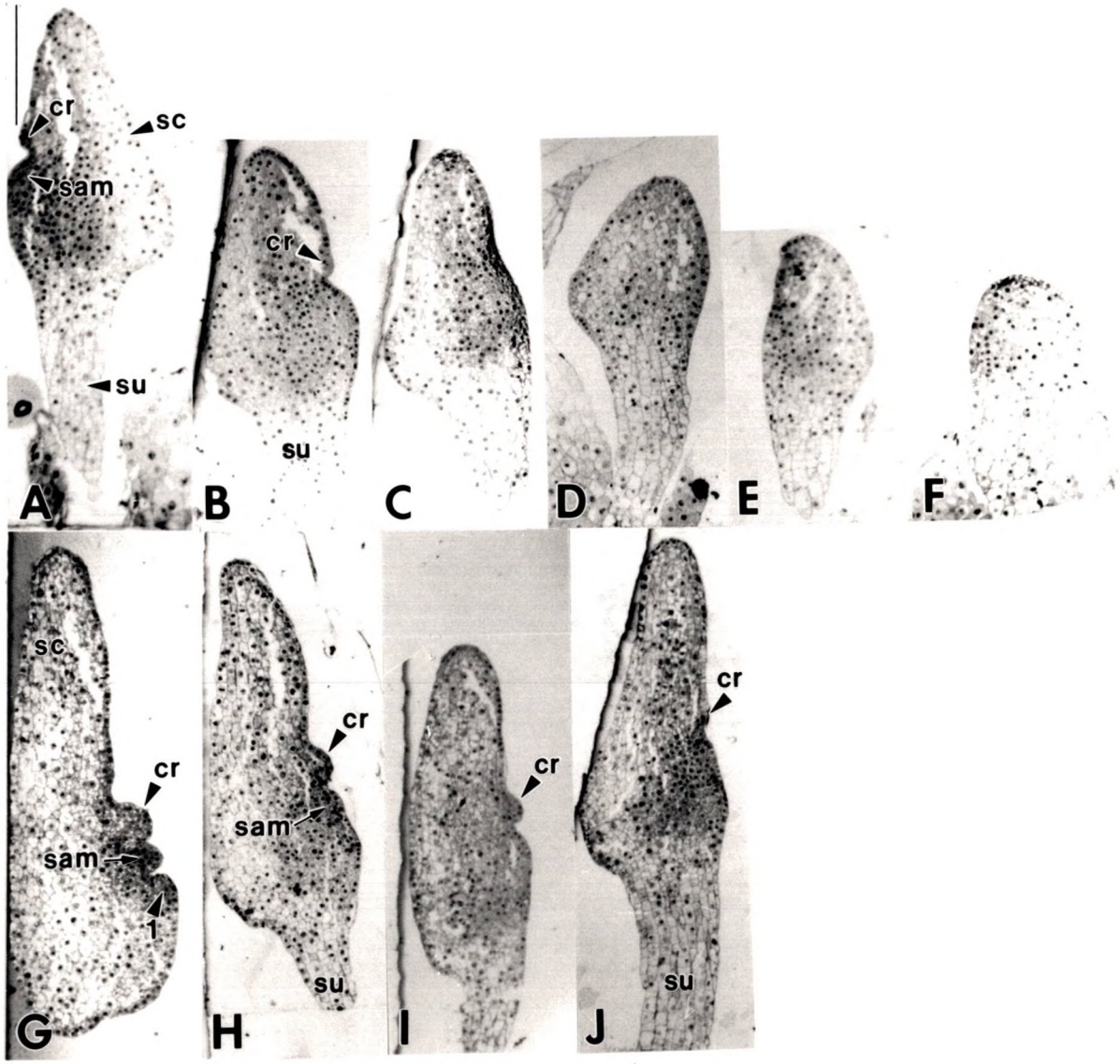
cr
sc
sam
su
A
cr
su
B
C
D
E
F
sc
cr
sam
1
G
cr
sam
su
H
cr
I
cr
su
J

Figure 6. Plastic sections (1 μm thick) of 14 dap embryos from field grown material.

A. Normal 14 dap embryo at stage 2.

B-D. Mutant 14 dap embryos at an abnormal stage 1. Note the flattened scutellum and well-formed root meristem (rm) and shoot apical meristem (sam). Abbreviations: cr = coleoptilar ring or ridge, sam = shoot apical meristem, sc = scutellum, su = suspensor, 1 = first leaf primordium, 2 = second leaf primordium. Scale bar = 0.25 mm.

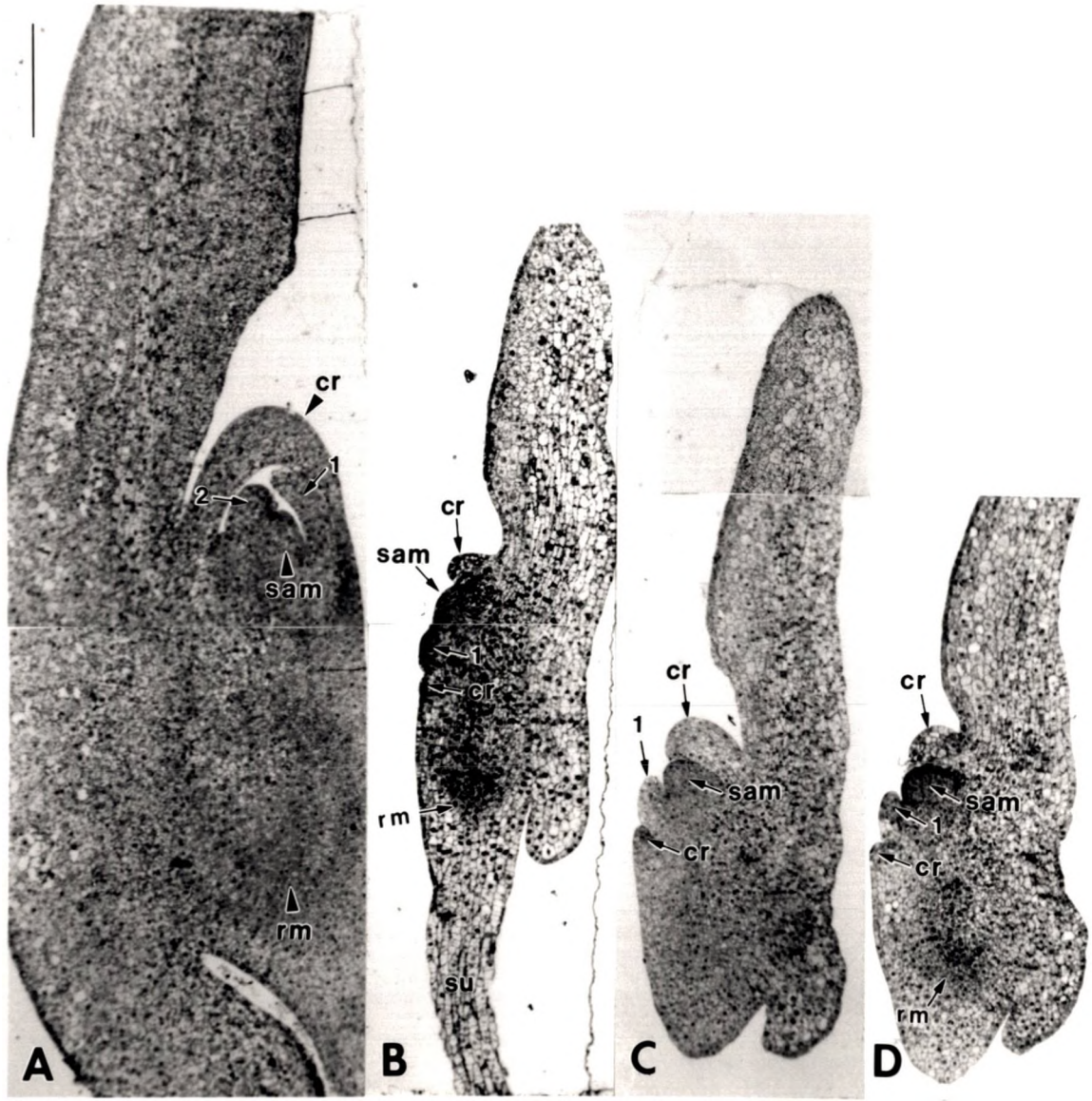
cr
1
2
sam
rm
A
cr
sam
1
cr
rm
su
B
cr
1
sam
cr
C
cr
sam
1
cr
rm
D

Figure 7. Plastic sections (1 μm thick) of mutant abnormal stage 1 embryos at 17 dap from field grown material. A-B. Mutant embryos had formed a coleoptilar ring or ridge (cr) and partially formed a shoot apical meristem (sam). Scutellum was flattened and somewhat pointed. Some necrosis (nec) had become evident in the shoot apex region and abaxial side of the scutellum. C. Embryo did not possess a completely separate shoot meristem and coleoptilar ring. Normal embryos at this age were at a late stage 2 to early stage 3 (not shown). Scale bar = 0.25 mm.


sc
cr
sam
nec
nec
nec
A
B
C

Figure 8. Plastic sections (1 μm thick) of mutant embryos at the flattened scutellum stage at 22 dap from field grown material.

A. Mutant embryo with partially differentiated coleoptilar ring (cr), shoot apical meristem (sam), and first leaf primordium (1).

B-D. Mutant embryos which failed to form or maintain a shoot apical meristem or coleoptilar ring. A root apical meristem (rm) is distinguishable in A, B, and D. Note the extensive necrosis (nec) in C which spans the region of the potential shoot apex through the backside of the scutellum. Scale bar = 0.25 mm.

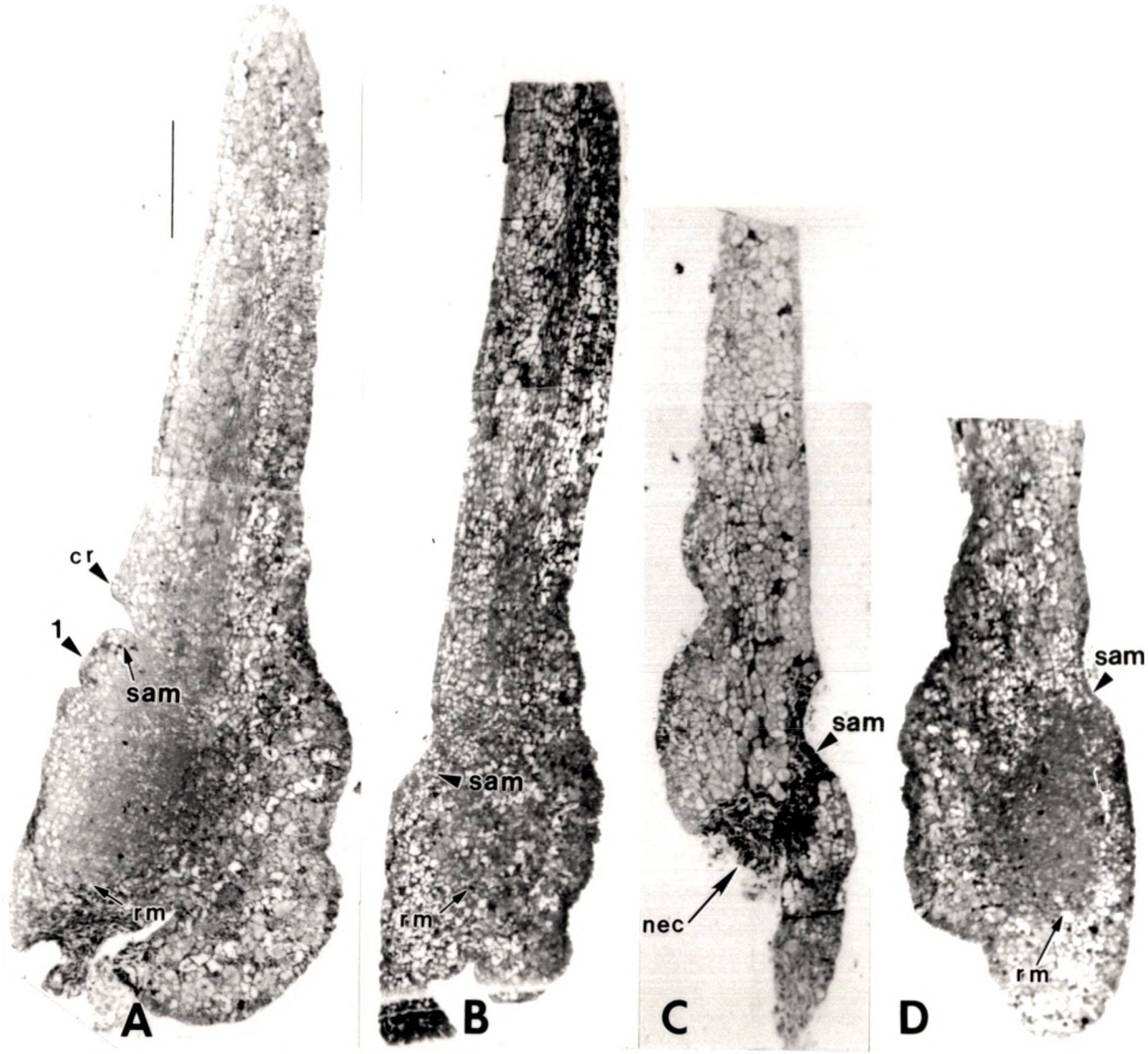
cr
1
sam
rm
A
sam
rm
B
sam
nec
C
sam
rm
D

Figure 9. A. Electron micrograph of 9 dap normal embryo (from Figure 5A) showing detail of cells of the coleoptilar primordia. Cells had few small vacuoles (V) and numerous mitochondria (M) and small nuclei (N). Magnification = 5300x.

B. Micrograph of 9 dap normal embryo from Figure 5C. Note the numerous plasmodesmata (pd). Magnification = 8000x.

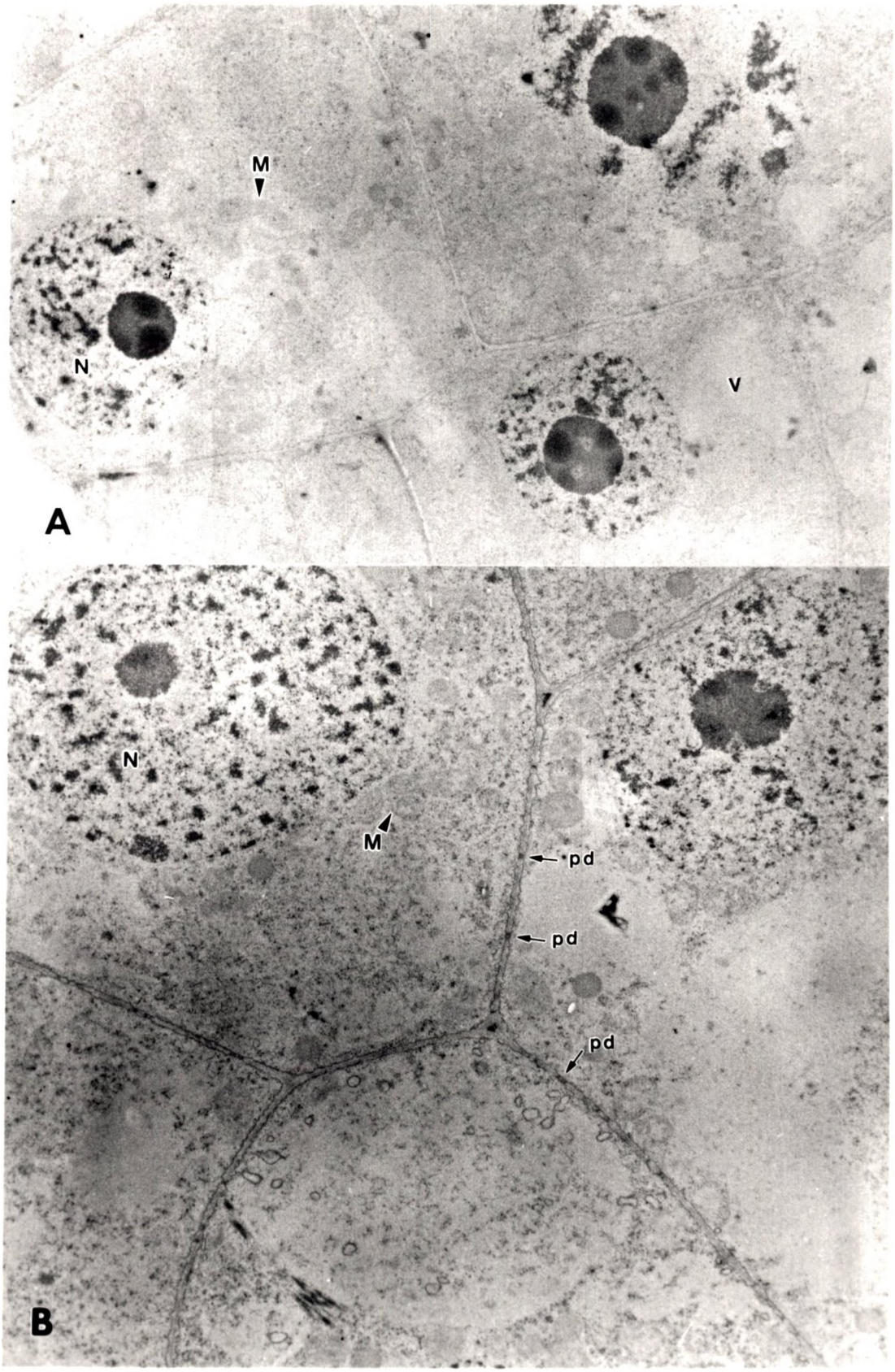
M
N
V
A
N
M
pd
pd
pd
B

Figure 10. A. Micrograph of 9 dap mutant embryo cells from the shoot apical meristem region (from Figure 5E). Note lobed appearance of the nucleus (N) and prominent nucleolus (Nu). Magnification = 8000x.

B. Micrograph of 9 dap mutant embryo cells from the shoot apical meristem region (from Figure 5F). Very large vacuoles (V) were prevalent, as well as numerous plasmodesmata (pd). Nuclei also appear more lobed than in normal cells of the same region. Magnification = 8000x.

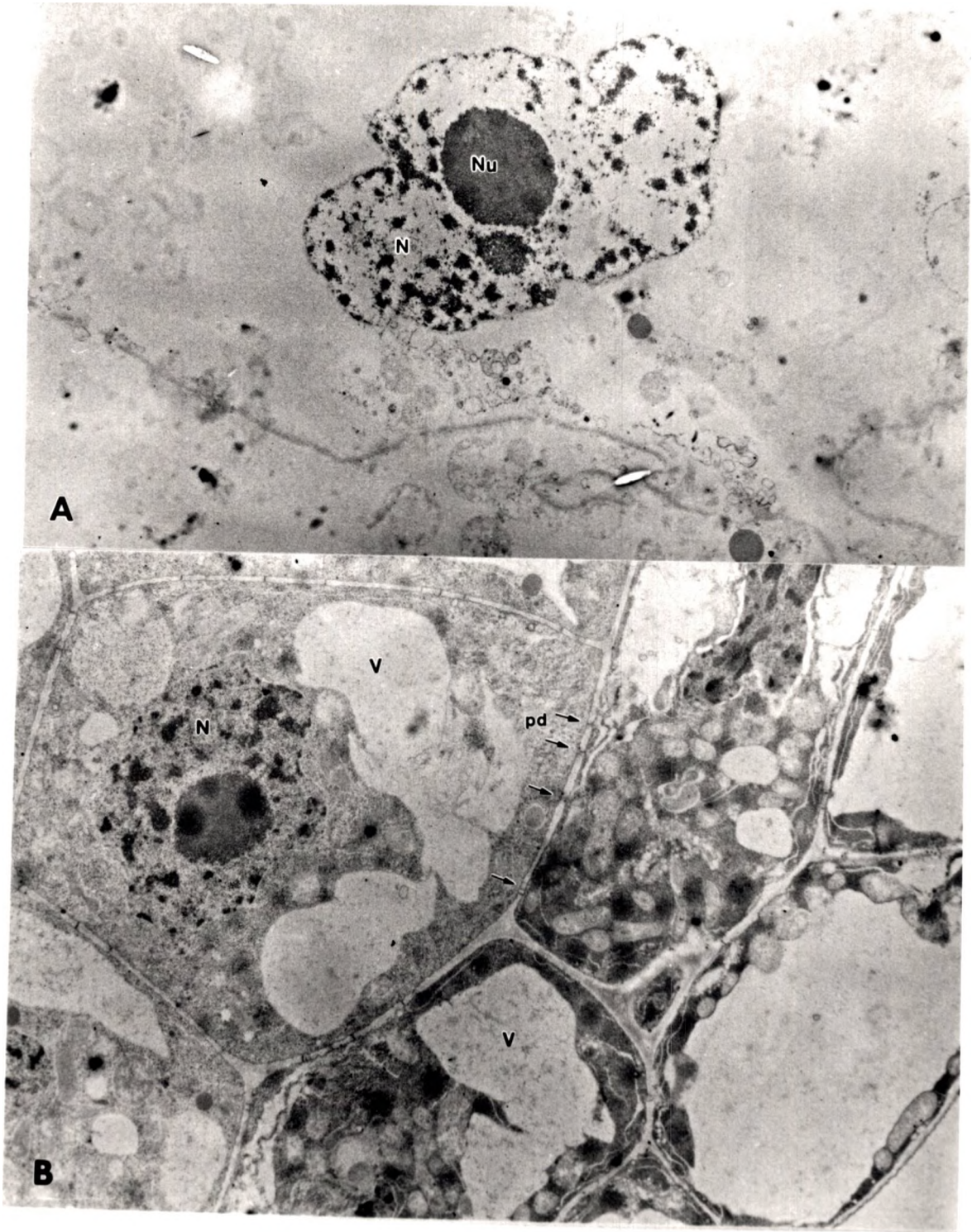
Nu
N
A
V
N
pd
V
B

Figure 11. Micrograph of 14 dap normal embryo (from Figure 6A) showing detail of shoot apical meristem. Lipid droplets (L) were very abundant as were plastids containing starch granules (S). Endoplasmic reticulum (ER) was also prevalent but very few vacuoles were observed. Note the relatively small nucleus (N) in relation to the cell volume. Magnification = 8000x.

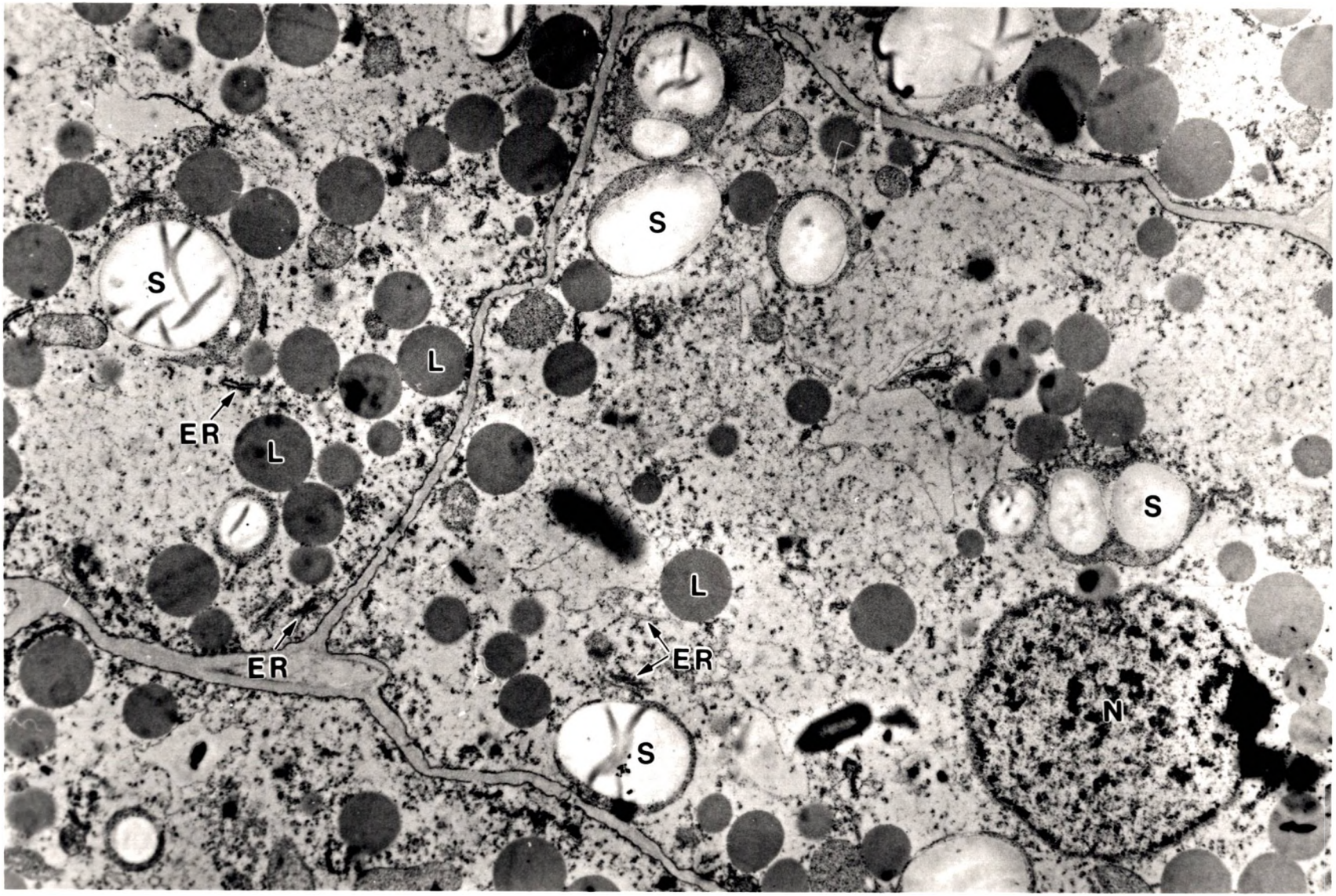
S
S
L
ER
L
S
L
ER
ER
S
N

Figure 12. Micrograph of 14 dap mutant embryo (from Figure 6B) showing detail of shoot apical meristem. Very large vacuoles were present and cells contained only a very few lipid droplets. Endoplasmic reticulum was less abundant than in normal cells and plastids (P) were present but contained no starch. Some appeared swollen and slightly distorted. Cells with osmiophilic cytoplasm may have begun to degenerate. Note the large nuclei (N) with convoluted nuclear membranes that take up much more of the cell volume than the nuclei of normal cells from the same region. Magnification = 8000x.

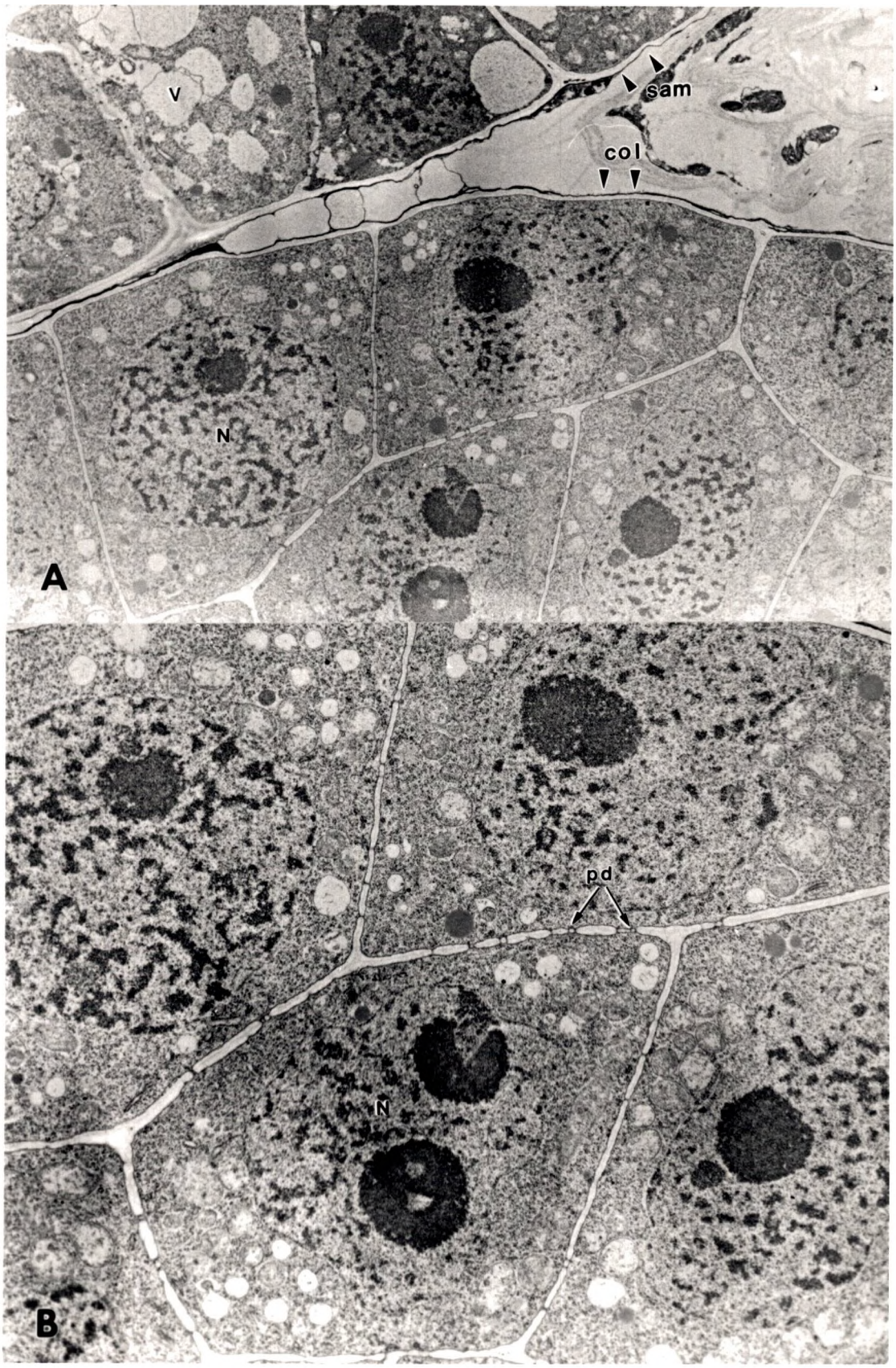
V
sam
col
N
A
pd
N
B

Figure 13. A. Micrograph of 14 dap mutant embryo (from Figure 6D) of shoot apical meristem (sam) and coleoptilar primordia (col). Shoot meristem cells have somewhat larger vacuoles (V) than coleoptilar cells. Darker osmiophilic cells may have begun to degenerate. Magnification = 5300x. B. Higher magnification of coleoptilar primordia cells in A. Note the numerous mitochondria and plasmodesmata and large nuclei (N) with convoluted nuclear membranes. Magnification = 8000x.

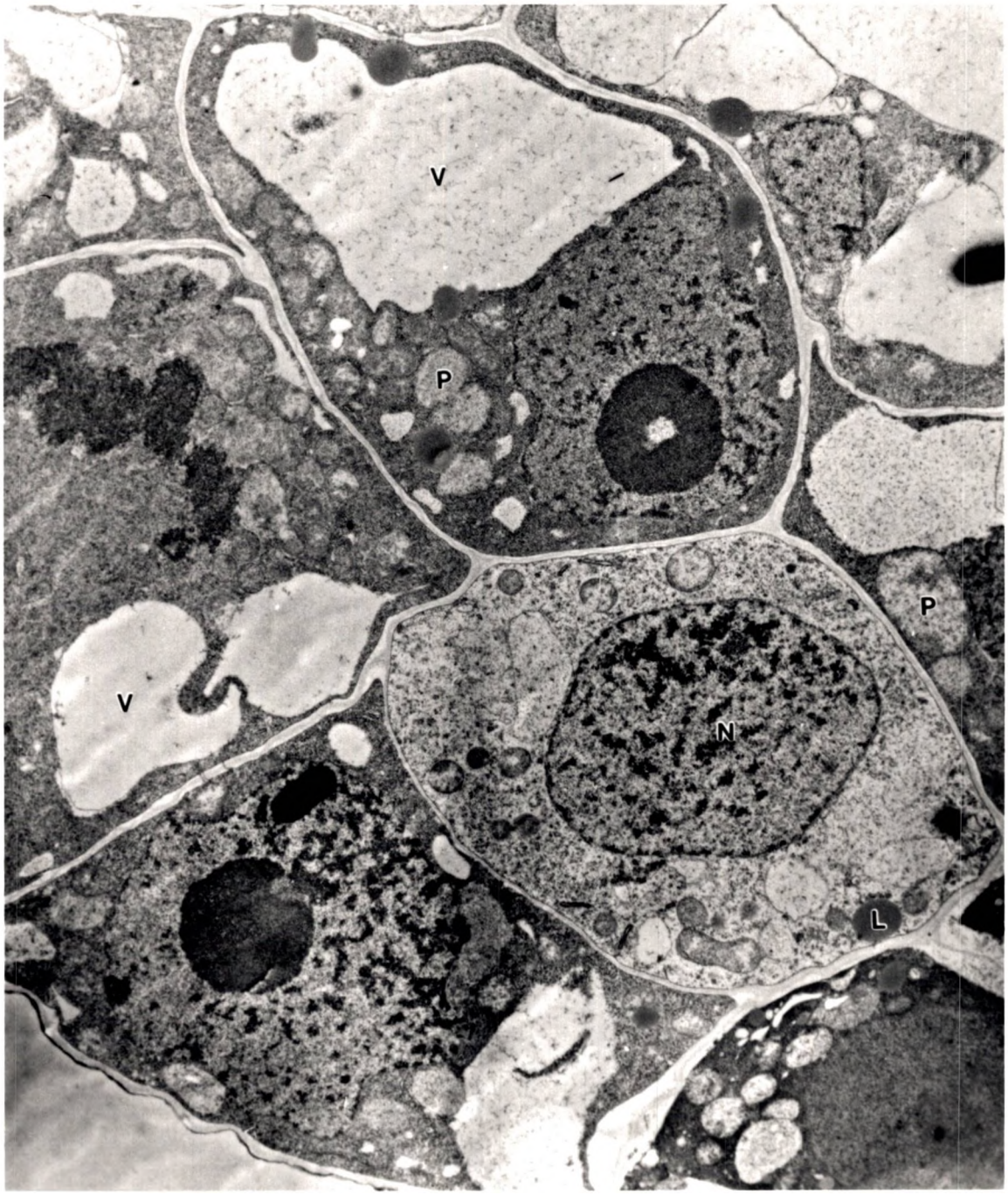
V
P
V
N
P
L

Figure 14. A. Micrograph of 17 dap normal embryo, detail of first leaf primordium. Cells contained large vacuoles (V), few mitochondria (M) and lipid droplets (L) and some plastids containing starch (S). Note the relatively small nucleus (N). Magnification = 8000x.

B. Detail of shoot apical meristem. Cells contained much greater number of mitochondria and lipid droplets than cells of the leaf primordium. Vacuoles were largely absent. Magnification = 8000x.

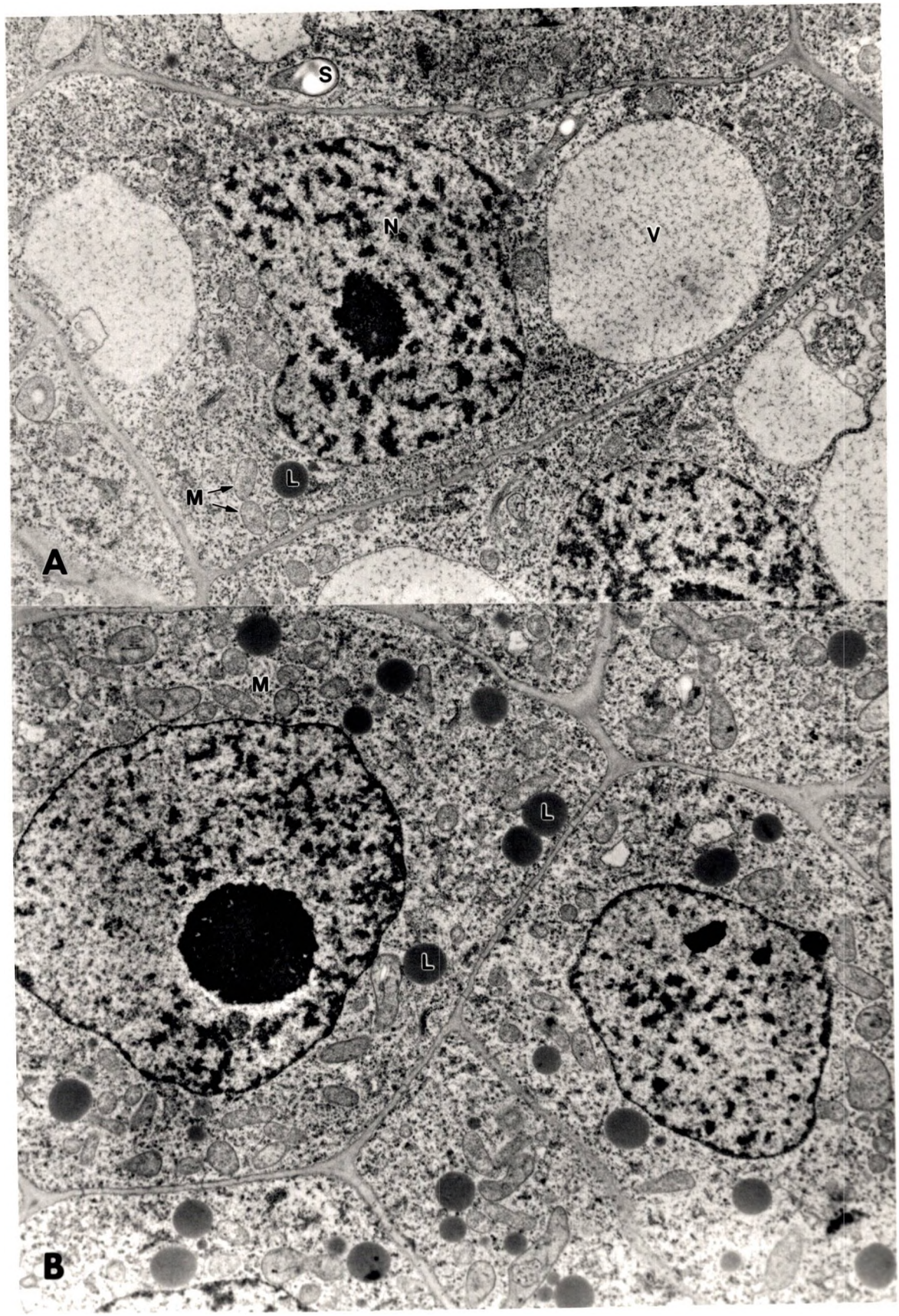
S
N
V
L
M
A
M
L
L
B

Figure 15. A. Micrograph of 17 dap mutant embryo cells from the shoot apical meristem region (from Figure 7B). Very electron dense cell had begun to degenerate and become necrotic (NEC), some vacuoles contained organelles and other cellular debris. Surrounding cells still appeared healthy. Note the highly lobed nucleus (N). Magnification = 5300x. B. Higher magnification of cells in A. Note the abundant large plastids, but no starch accumulation. Magnification = 8000x.

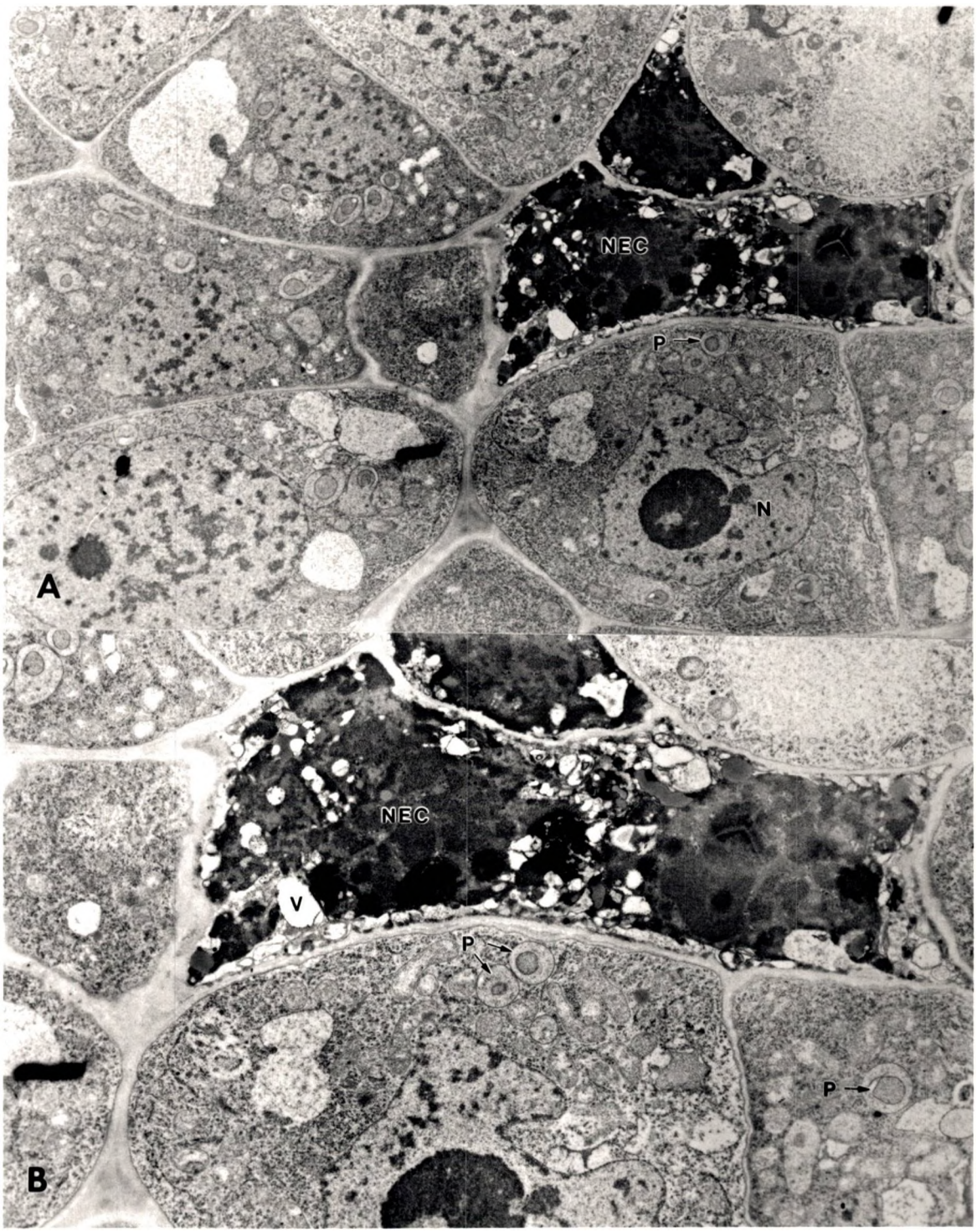
NEC
P
N
A
NEC
V
P
P
B

Figure 16. A. Micrograph of 17 dap mutant embryo cells from the shoot apical meristem region (from Figure 7A). Enlarged plastids (P) are very abundant. Magnification = 5300x. B. Micrograph of 17 dap mutant embryo cells from the shoot apical meristem region (from Figure 7C). Very large vacuoles were present in many cells, as well as a few lipid droplets. Some highly lobed nuclei (N) were apparent. Magnification = 5300x.

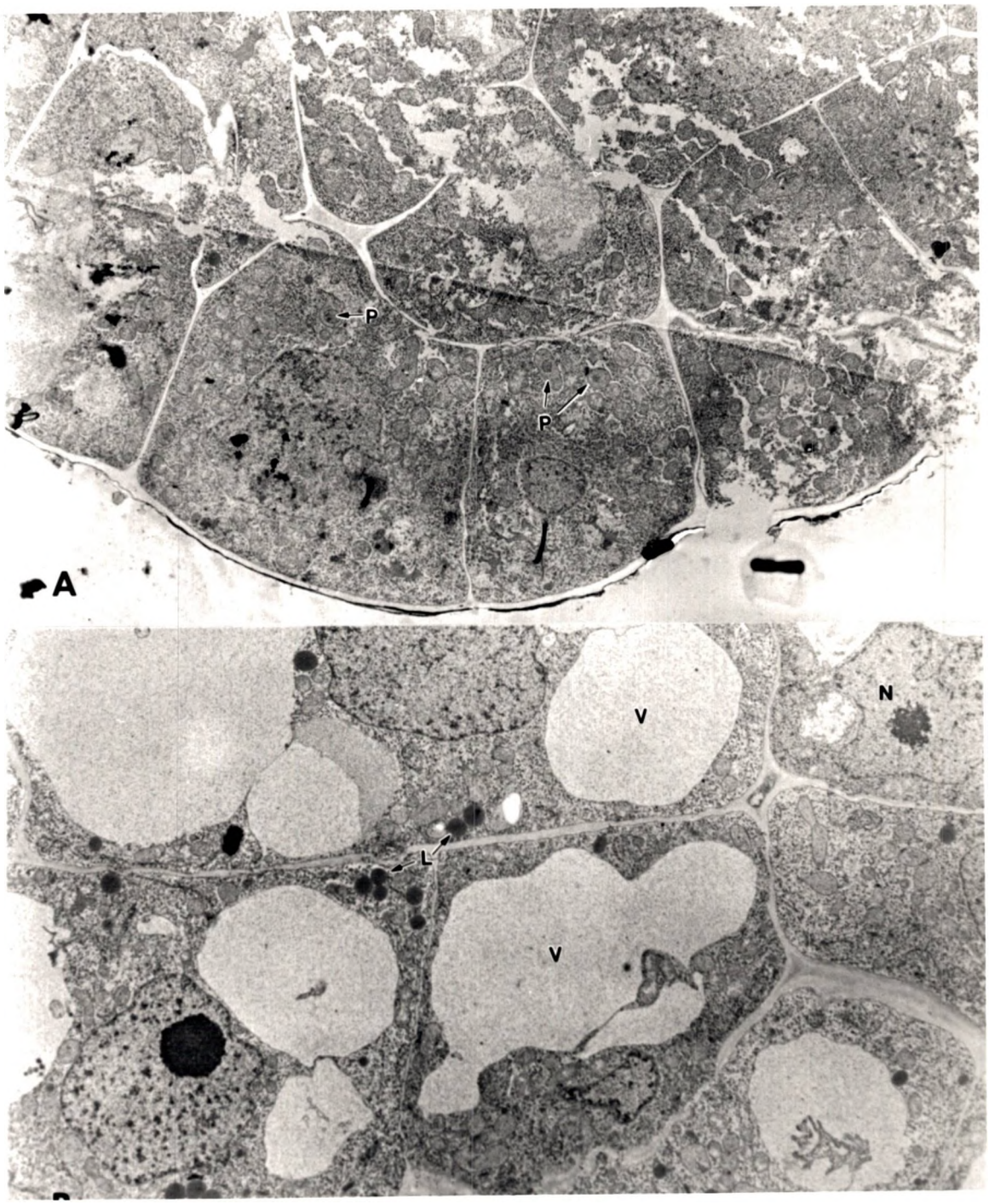
P
P
A
V
N
L
V

Figure 17. A. Micrograph of 22 dap mutant embryo (from Figure 8A) showing detail of shoot apex region. Several cells had become necrotic (NEC), and surrounding healthy cells showed large vacuoles which contained organelles. Magnification = 2650x.

B. Higher magnification of degenerating cells showing vacuoles containing organelles and plastids containing starch (S). Magnification = 8000x.

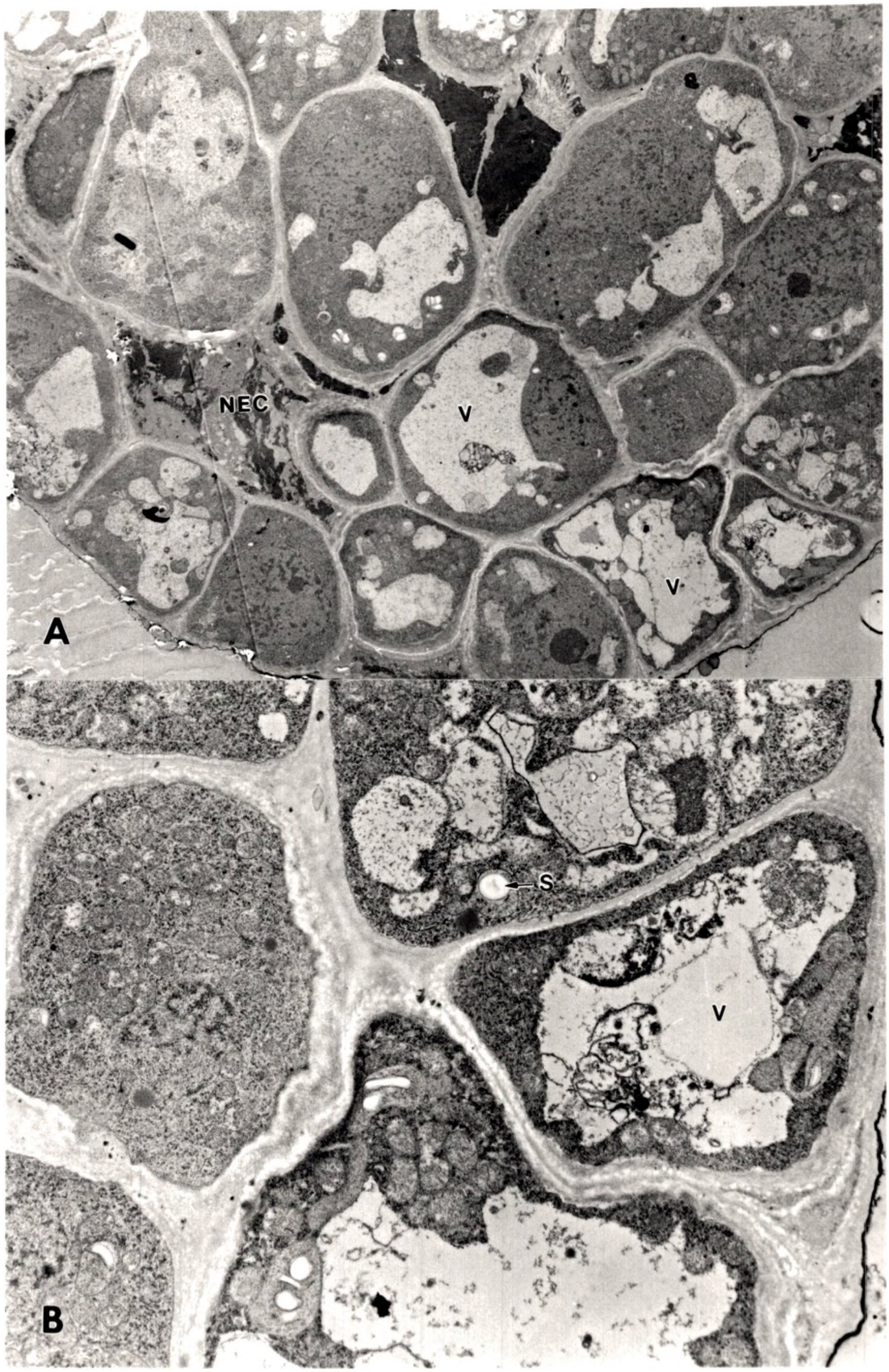
NEC
V
V
A
S
V
B

Figure 18. Micrograph of 22 dap mutant embryo cells from the degenerating region near the shoot apical meristem (from Figure 8C). Large necrotic (NEC) region is shown in detail. Degenerating cells had ruptured and nearby cells show signs that they had begun to degenerate also. Note the large vacuoles (V). Magnification = 2650x.

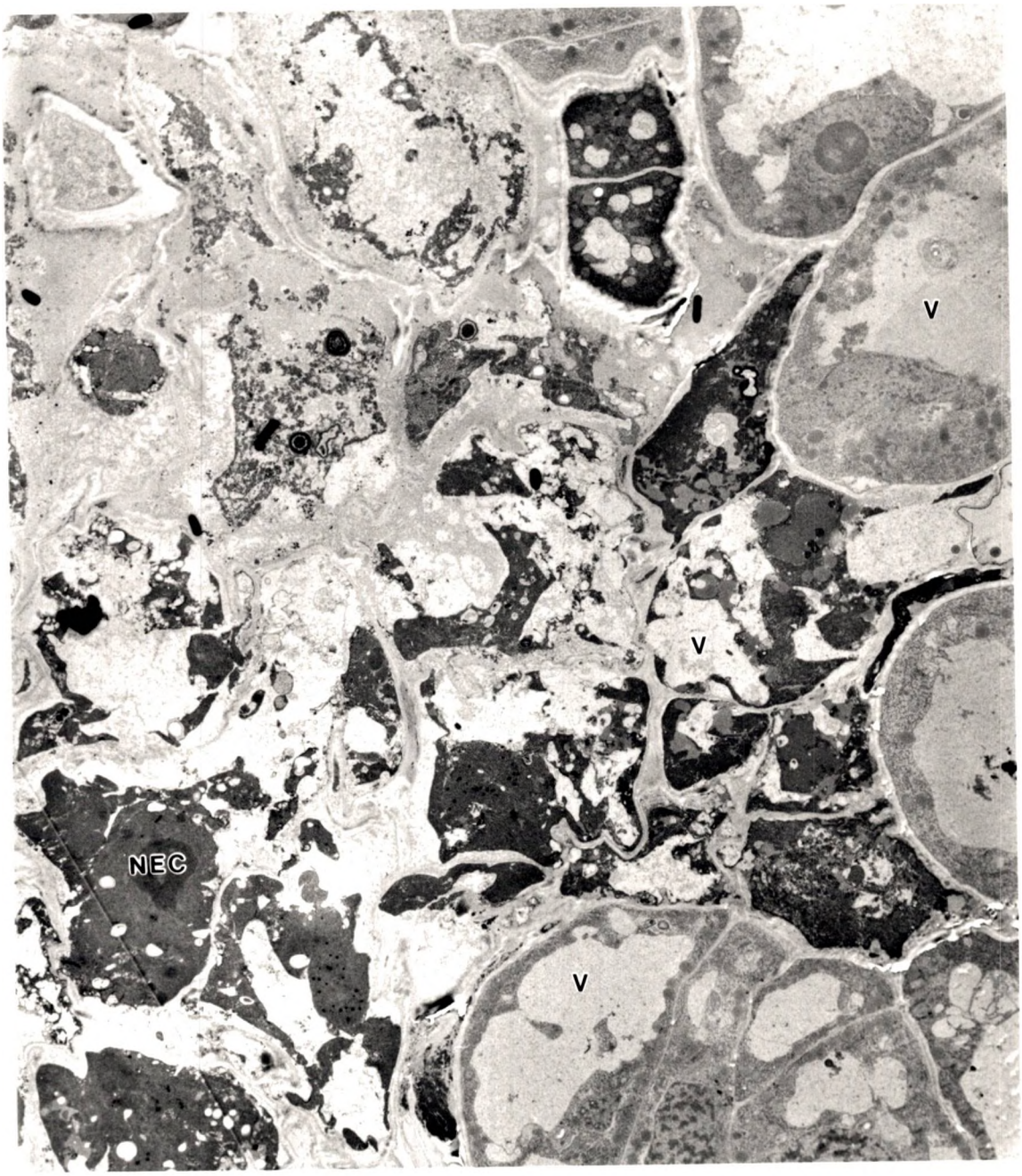
V
V
NEC
V

Figure 19. Higher magnification of necrotic cell in Figure 18. Cytoplasm had pulled away from cell wall and large vacuoles (V) were present. Several mitochondria and lipid droplets (L) persisted as well. Magnification = 8000x.

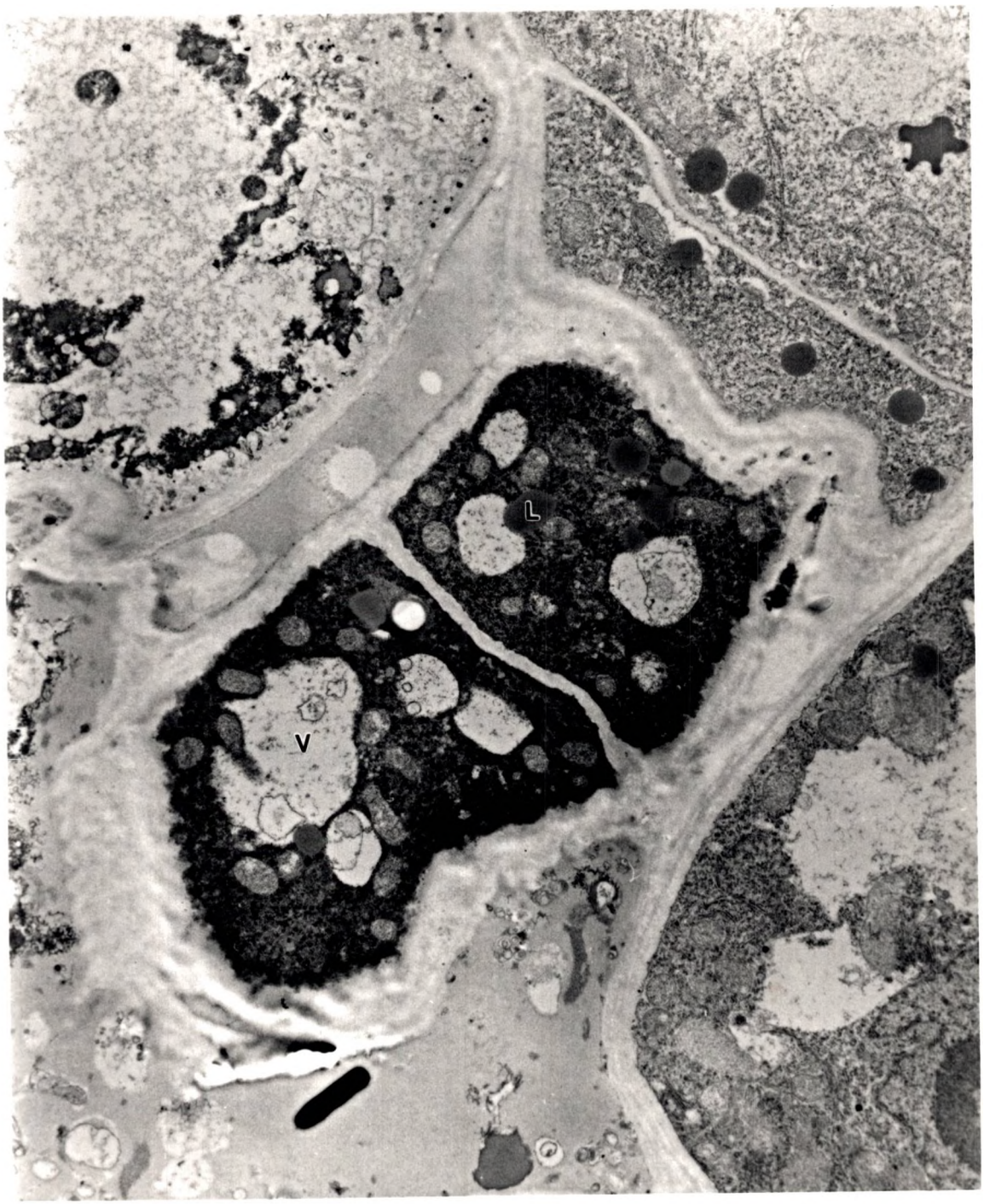
L
V

Discussion

Normal maize embryogenesis was examined using morphological and histological techniques. The role of the normal *dek23* gene in embryo development was assessed by comparison of mutant *dek23* embryos with normal embryos.

The first observable effect of the mutant *dek23* allele on embryogenesis was a delay in the normal timing of morphological events that give rise to the fully formed maize embryo. This delay became obvious at 9 dap, when normal embryos reached the coleoptilar stage and mutant embryos lagged in the transition stage (Figure 2). No abnormality other than the delay was detected in mutant embryos at 9 dap in either fresh dissections (Figure 2) or sectioned material (Figure 5). Electron micrographs of mutant embryos in the late transition stage at 9 dap revealed a slightly higher degree of vacuolization in mutant cells at the shoot apical meristem (sam) region (Figure 10), but this may be due to the delay in meristem organization in mutant embryos.

The developmental difference between mutant and normal embryos increased as mutant embryos subsequently did not differentiate normal shoot apical meristems or more than one

leaf primordium. At 14 dap, normal embryos had proceeded to stage 2, but mutant embryos produced only a single abnormal first leaf primordium at most (Figure 6). Previous investigations of the *dek23* mutant failed to note the degree of differentiation observed in this study (Clark and Sheridan 1986), but differing growth conditions and development of an earlier maturing genetic background may have influenced the phenotypic expression of this mutation. Clark and Sheridan (1986) reported no cases of mutant embryos forming a leaf primordium, whereas this study found that many mutant embryos were able to form some type of first leaf primordium.

Mutant embryos at 14 dap displayed some abnormalities at this developmental stage, termed abnormal stage 1. The scutellum was flattened and irregular, and cellular fine structure was altered as well (Figure 12). A higher degree of vacuolization in mutant sam cells along with osmiophilic cytoplasm (Gahan 1981) suggests a degeneration of cells in the shoot apex region in mutant embryos (Figure 13). The nuclei of mutant sam cells were quite large in relationship to the total volume of cytoplasm and had a lobed appearance (Figure 13). Gahan (1981) has observed these features in

cells whose genetic fate was to die. Vacuolization, electron dense cytoplasm, and large and convoluted nuclei may foreshadow the abnormal senescence of these cells that normally would contribute to the shoot apical meristem.

Degeneration of a few mutant cells in the shoot apex region was severe by 17 dap (Figure 15). Necrotic cells were apparent in the shoot apical meristem, and surrounding cells were showing signs of degeneration. Gahan (1981) reported two other features of senescent plant cells, vacuoles containing organelles, and enlarged or distorted plastids. These features were observed in some mutant sam cells (Figure 16), suggesting their pending degeneration. Cells in the sam in normal embryos had begun to accumulate starch in some plastids (Figure 14), and possessed a much greater number of lipid droplets than mutant sam cells.

Degeneration of mutant sam cells was apparent at the light micrographic level as well. Darkly staining areas of necrosis were evident in the shoot apex region (Figure 7), and sometimes along the abaxial side of the scutellum. Degeneration of the shoot apex region was also apparent. Observation of mutant embryos at different ages and developmental stages revealed that, although many mutant

embryos were able to initiate shoot apical meristem formation and one leaf primordium, they were unable to maintain this organization and elaborate on it.

By 22 dap, mutant embryos were in the abnormal flattened scutellum stage and the breakdown of organization in the shoot apex region was severe (Figure 8). Few mutant embryos possessed recognizable shoot apices, most having only a pit or indentation where the meristem should be. Necrosis in this region was prevalent as well, and often it had spread along the embryonic axis (Figure 8). Interestingly, the root meristem remained intact and generally appeared unaffected by necrosis. This supports the suggestion that shoot and root meristem formation or maintenance are separable (Sheridan and Clark 1987), and the normal *dek23* gene product is required only for formation and persistence of the shoot meristem. One embryo (Figure 8) had extensive necrosis emanating from the sunken shoot apex region back through the abaxial surface of the scutellum. The abaxial surface of the scutellum of all mutant embryos was convoluted and morphologically irregular.

A shootless mutation (*dks8*) generated in a stock carrying Robertson's Mutator (*Mu*) transposable element has

been reported by Sollinger and Rivin (1993) and provides additional support for the separate regulation of shoot and root apical meristem formation and maintenance. This mutant lacks a shoot apex, but has a complete scutellum, root meristem, and vascular structure and a normal endosperm. Tests in our lab confirm their finding that *dks8* is not allelic to *dek23* (data not shown).

Observation of mature mutant embryos in fresh dissection revealed some embryos with a proliferation of tissue just above where the shoot apex should be (Figure 4). This tissue seems to be derived from the upper portion of the coleoptilar ring. It is possible that failure of the shoot apical meristem to develop normally freed these cells from an inhibitory effect, allowing them to proliferate in an unorganized manner. Conversely, the degeneration of cells at the shoot apex may have released toxins or hormones capable of stimulating undifferentiated growth of nearby cells.

In conclusion, it appears that the *dek23* mutation affects embryogenesis very early, during the transition stage when an embryo is organizing the shoot apical meristem. Lack of the normal *dek23* gene product results in

a developmental delay causing mutant embryos to lag behind normal embryos on the same ear. Mutant embryos have often formed a shoot apical meristem and one leaf primordium by the time corresponding normal embryos have reached stage 2. But the mutant embryos subsequently lose the organization of their sam, and the cells of the shoot apex region undergo necrosis.

The defect caused by the *dek23* mutation is observable at the ultrastructural level. Shoot apex cells of mutant embryos are more highly vacuolated and the cells have larger nuclei with more convoluted nuclear membranes than normal sam cells. At this point there is no indication of necrosis. A proposed regulatory role of *dek23* in embryo development is supported by these ultrastructural observations. Cells that would normally become part of the long lived shoot apical meristem display characteristics of cells programmed to die (Gahan 1981). Many of the sam cells did die in mutant embryos before 22 dap, at the point where normal embryos had reached stage 3.

The sequence of genetic events leading to shoot apical meristem formation and maintenance was disrupted by the *dek23* mutation and this disruption resulted in loss of

organization of the sam and necrosis of many of the cells that would normally continue to divide and differentiate. It is possible that an altered metabolic pathway or missing structural protein could result in this significant shift in cell fate. A defect in a housekeeping gene should result in formation of slightly abnormal leaf primordia or other structures, or possibly the complete failure of any cell division to take place. The mutant embryo phenotype would likely be variable, with some mutant embryos being able to develop to a greater extent than others. The *dek23* mutant embryos are quite uniform in their phenotype, but the extent of necrosis is variable. It is possible that a protein that the *dek23* gene encodes is a shoot-apical-meristem-specific protein involved in cell to cell communication, or for uptake of nutrients. It seems more likely that a cascade of gene action triggered by the normal *dek23* gene product failed to occur, and this failure resulted in an embryo poised at the developmental stage where formation of the shoot apical meristem was about to occur upon receipt of the appropriate signals. It appears that sam cells of mutant *dek23* embryos attempt to form a shoot apical meristem and first leaf primordium, but do so in an abnormal way. The

onset of necrosis appears to be a secondary effect. When mutant sam cells are unable to proceed, a default program of senescence and cell death was initiated.

References

Abbe, E.C., and O.L. Stein, 1954 The growth of the shoot apex in maize: embryogeny. Am. J. Bot. 41:285-293.

Beckett, J.B., 1994 Locating recessive genes to chromosome arm with B-A translocations. Pp. 315-327. In: *The Maize Handbook*. Edited by M. Freeling and V. Walbot. Springer-Verlag, New York.

Clark, J.K., and W.F. Sheridan, 1988 Characterization of the two maize embryo-lethal defective kernel mutants *rgh*-1210* and *fl*-1253B*: effects on embryo and gametophyte development. Genetics 120:279-290.

Clark, J.K., and W.F. Sheridan, 1986 Developmental profiles of the maize embryo-lethal mutants *dek22* and *dek23*. J. Hered. 77:83-92.

Clark, J.K. and W.F. Sheridan, 1991 Isolation and characterization of 511 embryo-specific mutations of maize. The Plant Cell 3:935-951.

Demerec, M., 1923 Heritable characters of maize. XV-Germless seeds. J. Hered. 14:297-300.

Diboll, A.G., 1968 Fine structural development of the megagametophyte of *Zea mays* following fertilization. Am. J. Bot. 55:787-806.

Gahan, P.B., 1981 Cell senescence and death in plants. Pp. 145-169. In: *Cell death in biology and pathology*. Edited by I. D. Bowen and R.A. Lockshin. Chapman and Hall, New York.

Gavazzi, G., M. Nava-Rachi, and C. Tonelli, 1975 A mutation causing proline requirement in maize. Theor. Appl. Genet. 46:339-346.

Jones, D.F., 1920 Heritable characters of maize. IV. A lethal factor-defective seeds. J. Hered. 11:161-167.

Kiesselbach, T.A., 1949 *The Structure and Reproduction of Corn*. Univ. Nebr. Agric. Exp. Stn. Bull. 161:96pp., Lincoln, NB.

Manglesdorf, P.C., 1923 The inheritance of defective seed in maize. J. Hered. 14:119-125.

Manglesdorf, P.C., 1926 The genetics and morphology of some endosperm characters in maize. Conn. Agric. Exp. Stn. Bull. 279:509-614.

Neuffer, M.G., 1982 Mutant induction in maize. Pp. 61-64. In: *Maize for biological research*. Edited by W.F. Sheridan. Plant Molecular Biology Association, Charlottesville, VA.

Neuffer, M.G., and E.H. Coe, Jr., 1978 Paraffin oil technique for treating mature corn pollen with chemical mutagens. Maydica 23:21-28.

Neuffer, M.G., and W.F. Sheridan, 1980 Defective kernel mutants of maize. I. Genetic and lethality studies. Genetics 95:929-944.

Neuffer, M.G., M.T. Chang, J.K. Clark, and W.F. Sheridan, 1986 The genetic control of maize kernel development. Pp. 35-50. In: *Regulation of Carbon and Nitrogen Reduction and Utilization in Maize*. Edited by J.C. Shannon, D.P. Knievel and C.D. Boyer. American Society of Plant Physiologists, Rockville, MD.

Randolph, L.F., 1936 Developmental morphology of the caryopsis in maize. J. Agric. Res. 53:881-916.

Salamini, F., and C. Soave, 1982 Zein: genetics and biochemistry. Pp. 155-160. In: *Maize for biological research*. Edited by W.F. Sheridan. Plant Molecular Biology Association, Charlottesville, VA.

Sass, J.E., 1977 Morphology. Pp. 89-110. In: *Corn and corn improvement*. Edited by G.F. Sprague. American Society of Agronomy, Inc., Madison, WI.

Sass, J E., and G.R. Sprague, 1950 The embryology of "germless" maize. Iowa State College Journal of Science 24:209-218.

Scanlon, M.J., P.S. Stinard, M.G. James, A.M. Myers, and D.S. Robertson, 1994 Genetic analysis of sixty-three mutations affecting maize kernel development isolated from *Mutator* stocks. Genetics 136:281-294.

Schel, J.H.N., H. Kieft, and A.A.M. Van Lammeren, 1984 Interactions between embryo and endosperm during early developmental stages of maize caryopses (*Zea mays*). Can. J. Bot. 62:2842-2853.

Sheridan, W.F., 1988 Maize developmental genetics: genes of morphogenesis. Ann. Rev. Genet. 22:353-385.

Sheridan, W.F., and J.K. Clark, 1987 Maize embryogeny: a promising experimental system. Trends Genet. 3:3-6.

Sheridan, W.F. and J.K Clark, 1993 Mutational analysis of morphogenesis of the maize embryo. The Plant Journal 3:347-358.

Sheridan, W.F., and J.K. Clark, 1994 Fertilization and embryogeny in maize. Pp. 3-10. In: *The Maize Handbook*. Edited by M. Freeling and V. Walbot. Springer-Verlag, New York.

Sheridan W.F., and M.G. Neuffer, 1980 Defective kernel mutants of maize: II. Morphological and embryo culture studies. Genetics 95:945-960.

Sheridan, W.F., and M.G. Neuffer, 1981 Maize mutants altered in embryo development. Pp. 137-156. In: *Levels of genetic control in development*. Edited by S. Subtelney and U. Abbot. Alan R. Liss Inc., New York.

Sheridan, W.F., and M.G. Neuffer, 1982 Maize developmental mutants. Embryos unable to form leaf primordia. J. Hered. 73:318-329.

Sheridan, W.F., and M.G. Neuffer, 1983 Genetic control of embryo and endosperm development in maize. Pp. 105-122. In: *Gene structure and function in higher plants*. Edited by G.M. Reddy and E.H. Coe, Jr. Oxford and IBH Publishing Co., New Delhi, India.

Sheridan, W.F., and Y.R. Thorstenson, 1986 Developmental profiles of three embryo-lethal maize mutants lacking leaf primordia: *ptd*-1130, cp*-1418,* and *bno*-747B*. Dev. Genet. 7:35-49.

Sollinger J.D., and C. Rivin, 1993 dks8, a mutation specifically eliminating shoot formation during embryogenesis. Maize Genet. Coop. Newslett. 67:34-35.

Spurr, A.R., 1969 A low-viscosity epoxy resin embedding medium for electron microscopy. J. Ultrastructural Res. 26:31-43.

Suzuki, D.T., A.J.F. Griffiths, and R.C. Lewontin, 1981 *An introduction to genetic analysis*. Second edition. W.H. Freeman and Co., San Francisco.

Van Lammeren, A.A.M., 1986 Developmental morphology and cytology of the young maize embryo (*Zea mays* L.). Acta Bot. Neerl. 35:169-188.

Wentz, J.B., 1930 The inheritance of germless seeds in maize. Iowa Exp. Stn. Res. Bull. 121:347-379.

Wilson, C.M., 1978 Some biochemical indicators of genetic and developmental controls in endosperm. Pp. 405-422. In: *Maize breeding and genetics*. Edited by D.B. Walden. John Wiley and Sons, New York.

CHAPTER III. GENETICS, TRANSMISSION AND DOSAGE ANALYSES

Introduction

Embryogenesis in plants is believed to be under the control of a sequentially regulated genetic program (Sheridan and Neuffer 1981); expression of this program results in a well defined embryo possessing much of the basic structure and rudimentary organs of the vegetative plant (Sheridan and Clark 1994).

Maize (*Zea mays L.*) is particularly well suited for study of the role of genes in embryogenesis (Sheridan and Clark 1987a) due to its large embryo size, and significant organ and tissue development. Normal maize embryo development has been described in detail (Randolph 1936; Kiesselbach 1949; Abbe and Stein 1954) and a number of mutations affecting both embryo and endosperm development have been described (Neuffer and Sheridan 1980; Clark and Sheridan 1986; Sheridan and Thorstenson 1986; Clark and Sheridan 1988). These *defective kernel* (*dek*) mutations, located on several different chromosome arms, reveal that

many loci are required for normal embryo and endosperm development (Neuffer et al. 1986; Sheridan 1988) and examination of the *dek* mutant phenotypes gives insight into the function of these genes in normal development. Some mutations have been found to affect male gametophyte development as well (Clark and Sheridan 1988) and they serve to demonstrate the pleiotropic nature of all *dek* loci.

The *dek23* mutation on chromosome arm *2L* (Neuffer and Sheridan 1980) exhibits these pleiotropic characteristics. Mutant embryos are blocked at an early stage of development, at the time of shoot apical meristem formation (Clark and Sheridan 1986) and they are unable to germinate when mature or when cultured as young embryos (Sheridan and Neuffer 1980). The mature endosperm is greatly reduced and the kernel has a defective crown (dcr) phenotype (Neuffer and Sheridan 1980).

The *dek23* allele behaves as a Mendelian recessive, but displays aberrant segregation ratios on ears, indicating that it is also expressed in the gametophyte. Stocks carrying translocations between normal A chromosomes and supernumerary B chromosomes are available in maize and provide a powerful tool for the location of genes to

chromosome arm (Beckett 1994) and dosage analysis (Birchler 1994). Nondisjunction of the B centromere at the second pollen mitosis results in the formation of two sperm, one carrying two copies of the A chromosome arm involved in the B-A translocation, and one lacking that arm entirely.

When a plant that is heterozygous for the *dek23* allele and of normal chromosome constitution is crossed as a female by a pollen parent carrying the B-A translocation TB-1Sb-2L4464 carrying the normal allele at the *dek23* locus, then three classes of kernels are produced on the resulting ear. Two classes of nonconcordant kernels (having a genetically different embryo and endosperm) are produced when sperm from pollen grains carrying the B-A translocation fertilize embryo sacs that carry the mutant allele. One class of nonconcordant kernels, with mutant (hypoploid) endosperm and normal (hyperploid) embryos, is produced when the sperm carrying the two B-A chromosomes fertilizes the egg, and the sperm carrying only the A-B chromosome (lacking a B-A chromosome and therefore missing part of the A chromosome) fertilizes the central cell. The other class of nonconcordant kernels has a normal (hyperploid) endosperm and a mutant (hypoploid) embryo and is produced when the two

sperm switch roles. This second class of nonconcordant kernels occurs at just a slightly lower frequency than the first class due to pollen competition (Carlson 1994).

Concordant normal kernels, in which the embryo and endosperm are both phenotypically normal, are commonly produced in two ways. The first situation involves a pollen grain not carrying the B-A translocation landing on a silk, and the sperm from that pollen grain fertilizing both the egg and central cell of the embryo sac. The second situation in which concordant normal kernels are produced involves an embryo sac that does not carry the *dek23* allele. Fertilization of the egg and central cell will result in a phenotypically normal embryo and endosperm, regardless of which sperm participates in the fertilization.

Self pollinated ears that are heterozygous for the *dek23* allele produce concordant mutant kernels with mutant embryos containing two doses of the mutant *dek23* allele and a mutant endosperm. Heterofertilization can produce nonconcordant kernels with mutant embryos containing two doses of the *dek23* allele on a normal endosperm. These kernel classes allow comparison of the phenotype of a genetically mutant embryo when associated in a kernel with

either a normal or a mutant endosperm, thereby revealing the cell autonomy of the *dek23* gene product (Clark and Sheridan 1986). By comparing the effect of dosage of the mutant allele on the severity of phenotype it can be classified as an amorph (null allele) or hypomorph (partial loss of function) as described by Muller (1932).

This study reports on mapping of the *dek23* locus with known markers on chromosome 2, confirmation of dosage analysis of the *dek23* allele (Clark and Sheridan 1986), as well as sexual transmission and mutant kernel distribution studies to demonstrate the male gametophyte expression of this gene. Its specific effect on embryogenesis and role in endosperm development indicate that it is an essential gene for normal development in these different tissues.

Materials and Methods

Stocks: Linkage marker stocks were originally obtained from the Maize Genetics Cooperation Stock Center at the University of Illinois at Champaign-Urbana and from M.G. Neuffer at the University of Missouri, Columbia. Many of the markers as well as mutant *dek23* stocks were from non-inbred genetic stocks maintained in our laboratory.

Viable homozygous markers used included *virescent4* (*v4*), which results in a yellowish seedling that turns green and produces a fertile plant, and *white tip1* (*wt1*) which produces a green seedling in which the first leaf has a white distal margin.

Other marker stocks and the mutant *dek23* stocks were maintained as heterozygotes since these mutations are recessive lethals. The *white3* (*w3*) locus produces a lemon-white kernel which often displays vivipary, and when germinated, produces an albino seedling that dies shortly after emergence. Mutant *dek23* kernels produce nonviable embryos lacking a shoot apical meristem. The dominant marker *chocolate* (*Ch*) causes a brownish pigmentation of the maternal pericarp tissue. This marker was generally used in the heterozygous state although a few crosses were made to homozygous *Ch* plants.

Mapping studies: Normal kernels from ears segregating for *dek23* were grown and self-pollinated to confirm the presence of the mutant allele; at the same time pollen was crossed from these plants onto segregating marker plants (see Neuffer 1994 for protocols). The resulting outcross ears were harvested and kernels planted from those for which

the corresponding self-pollinated ear was found to segregate for the mutant phenotype, thereby confirming that the pollen parent of the outcross was heterozygous for the mutant *dek23* allele.

The F1 plants grown from the outcross kernels were also self-pollinated to confirm presence of the *dek23* allele (and the presence of the *w3* allele when appropriate) and usually backcrossed to the original marker. In those cases when the F1 plant was confirmed as carrying the *dek23* allele, backcross kernels were again grown out, scored for seedling traits, and self-pollinated to reveal the presence of *dek23* and *w3*. For three point linkage, the F1 plants were self-pollinated and crossed onto a second marker stock before backcrossing. For the lethal marker *w3*, backcrosses were made onto homozygous normal standard stocks. When the phenotypes of seedlings or kernels were difficult to score, kernels were planted in a sandbench and the resulting seedlings were scored to confirm presence of *w3* and *v4*.

Reduced transmission studies: Transmission of the *dek23* allele through the egg and through the pollen was tested by reciprocal crosses of a normal stock homozygous for all kernel color factors, and a colorless *dek23* stock

(Clark and Sheridan 1988), using the double pollination technique described by Sheridan and Clark (1987b). Colored kernels from the resulting ears were planted and the subsequent plants self-pollinated to uncover the presence of the mutant. The rate of transmission of the *dek23* allele through the egg was determined from the proportion of plants which produced segregating ears in families in which the mutant *dek23* stock had served as the female in the reciprocal crosses. Similarly the rate of transmission of the mutant allele through the pollen was given by the proportion of plants with segregating ears in families wherein the mutant stock served as the pollen parent. Observed versus expected ratios were analyzed using a replicated goodness of fit test utilizing log-likelihood ratios (Sokal and Rohlf 1981). Individual segregating ears of test families were analyzed by assessing the proportion of mutant kernels in the top one third of the ear as compared to the proportion in the bottom one third of the ear (Bianchi and Lorenzoni 1975). An analysis of variance (ANOVA) was carried out using a randomized block design (Sokal and Rohlf 1981).

Dosage studies: Pollen from plants carrying the B-A translocation TB-1Sb-2L4464 was crossed onto heterozygous *dek23* plants. This produced a small percentage of nonconcordant kernels with hyperploid phenotypically normal endosperm and hypoploid mutant embryos containing only one dose of the *dek23* allele. These kernels were compared to heterofertilized kernels (in which sperm from two different pollen grains participate in double fertilization) which occur at a frequency of 1-10% in maize (Sprague 1932), from self-pollinated *dek23* ears. The kernels of interest developed from ovules with embryo sacs containing the mutant *dek23* allele. In these kernels a genetically wild type sperm had fertilized the central cell producing a normal triploid endosperm, and a genetically mutant sperm from a different pollen grain carrying the *dek23* allele had joined with the egg cell, producing embryos which carry two doses of the *dek23* allele. Also used were concordant mutant kernels from a segregating self pollinated ear in which the mutant embryos contain two doses of the mutant allele and the triploid endosperm is also mutant. These mature kernels were soaked on moist filter paper for 36 hours and dissected

and photographed using a Wild M400 Photomacroscope and Kodak Gold 100 color print film.

Results

Two point linkage: The *dek23* locus has previously been located to chromosome arm *2L* (Neuffer and Sheridan 1980) and is uncovered by the B-A translocations TB-1Sb-2L4464 and TB-1Sb-2Lc, both of which have breakpoints on chromosome arm *2L* near *v4* (Rakha and Robertson 1970). Crosses between *dek23* and *wt* (on *2S*) show no linkage (Table 3). Linkage of *dek23* with *v4* indicated a map distance of 36.2 map units (m.u.) between loci (Table 4). A similar distance of 39.7 m.u. between *dek23* and *Ch* was also found (Table 5). Tighter linkage was observed with *w3*, a map distance of 21.9 m.u. was found between these two loci (Table 6). These data suggest a slight increase of the current map distances between *v4*, *w3*, and *Ch*, (Figure 20), but are otherwise consistent with published gene order and relative distances.

Table 3. Two point linkage of *wt* and *dek23*

	Parentals		Recombinants		
Ear	wt +	+ dek23	+ +	wt dek23	% Recombination
K 286	35	38	39	18	57/130 = 43.85%
K 287	26	27	37	21	58/111 = 52.25%
L 212	14	36	10	60	70/120 = 58.30%
Pooled	75	101	86	99	185/361 Recomb. = 51.24 %

Table 4. Two point linkage of *v4* and *dek23*

	Parentals		Recombinants		
Ear	v4 +	+ dek23	+ +	v4 dek23	% Recombination
K 278	36	34	28	9	37/107 = 34.58%
K 279	32	29	16	15	31/92 = 33.69%
K 286	37	41	37	15	52/130 = 40.00%
K 287	38	28	25	20	45/111 = 40.54%
L 218	59	26	24	10	34/119 = 28.57%
L 219	21	19	16	13	29/69 = 42.03%
L 222	39	27	23	13	36/102 = 35.29%
Pooled	187	135	107	60	264/730 Recomb. = 36.16%

Table 5. Two point linkage of *Ch* and *dek23*

	Parentals		Recombinants		
Ear	+ Ch	dek23 +	dek23 Ch	+ +	% Recombination
K 284	30	24	9	13	22/76 = 28.95%
K 285	53	42	31	45	76/171 =44.44%
Pooled	83	66	40	58	98/247 Recomb. = 39.68%

Table 6. Two point linkage of *w3* and *dek23*

	Parentals		Recombinants		
Ear	+ w3	dek23 +	dek23 w3	+ +	% Recombination
K 282	64	53	5	19	24/141 = 17.02%
L 217	26	24	2	17	19/69 =27.54%
L 847	29	28	6	14	20/77 = 25.97%
Pooled	119	105	13	50	# Recomb. = 63 Total = 287 Pooled = 21.95%

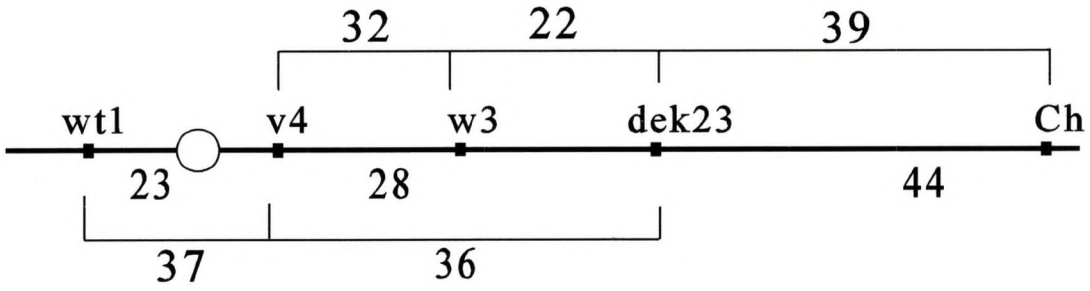

Figure 20. Integration of published map (distances on heavy line) and our linkage data (distances on brackets).

Three point linkage: Three point linkage between *wt*, *v4*, and *dek23* (Table 7) confirm the gene order suggested by B-A translocation crosses, namely that *dek23* is distal to *v4*; crosses by TB-1Sb-2Lc uncover *dek23* but not *v4*. These data also suggest a broadening of the established map. Three point linkage data between *v4*, *w3*, and *dek23* are presented in Tables 8,9,10 and are summarized in Table 11. Family N3740 (Table 10) showed a particularly high frequency of recombination in region II (*w3-dek23*). The small sample size and different coupling/repulsion configuration may have contributed to this finding, and cool wet environmental conditions during that growing season hampered accurate scoring of the dek and *w3* traits. Full maturation of the kernels (and thus color development in the kernel) did not take place, and small, immature normal kernels were difficult to distinguish from mutant kernels. Combined data suggest that *dek23* is located distal to *v4* and *w3*. These data again suggest a slightly larger distance between *v4* and *w3* than the established map. The distance of 21.4 m.u. between *w3* and *dek23* closely matches the two point distance of 21.9 m.u.; the distance of greater than 50 m.u. between

v4 and *dek23* reflects the expansion of map distances which occurs when a third point is introduced.

Table 7. Summary of three point linkage data of *wt v4* and *dek23*

Combined Data	Genotype	Number	Total
a) Parentals	wt v4 +	40	91
	+ + dek23	51	
b) C.O. I wt-v4	wt + dek23	18	53
	+ v4 +	35	
c) C.O. II v4-dek23	wt v4 dek23	21	62
	+ + +	41	
d) C.O. I & II	wt + +	21	35
	+ v4 dek23	14	
			Total = 241
Recombination in Region I		b+d/total	36.51%
Recombination in Region II		c+d/total	40.25%
Recomb. in Regions I+II combined		b+c+(dx2)/total	76.76%

C.O. = cross over

Table 8. Three point linkage of *v4 w3* and *dek23*

Ear M 8679	Genotype			Number	Total
a) Parentals	v4	+	dek23	22	36
	+	w3	+	14	
b) C.O. I v4-w3	v4	w3	+	14	20
	+	+	dek23	6	
c) C.O. II w3-dek23	v4	+	+	3	4
	+	w3	dek23	1	
d) C.O. I & II	v4	w3	dek23	0	1
	+	+	+	1	
					Total = 61
Recombination in Region I				b+d/total	34.43%
Recombination in Region II				c+d/total	8.20%
Recomb. in Regions I+II combined				b+c+(dx2)/total	42.62%

C.O. = cross over

Table 9. Three point linkage of *v4 w3* and *dek23*

Ear M 8680	Genotype			Number	Total
a) Parentals	v4	+	dek23	16	36
	+	w3	+	20	
b) C.O. I v4-w3	v4	w3	+	12	17
	+	+	dek23	5	
c) C.O. II w3-dek23	v4	+	+	8	10
	+	w3	dek23	2	
d) C.O. I & II	v4	w3	dek23	1	3
	+	+	+	2	
					Total = 66
Recombination in Region I				b+d/total	30.30%
Recombination in Region II				c+d/total	19.70%
Recomb. in Regions I+II combined				b+c+(dx2)/total	50.00%

C.O. = cross over

Table 10. Three point linkage of *v4 w3* and *dek23*

Ear N 3740	Genotype			Number	Total
a) Parentals	v4	+	+	10	18
	+	w3	dek23	8	
b) C.O. I v4-w3	v4	w3	dek23	3	9
	+	+	+	6	
c) C.O. II w3 dek23	v4	+	dek23	4	13
	+	w3	+	9	
d) C.O. I & II	v4	w3	+	2	6
	+	+	dek23	4	
					Total = 46
Recombination in Region I				b+d/total	32.61%
Recombination in Region II				c+d/total	41.30%
Recomb. in Regions I+II combined				b+c+(dx2)/total	73.91%

C.O. = cross over

Table 11. Summary of three point linkage data of *v4 w3* and *dek23*

Combined Data	Number	Total
a) Parentals	48 + 42	90
b) C.O. I	29 + 17	46
c) C.O. II	15 + 12	27
d) C.O. I & II	3 + 7	10
		Total =173
Recombination in Region I	b+d/total	0.3237
Recombination in Region II	c+d/total	0.2139
Recomb. in Regions I+II combined	b+c+(dx2)/total	0.5376

Transmission of the mutant *dek23* allele: Deficiency of mutant kernels (Table 13) on self-pollinated ears of heterozygous plants indicated possible expression of the *dek23* mutant allele in the gametophyte resulting in reduced sexual transmission. An average of 15.3% mutant kernels was seen where a frequency of 25% was expected (Table 13).

Rate of transmission through pollen and egg: Transmission of the *dek23* mutant allele through the egg was normal, 49.7% compared to the expected 50% (Table 12). Transmission through the pollen was found to be significantly reduced to 36.8% (Table 12). These rates were found to be significantly different from each other at the P=.001 level (see contingency X^2, Table 12). Because of the reduced transmission of the *dek23* allele through the pollen, the estimate of map distance between the *dek23* locus and marker loci may have been affected. To correct for this possibility, the recombination frequencies were recalculated using half classes. The parental and recombinant classes that contained the mutant *dek23* allele were removed from the calculation. The estimate of the distance between loci was not significantly altered by this recalculation (data not shown).

Distribution of mutant kernels on self-pollinated ears:

Pollen grains carrying the normal allele appear to have fertilized embryo sacs at a higher rate than pollen grains carrying the *dek23* mutant allele. Expression of the mutant allele may affect pollen germination rate or pollen tube growth rate. The difference in observed average percent mutant kernel distribution on the ears between the top one third by length, 17.1%, and bottom one third, 13.8%, (Table 13) and the low correlation coefficient suggest that the reduced transmission rate was due to disturbed pollen tube growth from pollen grains carrying the mutant *dek23* allele. A two-way ANOVA (Table 14) also showed that significant variation in percent mutant kernels was due to location on the ear. Reduced pollen germination should have uniform effects on mutant kernel percentage throughout the ear.

Table 12. Tests of transmission of *dek23* through pollen and egg

Transmission through pollen				Transmission through egg			
Test Family	Total No. ears	%ears seg. dek23	X^2	Test Family	Total No. ears	%ears seg. dek23	X^2
L 5659	37	35.1	3.32	L 5660	31	51.6	0.03
L 5661	37	27.0	8.12**	L 5662	54	55.5	0.67
L 5663	45	31.1	6.58*	L 5664	25	56.0	0.36
L 5665	34	41.2	1.06	L 5666	25	60.0	1.01
M 1749	41	31.7	5.62*	M 1750	32	50.0	0.00
M 1751	43	41.9	1.14	M 1752	53	39.6	2.30
M 1753	32	53.1	0.12	M 1754	63	55.5	0.78
M 1755	36	36.1	2.82	M 1756	34	44.1	0.47
M 1757	42	45.2	0.38	M 1758	48	47.9	0.08
M 1759	19	26.3	4.44*	M 1760	27	37.0	1.83
Total = 366 mean = 36.8% SE = 8.5%				Total = 392 mean = 49.7% SE = 7.6%			

Pollen transmission is expected to be 50%.
Pooled X^2 = 24.415***
Heterogeneity X^2 = 9.188 ns

Egg transmission is expected to be 50%.
Pooled X^2 = 0.010 ns
Heterogeneity X^2 = 7.527 ns

Pollen and egg transmission rate is the same.
Contingency X^2 = 12.209***

ns = not significant, * = P<0.05, ** = P<0.01, *** = P<0.001

Table 13. Segregation in top 1/3 and bottom 1/3 of self pollinated ears of *dek23*

Ear	Top 1/3		Bottom 1/3		Top and Bottom		
	Total kernels	%M[a]	Total kernels	%M[a]	Total kernels	%M[a]	X^2
L5659-32	138	15.2	155	11.6	293	13.3	16.01**
L5659-19	121	13.2	131	16.8	252	15.1	9.92**
L5659-40	128	15.6	135	12.6	263	14.1	12.57**
L5660-16	124	15.3	136	13.2	260	14.2	12.06**
L5660-31	163	16	163	15.3	326	15.6	11.41**
L5660-14	119	14.3	121	12.4	240	13.3	13.07**
L5661-2	140	17.9	167	15.6	307	16.6	8.64**
L5661-36	121	21.5	200	9	321	13.7	16.37**
L5661-24	150	16.7	189	11.6	339	13.9	16.81**
L5662-18	141	8.5	129	11.6	270	10	24.30**
L5662-51	136	19.9	159	8.8	295	13.9	14.54**
L5662-2	129	19.4	161	19.3	290	19.3	3.75
L5663-14	141	12.1	147	15.6	288	13.9	14.22**
L5663-28	169	17.2	173	13.3	342	15.2	13.13**
L5663-47	149	13.4	195	9.7	344	11.3	25.69**
L5664-7	144	16.7	190	10.5	334	13.2	18.68**
L5664-9	156	12.8	182	13.2	338	13	19.41**
L5664-4	159	17	193	11.9	352	14.2	16.41**
L5665-31	165	20	191	11.5	356	15.4	12.99**
L5665-11	142	22.5	166	18.6	308	20.4	2.55
L5665-9	179	25.1	159	22.6	338	24	0.15

Table 13 continued

L5666-9	180	18.3	229	18.3	409	18.3	7.26*
L5666-18	146	17.8	158	13.9	304	15.8	10.32**
L5666-8	120	25	126	14.2	246	19.5	2.96
Total	3460	17.1%[b]	3955	13.8%[b]	7415	15.3%[b]	

Do ears differ from a 3:1 ratio (25% mutant kernels)
Observed ratio (top + bottom) = 15.3% (6.5:1 ratio)
Pooled X^2 = 1038.02*** (23 df)
Heterogeneity X^2 = 25.58 ns

a = percent mutant kernels, b = mean

Table 14. Analysis of variance (ANOVA)

Source of variation	df	SS	MS	F_s
Location on ear	1	134.33	134.33	7.304*[a]
Individuals	23	423.01	18.391	1.98 ns[b]
Remainder	23	213.24	9.27	
Total	47	770.58		

$F_{.05[1,23]}$ = 4.28, $F_{.05[23,23]}$ = 2.02, df=degrees of freedom, SS=sum of squares, MS=mean square, F_s=sample variance ratio, * = P<0.05
a = Location on ear accounts for a significant amount of variance.
b = Individual ears do not account for a significant amount of variance.

Correlation between % mutant kernel segregation top vs.
% segregation bottom r = .33 ns, therefore the % of mutant kernels in the top 1/3 of an ear does not predict the % of mutant kernels in the bottom 1/3 of that ear.

Dosage effects: Dosage of the mutant *dek23* allele appears to have little effect on the size and degree of development of mutant embryos. Embryos carrying one copy versus two copies of the mutant *dek23* allele against a normal endosperm do not appear to differ in their severity of phenotype (Figure 21). Embryos carrying two copies of *dek23* against a mutant endosperm may be slightly larger than embryos carrying one copy of the mutant *dek23* allele, and occasionally exhibit some proliferation of tissue at the region of the coleoptilar ring (Figure 21).

Figure 21. Dissected mature kernels showing mutant embryo phenotype. A&D Concordant mutant kernels from self pollinated ear. Embryo and endosperm were phenotypically mutant, and the embryo carried two doses of *dek23*. Some slight proliferation of tissue from the coleoptilar ring area can be seen in D. B&E Nonconcordant kernels from the B-A translocation cross. Endosperm was phenotypically normal and genetically hyperploid for chromosome arm *2L*. Embryo was mutant in phenotype and genetically hypoploid carrying one dose of *dek23*. C&F Nonconcordant kernels due to heterofertilization. Endosperm was phenotypically normal, mutant embryo was diploid and carried two doses of *dek23*. All kernels were photographed at the same magnification.

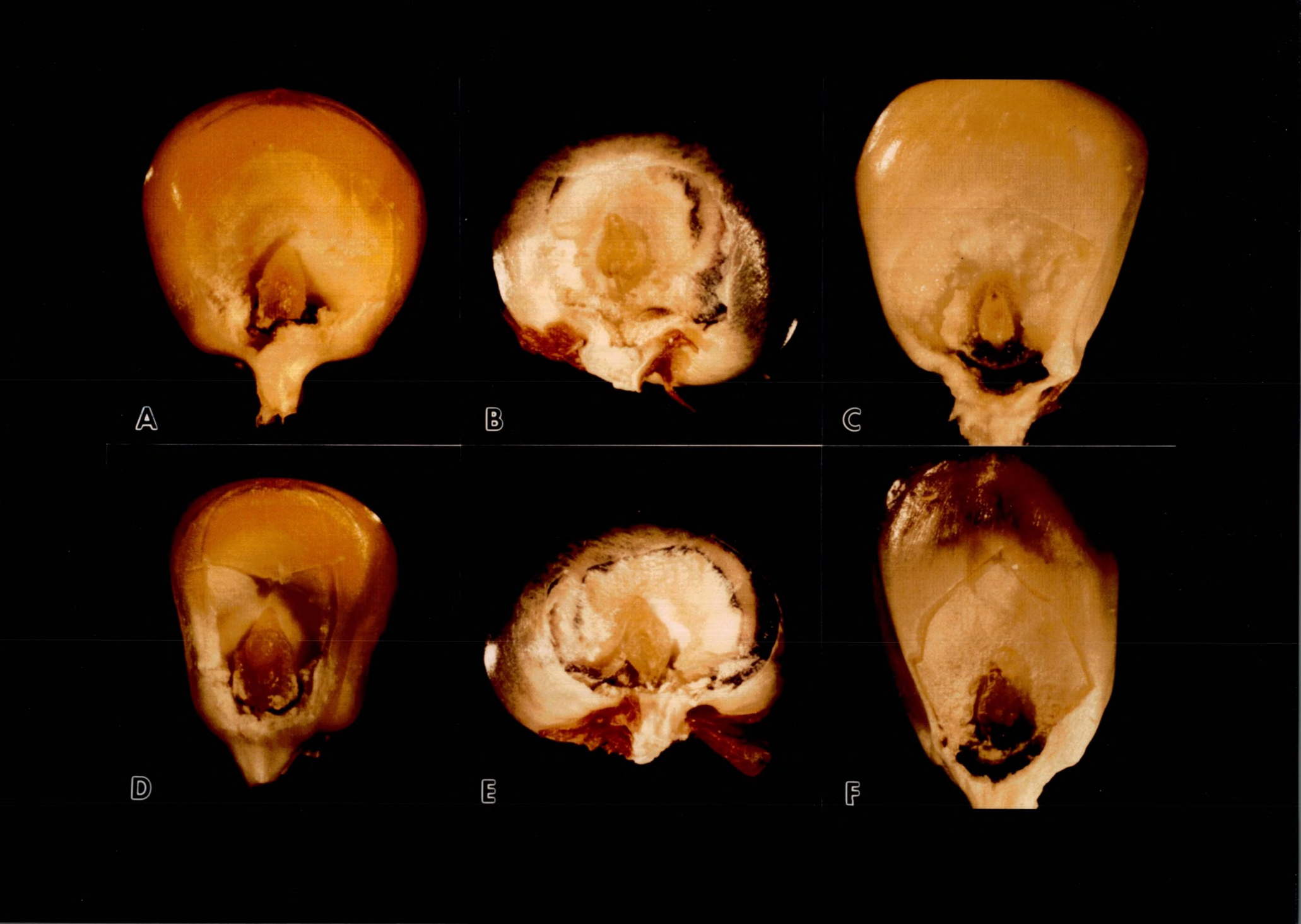
A
B
C
D
E
F

Discussion

The *dek23* locus is located toward the distal end of chromosome arm *2L*, about 22 m.u. distal to *w3* and proximal by 39 m.u. to *Ch*. Use of Haldane's mapping function to correct map distance suggests that these distances are even greater, 28 m.u. and 78 m.u. respectively (Haldane 1919). This large chromosomal region is relatively devoid of known markers, and contains several other loci involved in kernel development (Neuffer et al. 1986; Scanlon et al. 1994).

This mutant affects the embryo, the endosperm, and the gametophyte generation as well. Expression of the mutant *dek23* allele in the male gametophyte reduces sexual transmission of the mutant allele through the pollen. Ten paired reciprocal crosses from which 758 progeny were selfed and screened reveal that transmission of the mutant *dek23* allele through the pollen was about 13% lower than the expected 50% (36.8%, Table 12). Transmission through the egg was not affected.

That a gene which is expressed in the sporophyte, in this case the embryo, was also expressed in the gametophyte should not be surprising. Sari-Gorla et al. (1986) reported that 73% of genes expressed in maize pollen have a

homologous mRNA produced in the sporophyte. Only about 10% of the mRNA present in a pollen grain at anthesis is thought to be unique to the pollen grain (see review by Mascarenhas 1993). This overlap indicates that the organism utilizes many of the same genes in different tissues and in different generations.

From the unequal distribution of mutant kernels along the length of the ear, it can be inferred that a probable mechanism of reduced transmission is disturbed pollen tube growth (Mulcahy and Mulcahy 1987). Similar findings have been reported in *Arabidopsis* (Muller 1963; Meinke 1982) and in maize (Wentz 1930; Clark and Sheridan 1988). If pollen germination was affected, ratios of mutant kernels on the ear should be consistent along the length of the ear (Bianchi and Lorenzoni 1975; Clark and Sheridan 1988). There is the possibility that another closely linked mutation may be the cause of the reduced transmission. A gametophyte factor required for pollen tube growth may have been altered by the ethyl methane sulfonate treatment which presumably produced the *dek23* mutation. Mutations or deletions that include two gene loci are known in maize; these include *a1-x1*, *sh1-bz1-x2*, and *r-x1* and they have been

reviewed by Coe et al. (1988). The *Ga* factors also reviewed by Coe et al. (1988) commonly slow pollen tube growth unless the silk is of the same genotype. If a second factor is involved, recombinants between these loci should be recoverable by screening very large progeny pools. In this study, a large number of segregating ears have been examined and no evidence of recombinants (ears with a 25% ratio of mutant kernels, evenly distributed on the ear) has been discovered, nor have we seen any evidence suggesting that a deletion is responsible.

Dosage analyses reveal that the normal *dek23* gene product is cell autonomous at least to the extent that it cannot rescue mutant embryos via diffusion or transport from normal endosperm. The mutant allele is a classical amorph; one and two dose mutant embryos on a normal endosperm appear to have identical phenotypes. Diploid mutant embryos on a mutant endosperm showed slightly more tissue proliferation and may have a slight physiological advantage in competing with mutant endosperm for nutrients as compared with hypoploid mutant embryos.

The *dek23* mutation appears to have a very specific effect on embryo development in preventing organization and

maintenance of the shoot apical meristem, but not in the formation of the root meristem (Clark and Sheridan 1986). In addition, the normal allele of this locus is required for normal endosperm development and normal rate of pollen tube growth. The position of the *dek23* locus on the genetic map has been determined, thus providing a valuable marker on a chromosome arm otherwise devoid of many known loci.

References

Abbe, E.C., and O.L. Stein, 1954 The growth of the shoot apex in maize: embryogeny. Am. J. Bot. 41:285-293.

Beckett, J.B., 1994 Locating recessive genes to chromosome arm with B-A translocations. Pp. 315-327. In: *The Maize Handbook*. Edited by M. Freeling and V. Walbot. Springer-Verlag, New York.

Bianchi, A., and C. Lorenzoni, 1975 Gametophyte factors in *Zea mays*. pp. 257-263. In: *Gamete Competition in Plants and Animals*, Edited by D.L. Mulcahy. North-Holland, Amsterdam.

Birchler, J.A., 1994 Dosage analysis using B-A translocations. Pp. 328-329. In: *The Maize Handbook*. Edited by M. Freeling and V. Walbot. Springer-Verlag, New York.

Carlson, W.R., 1994 B-A translocation manipulation. Pp. 308-314. In: *The Maize Handbook*. Edited by M. Freeling and V. Walbot. Springer-Verlag, New York.

Clark, J.K., and W.F. Sheridan, 1986 Developmental profiles of the maize embryo-lethal mutants *dek22* and *dek23*. J. Hered. 77:83-92.

Clark, J.K., and W.F. Sheridan, 1988 Characterization of the two maize embryo-lethal defective kernel mutants *rgh*-1210* and *fl*-1253B*: effects on embryo and gametophyte development. Genetics 120:279-290.

Coe, E.H. Jr., M.G. Neuffer, and D.A. Hoisington, 1988 The genetics of corn. Pp. 83-258. In: *Corn and corn improvement,* Ed. 3. Edited by G.F. Sprague, and J.W. Dudley. American Society of Agronomy, Madison, WI.

Haldane, J.B.S., 1919 The probable errors of calculated linkage values and the most accurate method of determining gametic from certain zygotic series. J. Genet. 8:291-297.

Kiesselbach, T.A., 1949 *The Structure and Reproduction of Corn*. Univ. Nebr. Agric. Exp. Stn. Bull. 161:96pp., Lincoln, NB.

Mascarenhas, J.P., 1993 Molecular mechanisms of pollen tube growth and differentiation. The Plant Cell 5:1303-1314.

Meinke, D.W., 1982 Embryo-lethal mutants of *Arabidopsis thaliana*: evidence for gametophytic expression of the mutant genes. Theor. Appl. Genet. 63:281.

Mulcahy, D.L., and G.B. Mulcahy, 1987 The effects of pollen competition. Am. Sci. 75:44-50.

Muller, A.J., 1963 Embryonentest zum Nachweis rezessiver Letalfaktoren bei *Arabidopsis thaliana*. Biol. Zentralbl. 82:133-163.

Muller, H.J., 1932 Further studies on the nature and causes of gene mutations. Proc. Int. Cong. Genet. 6th 1:213-255.

Neuffer, M.G., 1994 Growing maize for genetic studies. Pp. 197-208. In: *The Maize Handbook*. Edited by M. Freeling and V. Walbot. Springer-Verlag, New York.

Neuffer, M.G., and W.F. Sheridan, 1980 Defective kernel mutants of maize. I. Genetic and lethality studies. Genetics 95:929-944.

Neuffer, M.G., M.T. Chang, J.K. Clark, and W.F. Sheridan, 1986 The genetic control of maize kernel development. Pp. 35-50. In: *Regulation of Carbon and Nitrogen Reduction and Utilization in Maize*. Edited by J.C. Shannon, D.P. Knievel and C.D. Boyer. American Society of Plant Physiologists, Rockville, MD.

Rakha, F.A., and D.S. Robertson 1970 A new technique for the production of A-B translocations and their use in genetic analysis. Genetics 65:223-240.

Randolph, L.F., 1936 Developmental morphology of the caryopsis in maize. J. Agric. Res. 53:881-916.

Sari-Gorla, M.C., C. Frova, and E. Redaelli, 1986 Extent of gene expression at the gametophytic phase in maize. Pp. 26-38. In: *Biotechnology and Ecology of Pollen*. Edited by D.L. Mulcahy, G.B. Mulcahy, and E. Ottaviano. Springer-Verlag, New York.

Scanlon, M.J., P.S. Stinard, M.G. James, A.M. Myers, and D.S. Robertson, 1994 Genetic analysis of sixty-three mutations affecting maize kernel development isolated from *Mutator* stocks. Genetics 136:281-294.

Sheridan, W.F., 1988 Maize developmental genetics: genes of morphogenesis. Ann. Rev. Genet. 22:353-385.

Sheridan, W.F., and J.K. Clark, 1987a Maize embryogeny: a promising experimental system. Trends Genet. 3:3-6.

Sheridan, W.F., and J.K. Clark, 1987b Allelism testing by double pollination of lethal maize *dek* mutants. J. Hered. 78:49-50.

Sheridan, W.F., and J.K. Clark, 1994 Fertilization and embryogeny in maize. pp. 3-10. In: *The Maize Handbook*. Edited by M. Freeling and V. Walbot. Springer-Verlag, New York.

Sheridan W.F., and M.G. Neuffer, 1980 Defective kernel mutants of maize: II. Morphological and embryo culture studies. Genetics 95:945-960.

Sheridan, W.F., and Y.R. Thorstenson, 1986 Developmental profiles of three embryo-lethal maize mutants lacking leaf primordia: *ptd*-1130, cp*-1418,* and *bno*-747B*. Dev. Genet. 7:35-49.

Sokal, R.R., and F.J. Rohlf, 1981 *Biometry*, Ed. 2. W.H. Freeman, San Francisco.

Sprague, G.F., 1932 The nature and extent of heterofertilization in maize. Genetics 17:358-368.

Wentz, J.B. 1930 The inheritance of germless seeds in maize. Iowa Exp. Stn. Res. Bull. 121:347-379.

CHAPTER IV. NORMAL MAIZE EMBRYOGENY: ANALYSIS OF TWO-DIMENSIONAL PROTEIN PATTERNS OF MAIZE EMBRYOS FROM THE TRANSITION STAGE THROUGH KERNEL MATURITY.

Introduction

The morphological features of maize (*Zea mays* L.) embryo development have been well characterized (Randolph 1936; Abbe and Stein 1954) but the molecular processes underlying embryogenesis are not well understood.

Two-dimensional electrophoresis is a powerful tool (O'Farrell 1975) that has been used to visualize a large number of the polypeptides synthesized and stored in maize (Sanchez de Jimenez and Aguilar 1984; Sanchez-Martinez et al. 1986; Boothe and Walden 1989), and other plants (Sung and Okimoto 1983; Aspart et al. 1984; Galau et al. 1987; Gottlieb and de Vienne 1988; Stabel et al. 1990). Two-dimensional electrophoresis has been utilized to detect variation between populations (Zivy et al. 1983; Damerval et al. 1986; Damerval et al. 1987), to identify tissue and organ specific patterns of protein synthesis (Sachs et al. 1980; Harrison and Black 1982; Zivy et al. 1984; Leonardi et

al. 1988), and to observe the effect of a single gene mutation or a single allele substitution on normal patterns of protein expression (Gottlieb and de Vienne 1988; Fearn and LaRue 1990; Rivin and Grudt 1991).

Several comprehensive analyses of mouse embryogenesis using 2-D electrophoresis have been performed. Cullen et al. (1980) isolated radioactively labelled proteins from unfertilized eggs and from embryos up through the tenth day of gestation. They were able to identify the putative onset of zygotic mRNA translation between the second and third day of gestation. Nieder (1989) noted significant differences in secreted proteins produced by blastocysts when they were incubated *in vivo* and *in vitro*. Latham et al. (1991) established a computerized database of protein patterns of early stages of mouse embryogenesis and was able to demonstrate a significant quantitative change in spots during the switch from maternal to zygotic mRNA translation. Latham et al. (1993) described specific pattern changes that occurred during the differentiation of the primitive germ layers in mouse embryos.

Two-dimensional studies on plant embryogenesis have focused on somatic embryogenesis in carrot (Schnall et al.

1991), and in *Trifolium* (McGee et al. 1989). Early studies in maize were concerned primarily with the proteins synthesized during germination of mature embryos (Sanchez de Jimenez et al. 1984; Higginbotham et al. 1991) or the effects of premature desiccation and subsequent germination of embryos (Oishi and Bewley 1992). The only comprehensive 2-D gel analysis of early embryonic stages of maize covered the ages from 20 days after pollination (dap), which probably coincides with stage 2 or 3, to maturity and the period from 2-8 hours after imbibition (Sanchez-Martinez et al. 1986). Boothe and Walden (1989) examined protein patterns of embryos from 15-52 dap, covering stages 1 to 6, but they did not look at individual spot differences. Instead, they assessed abundance of spots in 16 regions on the gels, and used multivariate statistical analyses to estimate genotypic variation between inbred lines. This effectively lowered the number of variables in each sample from several hundred spots to 16 numeric scores given to the regions in the grid. This greatly underestimates the variation present, and virtually ignores the contribution of individual spots. In none of these studies did the

investigators report the developmental stage of immature embryos, only their chronological age.

The purpose of this study was to describe some of the molecular events taking place during normal maize embryogenesis by obtaining protein profiles of embryos at stages of development ranging from the transition stage through stage 5/6. These profiles reveal the changing pattern of proteins produced by genes that are active during embryogenesis. Integration of these protein patterns with stages of morphological differentiation may indicate specific proteins or groups of proteins that are associated with morphological events. Analysis of mutations that alter or block formation of specific morphological structures could be facilitated by identification of a group of proteins that are candidates for affectors or indicators of developmental processes.

In order to further characterize some of the *defective kernel* (*dek*) mutations being studied in our laboratory, we have developed a strategy for obtaining protein profiles of maize embryos at each developmental stage of morphogenesis. These profiles provide a reproducible baseline for comparison with mutant embryo protein profiles in a similar

background, and can be performed more quickly than the methods used by the previously mentioned investigators which involve mRNA isolation and *in vitro* translation, or uptake of radioactive amino acids during protein synthesis *in vivo*. In addition, this study covers the stages of embryogenesis from the transition stage (9-10 dap) through stage 5/6. While a grid system was employed to facilitate comparison of gels, all spots on the gels were used in the analysis. The use of highly sensitive colored silver stain is approximately as sensitive as ^{35}S-methionine labelling of proteins (Dunbar 1987) and provides enhanced resolution of closely grouped protein spots.

Materials and Methods

Stocks: Kernels were grown in the greenhouse from a self-pollinated ear of a genetic stock that was segregating for *dek23*. These kernels produced homozygous normal plants and plants heterozygous for *dek23*. Ears of both types of plants were self-pollinated; normal embryos were collected from ears that did not segregate for *dek23*, and segregating ears were used for subsequent analysis of mutant embryos. This provided an almost identical background to facilitate

comparisons between mutant and normal proteins in the next chapter.

Protein extraction: A portion of an ear was removed and kernels were dissected to expose the developing embryo. Embryos were staged according to the criteria of Abbe and Stein (1954) and collected on ice. Several embryos were pooled for each sample of early stages, 35-50 for transition and coleoptilar stages, 15-25 for stage 1, 2-5 for stage 2, 1-5 for stage 3, and only one embryo was needed per sample for stages 4 and 5/6. Embryos were crushed to a fine powder in liquid nitrogen and placed in 500 µl of boiling buffer which contained 62.5 mM Tris-HCl, pH 6.8, 5% (w/v) sodium dodecyl sulfate (SDS), 5% (v/v) β-mercaptoethanol, and 10% (v/v) glycerol (Hussey et al. 1988). This solution was boiled for 5 minutes to inhibit proteases (Colas des Francs et al. 1985), and then spun in a microfuge at 10,000 x g for 3 minutes to remove cellular debris.

The supernatant was drawn off and was precipitated with 9 volumes of acetone at -20° C for at least two hours. The sample was again spun in a microfuge for 10 minutes and the pellet dried. The precipitate was resuspended in 20 µl

of a lysis buffer containing 20 mM Tris-HCl, pH 7.6, 5mM $MgCl_2$, 10% (v/v) Nonidet P-40, and 50 µg/ml leupeptin to form a thick slurry. To this slurry was added 1 µl each of 2 mg/ml DNase I and 1 mg/ml RNase and the mixture was incubated on ice for 15 minutes. This mixture was then adjusted to 9.5 M urea, and 40 µl of sample buffer containing 2% (v/v) Nonidet P-40, 2% (v/v) ampholytes (Bio Rad Biolyte™), 5% (v/v) β-mercaptoethanol and 9.5 M urea was added, followed by vigorous mixing.

At this point in the extraction a 10 µl aliquot was removed from each 70 µl sample and precipitated with 9 volumes of acetone at -20° C. This precipitate was redissolved in 700 µl of 0.1 N NaOH and used to assay protein concentration, using a standard Lowry assay (Lowry et al. 1951) and read at 750 nm on a Hitachi Model 124 Dual Beam Spectrophotometer. The remaining sample was stored at -80° C until used.

Isoelectric focusing: Isoelectric focusing was carried out in 2 x 120 mm tube gels. Focusing gels were 6.4% T (total acrylamide), 0.4% C (crosslinker, piperizine

diacrylamide) and contained 10% v/v of a 3:1 ratio of ampholytes (3 parts pH 5-7, 1 part pH 3-10). Samples were focused by the method of Dunbar (1987) for 20 hours at 500 volts plus 4 hours at 800 volts for a total of 13,200 volt-hours (Vh). Gels were equilibrated in buffer containing 125 mM Tris-HCl pH 6.8, 2% (w/v) SDS, and 10% (v/v) glycerol plus a small amount of bromophenol blue. Gels were stored at -20° C.

Second dimension: Separation of focused proteins was carried out on a uniform 12.5% polyacrylamide gel (12.5% T, 3.3% C) at pH 8.8. Isoelectric tube gels were thawed and placed horizontally on top of the second dimension slab gel. The tube gels were sealed onto the slab gel with an agarose overlay solution containing 25 mM tris base, 192 mM glycine, 0.1% SDS, and 0.5% agarose. Second dimension gels were 16 x 18 cm wide and 1.5 mm thick and were run at 60 mA per gel constant current for about 5 hours (until the bromophenol blue dye front reached the bottom edge of the gel). Gels were fixed in 50% (v/v) ethanol, 5% (v/v) acetic acid overnight and stained with the colored silver stain Gelcode™ (Pierce) as described by Sammons et al. (1981).

Gels were photographed using Kodak T-max 100 black and white film.

Five to eight independent protein isolates were obtained for each of the embryonic stages of Abbe and Stein (1954) except the transition stage for which only two samples were obtained. Each sample was run at least twice to determine the quality of the sample and to control for run to run variation. Different amounts of total protein were loaded to optimize the resolution of proteins with low or high abundance. Four or more independent samples for each stage were photographed, except the transition stage for which only one sample gave satisfactory results. A total of 85 second dimension gels were run and scored visually for quality of isoelectric focusing, completeness of size separation, and overall quality of staining. Gels were rejected for further analysis if they contained diffuse or poorly separated spots, or if significant defects such as bubbles were present in the gel matrix.

Analysis: Protein patterns were analyzed by establishing a grid framework, based on protein size standards and several landmark spots which appeared on all the gels (Boothe and Walden 1989). This produced a 3

column, 5 rowed grid, which was overlaid each gel and used to facilitate gel to gel comparisons (Figure 22). Rows and columns were given letter and number designations respectively, and the zones delimited will be referred to by those designations below. This grid also assisted in determining gel to gel reproducibility and accuracy in identifying spots in crowded regions of the gel.

One gel for each stage was chosen for comparison to gels of other stages. When differences between gels within a stage were detected, the gel containing the most spots or the most tightly focused spots was chosen as the representative for that stage.

Results

Measurement of wet weight and dry weight of embryos (Table 15) at stages 1 through 5/6 were taken. The data show a steady increase in wet and dry embryo weight, an increase in percentage of dry weight to wet weight, and a decrease in percentage of protein to dry weight.

Table 15. Measurement of embryo weights and percent protein.

Stage	Age	wet weight (mg)	dry weight (mg)	% dry to wet weight	Protein conc. (mg/mg tissue)	Protein % of dry weight
1	14 dap	0.488	0.044	9.0%	0.0087	19.8
1	14 dap	2.200	0.190	8.6%	0.0214	11.3
2	16 dap	3.5518	0.706	10.3%	0.0267	7.4
3	20 dap	16.443	3.712	22.6%	0.0958	2.6
3	23 dap	24.342	6.650	27.3%	0.1625	2.4
4	29 dap	26.540	10.670	40.2%	0.6110	5.7
5/6	44 dap	51.088	23.553	46.1%	0.8950	3.8

Reproducible developmental profiles of normal maize embryogenesis based on 2-D protein patterns were obtained. The methodology employed a rapid extraction of total soluble protein from isolated embryos. Isoelectric focusing and second dimension separation could be completed in two days and non-radioactive detection of spots was rapid (6 hours) and extremely sensitive.

Reproducibility of replicate gels was judged to be very good. Multiple two-dimensional separations of each sample were performed, and comparison of these gels revealed very few differences between them. Occasional flaws in the gel matrix or isoelectric pH gradient were detected, and in these cases the best gel was chosen as representative for that stage. Comparison of gels from different protein samples within an embryo stage did reveal some differences in number of spots present; these differences may be attributable to slightly different chronological ages or physiological variation between plants sampled. The genetic stock used was not isogenic, therefore some heterozygosity was present that may have contributed to these spot differences also. In all cases, the gel with the greatest number of spots within a stage was chosen as representative

for that stage. Other gels were used to confirm the identification of stage specific spots or overall trends in spot patterns, but are not shown here.

Transition stage embryos were the most difficult to isolate due to their small size and fragile consistency. A relatively large number of embryos (35-50) were required to provide an adequate amount of tissue for protein extraction. Gel patterns contained relatively few spots and these stained with low overall intensity (Figure 23) despite the fact that more than 200 µg of protein were loaded, based on Lowry assay results. Several landmark spots were identified and used in comparison with other gels. Two spots produced at high intensity (11 and 12, Figure 23) were found at fairly consistent levels on gels of all seven developmental stages observed. Two other spots, termed early embryonic, were found at their highest level on transition stage gels; they decreased in intensity and disappeared after stage 1. Several other spots were present at low levels.

Coleoptilar stage embryos were relatively easy to isolate and produced a pattern with significantly more and darker spots (Figure 24) than transition stage embryos when

an equal amount (200 µg) of total protein was loaded onto gels. Two stage specific (SS) spots were detected with a relative molecular weights (M_r) of 60 kD and 19 kD. These spots were not detected on earlier or later stage gels, but were found on other coleoptilar stage gels (not shown). A spot near 28 kD was labelled constitutive maturation (CM) because it was found at low levels on almost all gels up to stage 3, after which it increased significantly. Several more spots increased in size and intensity until stage 3 and subsequently decreased or disappeared.

Stage 1 embryo patterns were generated using 100 µg of protein per gel, as were all subsequent stage gels. This method allowed direct comparison among later stage gels, and reduced the overloading of some abundant proteins found in 29 dap and 40 dap gels which. Comparisons made between stage 1 and the coleoptilar stage are qualitatives (presence or absence of spots) as any quantitative (spot intensity) evaluation may not compensate for total protein concentration difference. While some estimate of relative spot intensity can be made, silver staining does not produce a linear change in spot density or intensity (Dunbar 1987).

Despite these limitation, some quantitative differences can be detected. Notably two spots in zone D3 (unlabelled arrows) appear darker in Figure 25 than in Figure 24, indicating a gain in intensity. Also the SS spots seen in coleoptilar stage (Figure 24) are absent in stage 1 (Figure 25).

Stage 2 patterns (Figure 26) exhibit an overall increase in spot intensity from stage 1. A group of spots labelled EM (early maturation) have begun to increase in number and intensity. These may include precursors to the globulin (GLB) proteins that have been reported to appear at about this chronological age (Kriz 1989), although their apparent M_r of 56-57 kD is too small to be GLB 1 (Kriz and Schwartz 1986). Some inbred lines have been reported to have globulin proteins in this size class (Cross and Adams 1983). Spots labelled EE in previous gels have disappeared from stage 2 gels, and spots marked with unlabelled arrows have begun to increase in intensity.

Stage 3 embryo patterns reveal an increase in intensity of spots, as well as a number of unique quantitative and qualitative changes (Figure 27). Three potentially stage specific spots were identified, with M_r of

39.6 kD, 28.8 kD and 27.8 kD. A spot (labelled PC on Figure 27) also appeared to shift toward a more acidic isoelectric point in relation to nearby spots. Spots marked with unlabelled arrows reached their peak intensity at stage 3 and maturation or storage proteins labelled EM (probably globulins) also began to increase. Color-based silver staining revealed an increase of several spots that stain yellow or orange (light spots in Figure 27). These color changes are thought to be due to reaction of the stain with modified side chains, sugars, or lipids on the polypeptides (Sammons et al. 1981).

The pattern of stage 4 embryos was predominated by the increase in basic pI proteins with an M_r between 50 and 70 kD. An acidic group was also present in this size class as well as a smaller M_r group near 28.5 kD (Figure 28). These spots are likely to be members of the globulin protein family as they closely resemble the size and behavior of those proteins as reported by Khavkin et al. (1978), Cross and Adams (1983), Kriz and Schwartz (1986), and Kriz (1989). Also notable was the reduction in intensity of spots marked by unlabelled arrows, which were quite dark at stage 3 (compare Figure 27 and Figure 28).

By stage 5/6 (approximately 40 dap) the accumulation of putative globulins had reached a very high level (Figure 29). Putative globulin subunits of heterogeneous charge but similar M_r were found in the 50-60 kD range and also in the 26-29 kD range. Two potentially stage specific spots were detected, one quite basic with an M_r of 30 kD and one quite acidic at 28 kD. Some of the arrow-marked spots had disappeared, or diminished to the limit of sensitivity of the silver staining.

Proteins that are present at very low levels in a cell, such as transcription factors, have been shown to activate promoters in *in vivo* assays at a concentration of 10,000 molecules per cell (Katagiri and Chua 1992). At this concentration a transcription factor with an M_r of 60 kD would be below the limit of resolution of a silver stained gel. Given an embryo of 1×10^4 cells: 6×10^4 gm/mol ÷ 6×10^{23} molecules/mol = 1×10^{-19} gm/molecule x 10,000 molecules/cell x 1×10^3 cells/embryo = 1×10^{-12} gm/embryo or 1 picogram/embryo. The detection limit of silver staining is reported to be 100 to 500 picograms (Ochs et al. 1981; Gottlieb and de Vienne 1988) therefore all of the protein from at least 100 embryos of this size (stage 1-2)

would have to be loaded on a gel (assuming the protein is present at this level in all cells) in order for that protein to be detectable at the lowest level.

Figure 22. Pattern of 23 dap stage 3 embryo showing grid overlay. Horizontal lines were keyed to molecular weight markers, vertical lines were keyed to specific landmark spots which appeared in all gels (numbered 1,2,3 and 4). This system allowed easy comparison of regions from gel to gel, despite minor differences in isoelectric focusing or size separation.

Figure 23. Pattern of 9 dap transition stage embryos, 200 µg total protein. Gel shows only about 71 spots that can be readily detected. Sixteen landmark spots were identified and four of those (1-4) used to establish grid lines. Spots 11 and 12 appeared to be produced at very consistent levels throughout development. Spots labelled EE (early embryonic) in zone C3 were present from transition through stage 1. Short unlabelled arrows indicate spots which were present at low levels at transition stage, increased to maximum intensity by stage 3, and decreased or disappeared by stage 5/6.

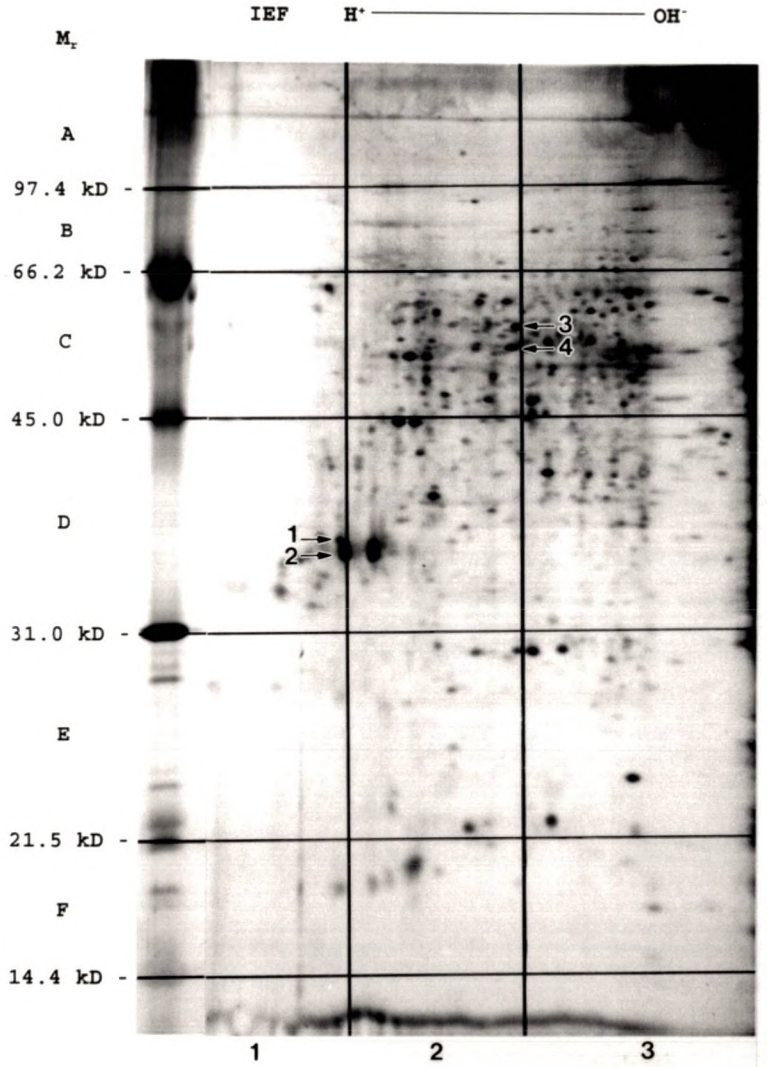

Figure 22

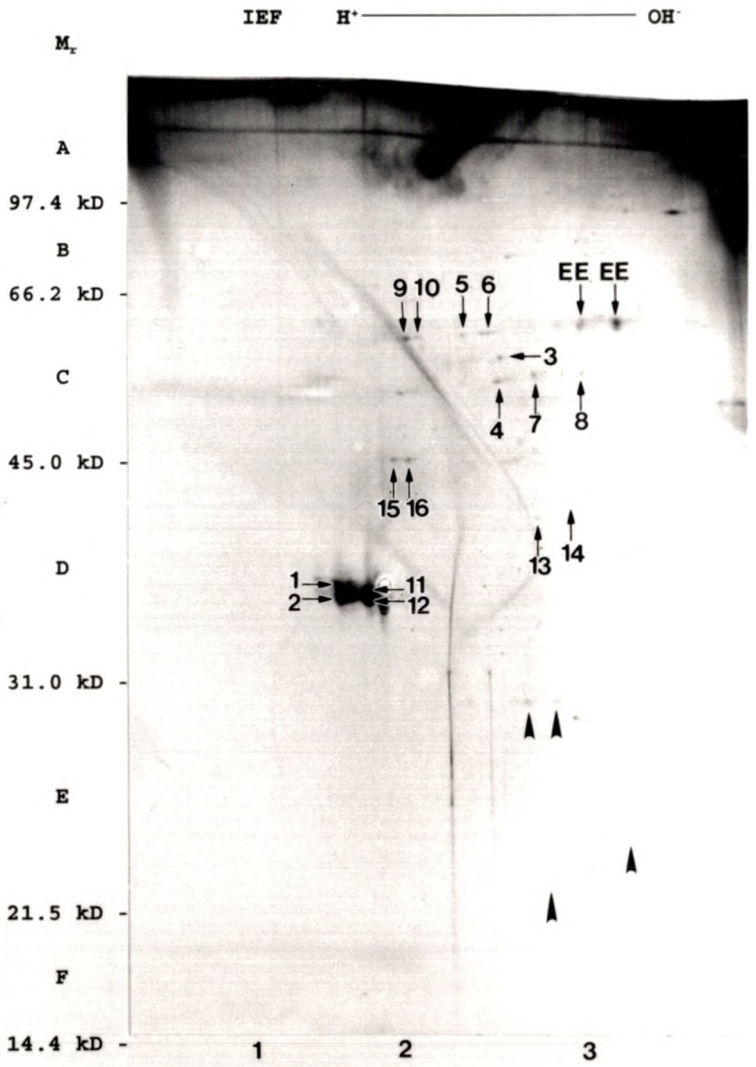

Figure 23

Figure 24. Pattern of 10 dap coleoptilar stage embryos, 200 µg total protein. Arrows labelled SS (stage specific) in zones C3 and F2 appear only on gels of this stage (coleoptilar). Spot labelled CM (constitutive maturation) in zone E2 was present at low levels in coleoptilar, stage 1 (Figure 25), stage 2 (Figure 26) and increased significantly in stage 3 (Figure 27) and later. Unlabelled arrows indicate spots which had peak intensities at stage 3 and subsequently decreased. EE indicates spots which were present through stage 1 but not after.

Figure 25. Pattern of 14 dap stage 1 embryos, 100 µg total protein. Note the absence of stage specific (SS) spots from Figure 24, and the increase in intensity of two spots marked by unlabelled arrows in zone D3. This increase is apparent even though one-half the total amount of protein was used in Figure 25 as compared to Figure 24.

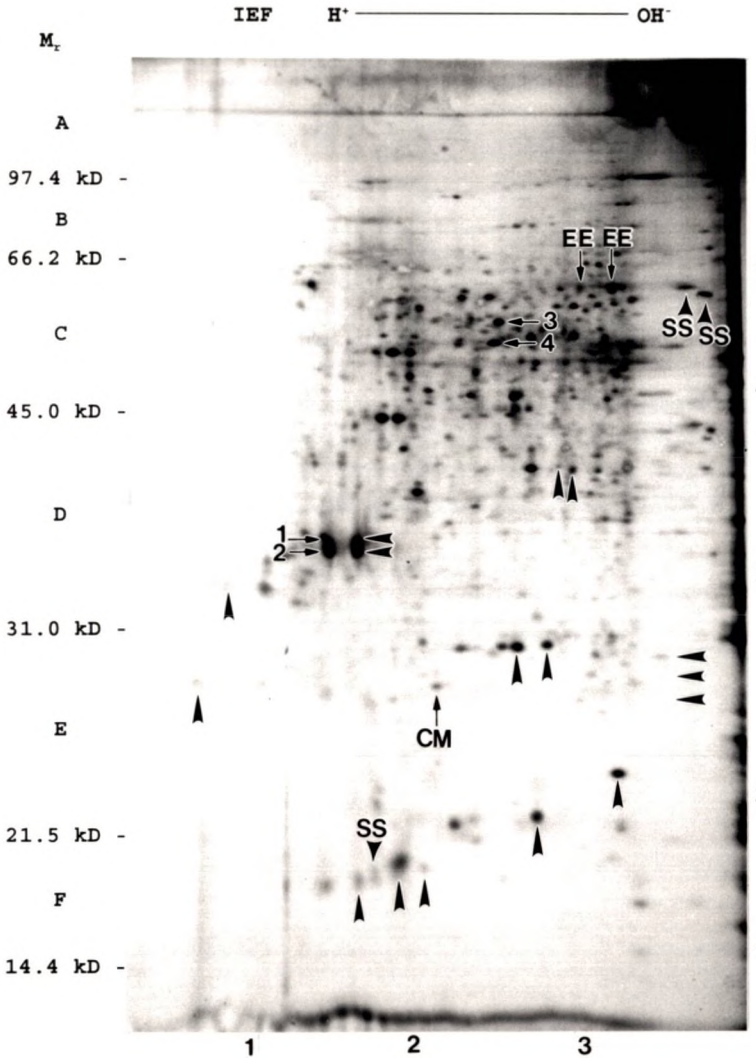

Figure 24

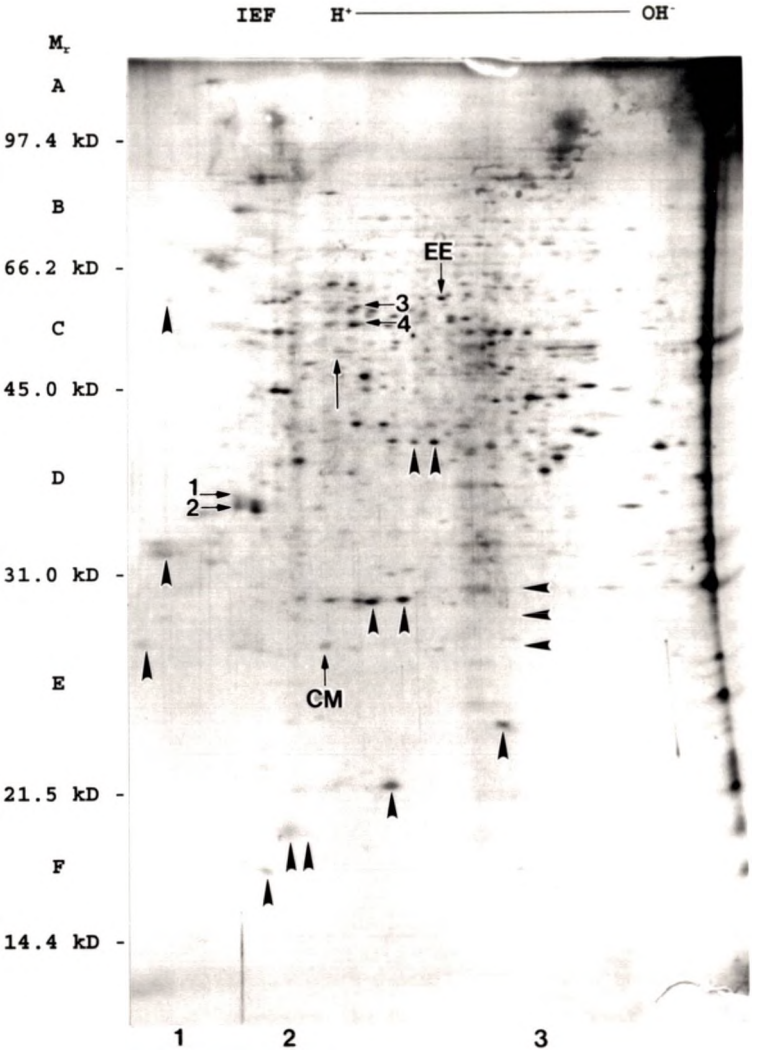

Figure 25

Figure 26. Pattern of 19 dap stage 2 embryos, 100 µg total protein. EE spots were no longer detectable. Several of the spots marked with unlabelled arrows had begun to increase in size and intensity, particularly those having basic isoelectric points. Spots marked EM (early maturation) appeared for the first time at this stage and increase dramatically by stage 5/6 (see Figure 29).

Figure 27. Pattern of 23 dap stage 3 embryos, 100 µg total protein. This stage was marked by significant increase in size and intensity of most spots, notably those marked with unlabelled arrows. Two stage specific (SS) spots were identified with molecular weights of 39.6 and 27.6 kD. The spot labelled CM had increased in intensity over the previous stages. Spots labelled EM had also increased significantly. One spot labelled PC (pI change) was present at a different isoelectric point relative to nearby spots than a similar spot in stage 2 gels. Several spots also showed a color change (light colored spots) due to reaction of the color-based silver stain with charged side groups, sugars, or lipids on polypeptides (Sammons et al. 1981).

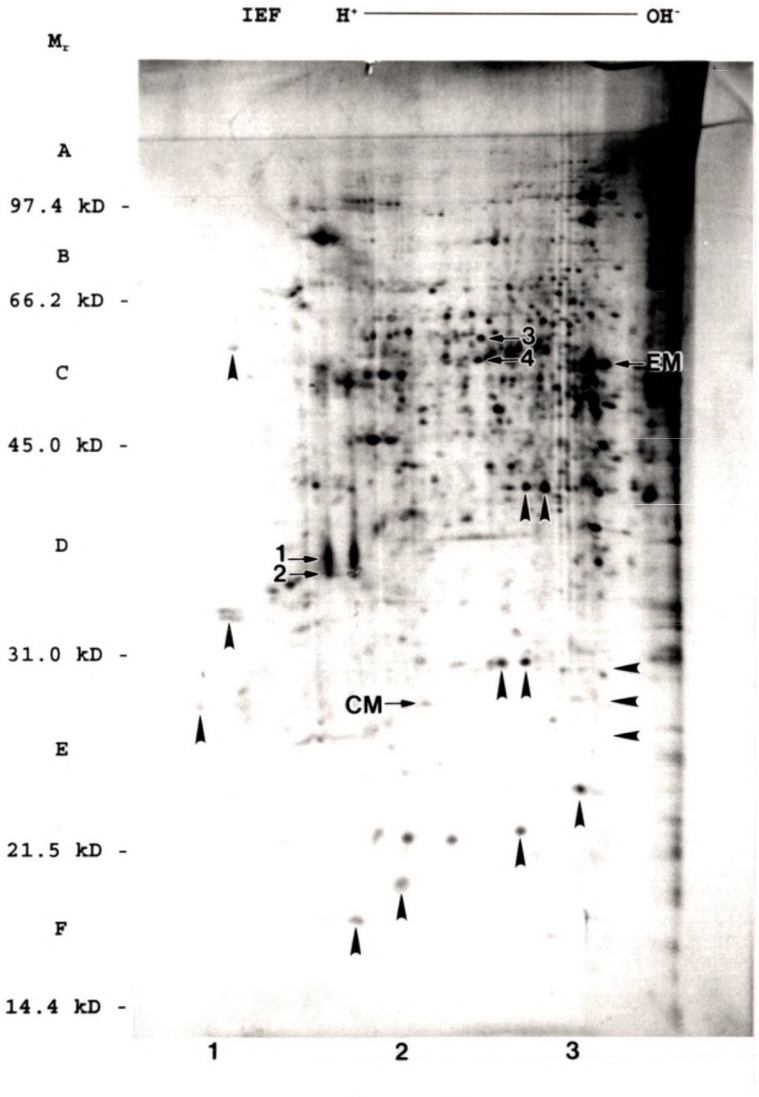

Figure 26

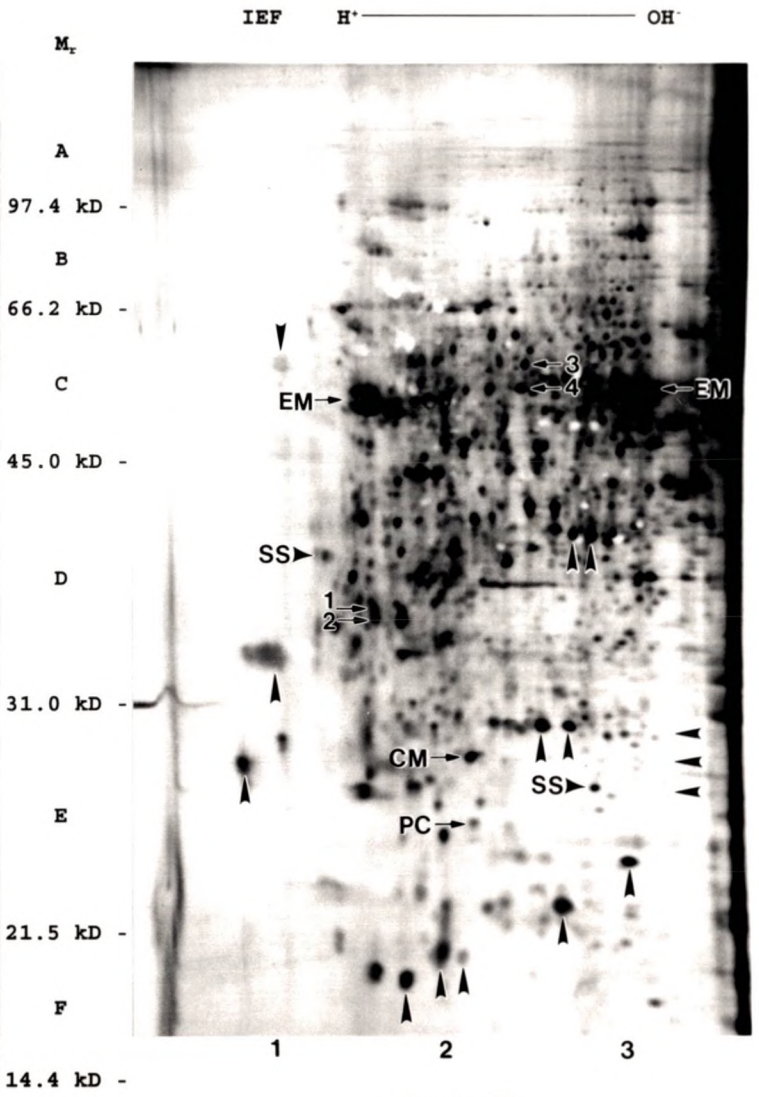

Figure 27

Figure 28. Pattern of 29 dap stage 4 embryos, 100 µg total protein. Spots marked with unlabelled arrows appeared diminished in intensity from the previous profile of stage 3 embryos. The group of spots labelled EM had increased in intensity and new spots had appeared within the group. Spots labelled LM (late maturation) had also appeared in the 65-67 kD range and near 28 kD that were not present in the stage 3 profile (Figure 27).

Figure 29. Pattern of 40 dap embryo stage 5/6, 100 µg total protein. A significant increase in EM, LM and CM spots was evident from the previous stage 4 profile (Figure 28). Potential stage specific (SS) spots were identified with molecular weights at 30.2 kD and 27.8 kD. Spots marked with unlabelled arrows continued to decrease in intensity from the preceding two developmental stages, some disappearing altogether.

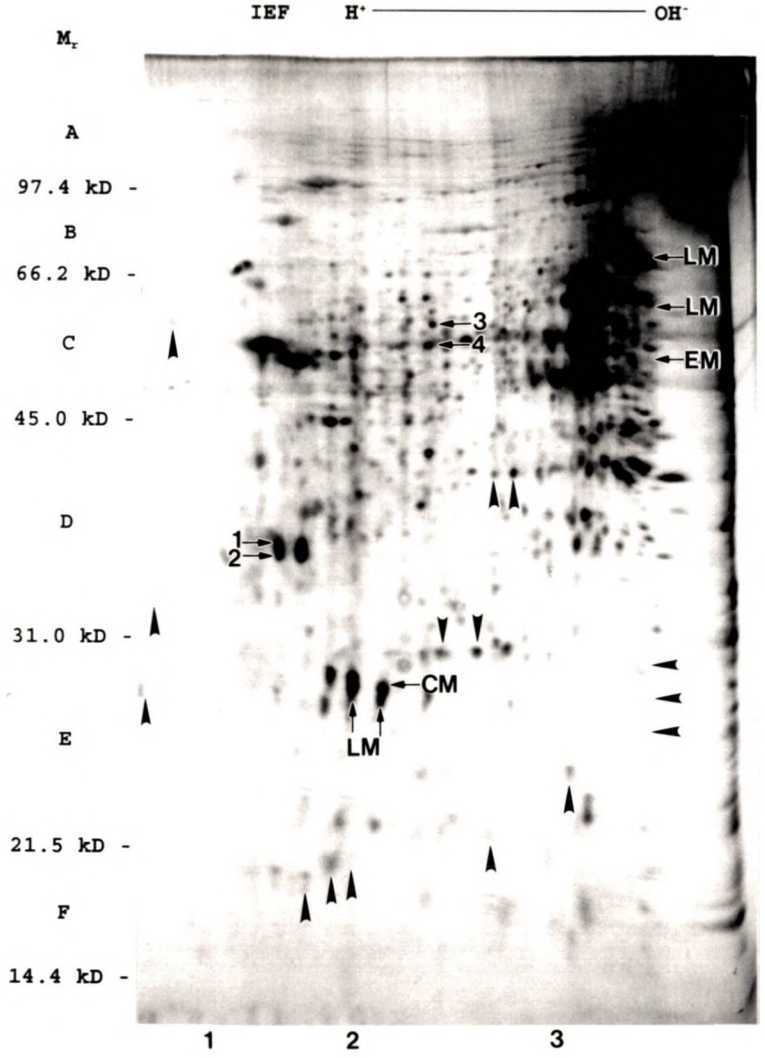

Figure 28

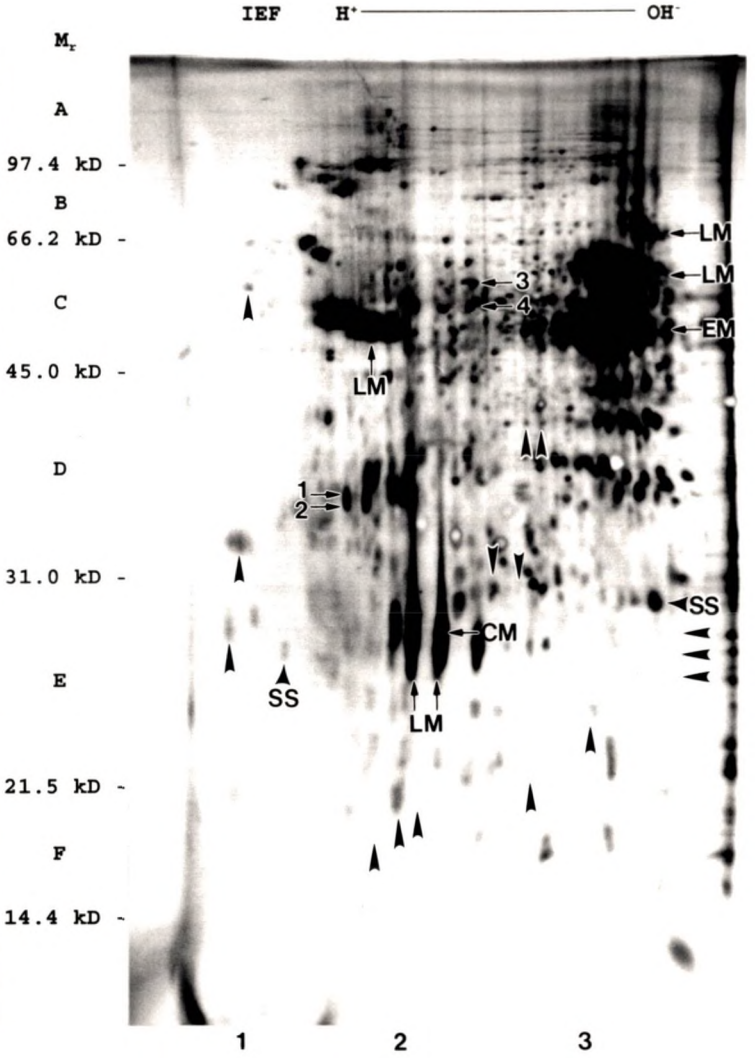

Figure 29

Discussion

Two-dimensional protein patterns produced from developing maize embryos reveal the developmentally regulated program of gene expression that is occurring during embryogenesis. The quantity, timing, and modification of numerous gene products can be observed and comparisons made between developmental stages. Analysis of the protein patterns of normal embryogenesis will provide a baseline for subsequent mutant analysis and identification of genes that are required for normal embryo development.

The protein profiles in this study reveal several interesting features of maize embryo development. Very young transition stage embryos (9-10 dap) exhibit patterns with very few spots as compared to older embryos (Figures 4 and 5). This finding is intriguing since the amount of total protein loaded from transition stage embryos was twice the amount loaded for later stage embryos. These later stage embryos produced patterns with numerous dark spots. One-dimensional analysis did not reveal any observable small polypeptides running off the gel (data not shown), however there is some evidence that many di- or tri-peptides may be

present in very young embryos as a mechanism for maintaining high osmotic potential (W.F. Sheridan pers. comm.).

After the initial stages of embryogenesis, the majority of the spots do not change qualitatively; they are present in gels of most stages. Many of those spots likely represent normal structural and metabolic polypeptides and vary only in the amount present at any given stage as controlled by regulatory elements (Leonardi et al. 1987). They can be used as landmarks for the comparison of other spots that do vary in relative molecular weight or isoelectric point, and some of these landmark spots have been identified in the patterns of all of the stages of embryogenesis examined in this study (see Figure 22).

A few stage specific-spots (SS) have been observed and these can be used to identify specific developmental events or stages. The SS spots in the coleoptilar stage embryos may be related to the switch those embryos were making prior to initiation and proliferation of leaf primordia (Sheridan and Clark 1994). The spots termed early embryonic (EE) were present only in young embryos through stage 1, and also may be involved with processes of organization and differentiation of the shoot and root meristems. They may

not be required after the embryonic axis has been established.

Stage 3 embryos possessed the greatest number of spots at their highest intensity, as well as two SS spots. These embryos were undergoing the transition from rapid cell division and proliferation of leaf primordia, to one of cell expansion, maturation, and preparation for desiccation (Kriz et al. 1990; Rivin and Grudt 1991). One spot was apparently modified in charge, as its apparent pI shifted in relation to nearby spots.

At stage 4, protein patterns showed some reduction in intensity of many spots, but new intensely staining spots appeared at 50-70 kD. These spots, some of which are probably members of the globulin family (Khavkin et al. 1978), are thought to be secondary storage proteins in the embryo and to some degree in the endosperm (Dierks-Ventling and Ventling 1982). They may provide an immediate source of nitrogen for the germinating seedling (Higgins 1984; Kriz 1989).

Stage 5/6 patterns continued the proliferation of putative globulin polypeptides. Some of these proteins in the 26-28 kD range may be subunits of larger globulin

complexes (Kriz 1989). Two possible SS spots may also signal the onset of dormancy as desiccation of the seed proceeds.

While this study made no attempt to specifically identify any particular polypeptides, it was able to identify spots that are specific to some phases or stages of embryo development. The overall profile at any one stage also provides insight into the molecular processes taking place by revealing the amount and timing of gene expression in the embryo.

One of the strengths of this study over previous analyses is the number of replicates assayed. The fairly rapid protein isolation and colored silver staining technique allowed a large number of samples to be analyzed with several replicates of each embryonic stage. Studies involving mRNA isolation, *in vitro* translation, and fluorography or autoradiography of gels are much more time consuming and can limit the number of samples or stages utilized. The large format of gels used in this study also increased the number of data points (spots) observed and provided enhanced resolution of closely spaced spots. The colored silver stain adds an additional method of

identifying closely spaced spots, or spots which have changed position. By silver staining the total protein, degradation of some spots was detected that would not have been detected using radioactive labelling of newly synthesized proteins. By comparing regions of gels using a coordinate system, small changes in spot mobility were detected and no artificial condensation of data was used.

Potential problems with this method were identified as well. Use of total protein staining cannot identify proteins that were synthesized for a short period, and then remained in cells unchanged afterward. These spots could be interpreted as those proteins being produced at a constant level in different developmental stages. No identification of specific proteins by western blotting and antibody binding was attempted. The physiological differences in kernel development among different plants could have been accounted for and plants that varied in size could have been eliminated. Some variation within a developmental stage may have been due to differences in plant health or exact chronological age of the embryos, or due to heterozygosity in the non-inbred genetic stock used in this analysis.

Future 2-D gel analyses of maize embryogenesis might include isolation of stage specific or other interesting proteins from gels. These proteins could be sequenced or used as antigens for antibody production. The resulting antibodies could then be used for identification of these proteins on western blots. Differential dissection of the scutellum away from the embryonic axis can be done easily at later stages of embryogenesis; the differing fates of these tissues should yield differing protein profiles and these differences may identify proteins that correspond to the differing cell fates. Isolation of transition stage and younger embryos and possibly embryo sacs may also provide data on the utilization of maternal mRNA and the switch to zygotic control of protein synthesis, as was demonstrated in the mouse (Cullen et al. 1980).

These baseline data should provide a context for the analysis of mutant embryo proteins. Disturbances in the landmark (Figure 22) or maturation and storage polypeptides should be readily distinguishable, and the profiles of mutant embryos during different developmental stages or chronological ages will provide information about the extent

and timing of gene expression that is taking place, regardless of morphological changes.

References

Abbe, E.C., and O.L. Stein, 1954 The growth of the shoot apex in maize: embryogeny. Am. J. Bot. 41:285-293.

Aspart, L., Y. Meyer, M. Laroche and P. Penon, 1984 Developmental regulation of the synthesis of proteins encoded by stored mRNA in radish embryos. Plant Physiol. 76:664-673.

Boothe, J.G. and D.B. Walden, 1989 Multivariate analyses of polypeptide synthesis in developing maize embryos. Theor. Appl. Genet. 77:495-500.

Colas des Francs, C., H. Thiellement and D. de Vienne, 1985. Analysis of leaf proteins by two-dimensional gel electrophoresis. Protease action as exemplefied by ribulose bisphosphate carboxylase/oxygenase degradation and procedure to avoid proteolysis during extraction. Plant Physiol. 78:178-182.

Cross, J.W. and W.R. Adams Jr., 1983 Embryo-specific globulins from *Zea mays* L. and their subunit composition. J. Agric. Food Chem. 31:534-538.

Cullen, B.R., K. Emigholz, and J.J. Monahan, 1980 Protein patterns of early mouse embryos during development. Differentiation 17:151-160.

Damerval, C., Y. Hebert and D. de Vienne, 1987 Is the polymorphism of protein amounts related to phenotypic variability? A comparison of two-dimensional electrophoresis data with morphological traits in maize. Theor. Appl. Genet. 74:194-202.

Damerval, C., D. de Vienne, M. Zivy and H. Thiellement, 1986 Technical improvements in two-dimensional electrophoresis increase the level of genetic variation detected in wheat-seedling proteins. Electrophoresis 7:52-54.

Dierks-Ventling, C. and D. Ventling, 1982 Tissue specific immunofluorescent localization of zein and globulin in *Zea mays* L. seeds. FEBS Letters 144:167-172.

Dunbar, B.S., 1987 *Two-dimensional electrophoresis and immunological techniques*. Plenum Press, New York.

Fearn, J.C. and T.A. LaRue, 1990 An altered constitutive peptide in *sym5* mutants of *Pisum sativum* L. Plant Mol. Biol. 14:207-216.

Galau G.A., N. Bijaisoradat and D.W. Hughes, 1987 Accumulation kinetics of cotton late embryogenesis-abundant mRNAs and storage protein mRNAs: coordinate regulation during embryogenesis and the role of abscisic acid. Dev. Biol. 123:198-212.

Gottlieb, L.D. and D. de Vienne, 1988 Assessment of pleiotropic effects of a gene substitution in pea by two-dimensional polyacrylamide gel electrophoresis. Genetics 119:705-710.

Harrison, P.A. and C.C Black, 1982 Two-dimensional electrophoretic mapping of proteins of bundle sheath and mesophyll cells of the C4 grass *Digitaria sanguinalis* L. Scop. (Crabgrass). Plant Physiol. 70:1359-1366.

Higginbotham, J.W., J.S.C. Smith and O.S. Smith, 1991 Quantitative analysis of two-dimensional protein profiles of inbred lines of maize *Zea mays* L. Electrophoresis 12:425-431.

Higgins, T.J.V., 1984 Synthesis and regulation of major proteins in seeds. Ann. Rev. Plant Physiol. 35:191-221.

Hussey, P.J., C.W. Lloyd and K. Gull, 1988 Differential and developmental expression of β-tubulins in a higher plant. J. Biol. Chem. 263:5474-5479.

Katagiri, F. and N.-H. Chua, 1992 Plant transcription factors: present knowledge and future challenges. Trends Genet. 8:22-27.

Khavkin, E.E., S.I. Misharin, Y.Y Markov and A.A. Peshkova, 1978 Identification of embryonal antigens of maize: globulins as primary reserve proteins of the embryo. Planta 143:11-20.

Kriz, A.L., M.S. Wallace and R. Paiva, 1990 Globulin gene expression in embryos of maize viviparous mutants. Plant Physiol. 92:538-542.

Kriz, A.L., 1989 Characterization of embryo globulins encoded by the maize *Glb* genes. Biochem. Genet. 27:239-251.

Kriz, A.L. and D. Schwartz, 1986 Synthesis of globulins in maize embryos. Plant Physiol. 82:1069-1075.

Latham, K.E., J.I. Garrels, C. Chang and D. Solter, 1991 Quantitative analysis of protein synthesis in mouse embryos. I. Extensive reprogramming at the one- and two-cell stages. Development 112:921-932.

Latham, K.E., R.S.P. Beddington, D. Solter and J.I. Garrels, 1993 Quantitative analysis of protein synthesis in mouse embryos. II. Differentiation of endoderm mesoderm and ectoderm. Mol. Reprod. Dev. 35:140-150.

Leonardi, A., C. Damerval and D. de Vienne, 1987 Inheritance of protein amounts: comparison of two-dimensional electrophoresis patterns of leaf sheaths of two maize lines (*Zea mays* L.) and their hybrids. Genet. Res. Camb. 50:1-5.

Leonardi, A., C. Damerval and D. de Vienne, 1988 Organ-specific variability and inheritance of maize proteins revealed by two-dimensional electrophoresis. Genet. Res. Camb. 52:97-103.

Lowry, O.H., N.J. Rosenbrough, A.L. Farr and R.J. Randall, 1951 Protein measurement with the Folin phenol reagent. J. Biol. Chem. 193:265-276.

McGee, J.D., E.G. Williams, G.B. Collins and D.F. Hildebrand 1989 Somatic embryogenesis in *Trifolium:* protein profiles associated with high- and low-frequency regeneration. J. Plant. Physiol. 135:306-312.

Nieder, G.L., 1989 Analysis of proteins secreted by mouse embryos developing *in vivo* and *in vitro*. J. Exp. Zool. 252:134-142.

O'Farrell, P.H., 1975 High resolution two-dimensional electrophoresis of proteins. J. Biol. Chem. 250:4007-4021.

Ochs, D.C., E.H. McConkey and D.W. Sammons, 1981 Silver stains for proteins in polyacrylamide gels: A comparison of six methods. Electrophoresis 2:304-307.

Oishi, M.Y. and D. Bewley, 1992 Premature drying, fluridone-treatment, and embryo isolation during development of maize kernels *Zea mays* L. induce germination, but the protein synthetic responses are different. Potential regulation of germination and protein synthesis by abscisic acid. J. Exp. Bot. 43:759-767.

Randolph, L.F., 1936 Developmental morphology of the caryopsis in maize. J. Agric. Res. 53:881-916.

Rivin, C.J. and T. Grudt, 1991 Abscisic acid and the developmental regulation of embryo storage proteins in maize. Plant Physiol. 95:358-365.

Sachs, M.M., M. Freeling and R. Okimoto, 1980 The anaerobic proteins of maize. Cell 20:761-767.

Sammons, D.W., L.D. Adams and E.E. Nishizawa, 1981 Ultrasensitive silver-based color staining of polypeptides in polyacrylamide gels. Electrophoresis 2:135-141.

Sanchez de Jimenez, E. and R. Aguilar, 1984 Protein synthesis patterns. Relevance of old and new messenger RNA in germinating maize embryos. Plant Physiol. 75:231-234.

Sanchez-Martinez, D., P. Puigdomenech and M. Pages, 1986 Regulation of gene expression in developing *Zea mays* embryos. Protein synthesis during embryogenesis and early germination of maize. Plant Physiol. 82:543-549.

Schnall, J.A., C.H. Hwang, T.J. Cooke and J.L. Zimmerman, 1991 An evaluation of gene expression during somatic embryogenesis of two temperature-sensitive carrot variants unable to complete embryo development. Physiol. Plant. 82:498-504.

Sheridan, W.F. and J.K. Clark, 1987 Maize embryogeny: a promising experimental system. Trends in Genet. 3:3-6.

Sheridan, W.F., and J.K. Clark, 1994 Fertilization and embryogeny in maize. Pp. 3-10. In: *The Maize Handbook*. Edited by M. Freeling and V. Walbot. Springer-Verlag, New York.

Stabel, P., T. Eriksson and P. Engstrom, 1990 Changes in protein synthesis upon cytokinin-mediated adventitious bud induction and during seed development in Norway spruce *Picea abies*. Plant Physiol. 92:1174-1183.

Sung, Z.R. and R. Okimoto, 1983 Coordinate gene expression during somatic embryogenesis in carrots. Proc. Nat. Acad. Sci. USA 80:2661-2665.

Zivy, M., H. Thiellement, D. de Vienne and J.-P. Hofmann, 1983 Study on nuclear and cytoplasmic genome expression in wheat by two-dimensional gel electrophoresis. 1.First results on 18 alloplasmic lines. Theor. Appl. Genet. 66:1-7.

Zivy, M., H. Thiellement, D. de Vienne and J.-P. Hofmann, 1984 Study on nuclear and cytoplasmic genome expression in wheat by two-dimensional gel electrophoresis. 2.Genetic differences between two

lines and two groups of cytoplasms at five developmental stages or organs. Theor. Appl. Genet. 68:335-345.

CHAPTER V. THE ROLE OF THE *dek23* GENE IN NORMAL MAIZE EMBRYOGENY: EFFECTS ON PROTEIN PROFILES OF MUTANT EMBRYOS

Introduction

Understanding the role of genes in plant embryo morphogenesis is one of the fundamental questions facing investigators today (Sheridan 1988; Meinke 1991). The analysis of mutations which disrupt genes that are essential for normal embryogenesis will give insight into the mode of action of these genes (Sheridan and Clark 1987; Sheridan 1988).

Over 200 maize (*Zea mays* L.) *dek* mutants have been isolated and characterized genetically and morphologically (Neuffer and Sheridan 1980; Sheridan and Neuffer 1982; Clark and Sheridan 1986; Sheridan and Thorstenson 1986; Clark and Sheridan 1988) and at the molecular level (Scanlon et al. 1994). In addition, 51 *embryo-specific* (*emb*) mutations have been isolated and characterized (Clark and Sheridan 1991; Sheridan and Clark 1993).

A subset of these *dek* mutants, including *dek23*, was chosen for detailed analysis because of morphological

features that suggested they may be regulatory in nature (Sheridan and Neuffer 1982; Sheridan and Clark 1987). The *dek23* mutation has the specific effect of blocking shoot apical meristem and coleoptilar ring formation but not root meristem formation (Clark and Sheridan 1986), indicating that the normal gene product is necessary during phase 2 of embryogeny when the meristems and embryonic axis are established (Sheridan and Clark 1994). Mutant *dek23* embryos are affected quite early in development, 8-10 days after pollination (dap), but produce enough tissue for biochemical analysis.

Previous studies of maize embryo proteins have focused on later stages of embryogenesis, 15-20 dap (around stage 1-2) and later (Sanchez-Martinez et al. 1986; Boothe and Walden 1989; Rivin and Grudt 1991) and early stages of germination (Sanchez de Jimenez and Aguilar 1984). The important early events establishing the embryonic axis and shoot apical meristem occur prior to this time, during the transition and coleoptilar stage. Furthermore, these studies all employed the uptake of radiolabelled amino acids or *in vitro* translation of isolated mRNA and autoradiographic visualization of gels, thus limiting the

number of replicates. This study used two-dimensional gel electrophoresis to analyze the soluble proteins extracted from mutant *dek23* maize embryos and compared their protein patterns with those of their normal counterparts. The use of total soluble protein and colored silver staining of gels allowed for rapid and sensitive visualization of protein patterns from very early stages of embryogenesis, when cell fate is being determined.

Materials and Methods

Protein extraction and two-dimensional electrophoresis were performed as described in the preceding chapter.

Mutant *dek23* embryos are delayed in development as compared to normal embryos on the same ear when the normal embryos enter the coleoptilar stage (Clark and Sheridan 1986). At this point, mutant embryos remain in the transition stage and are unable to form a normal coleoptilar ring or leaf primordia. Since the staging system of Abbe and Stein (1954) uses the formation of the coleoptilar ring and leaf primordia as morphological markers for developmental stages, new criteria have been developed to identify the developmental stages of *dek23* mutant embryos.

At 9 dap, mutant and normal embryos cannot be distinguished from each other in field grown material. At 10-11 dap, mutant embryos are at an abnormal (timing) late transition stage and normal embryos are at the coleoptilar stage. At 15 dap, mutant embryos are at an abnormal coleoptilar stage (they possess only a slight bulge where the coleoptilar ring should form) and normal embryos are at stage 1. At 18 dap, mutant embryos are at an abnormal stage 1, a shoot apical meristem is present and some mutant embryos possess a lower coleoptilar bulge and a small second bulge corresponding to the first leaf primordium. Normal embryos on the same ear are at stage 2. Mutant embryos cease to form recognizable morphological structures at this point so subsequent stages are identified by changes in the scutellum. At 29 dap, the mutant embryo has a broad flat scutellum, and is thus at the flattened scutellum stage. Normal embryos are at stage 4. At 40 dap, many mutant embryos have necrotic regions and are at the degenerative stage while normal embryos are at stage 5/6. These developmental stages will be used in subsequent descriptions of mutant embryos.

Four independent samples of mutant embryo proteins were separated by 2-D electrophoresis for each developmental stage except the abnormal late transition stage. Two independent samples were separated for that stage. A total of 37 second dimension gels were run using mutant embryo proteins. Two replicates were run to assess the reproducibility of the 2-D separation and to control for variation in the pH gradient and gel matrix. When differences between gels within a stage were present, the gel with the most spots or the most tightly focused spots was chosen as representative for that stage. One representative gel from each stage was compared to 2-D patterns of normal embryos at a similar developmental stage.

Results

Two-dimensional gels of mutant *dek23* proteins were prepared from mutant embryos at five unique developmental stages. These gels were compared to each other and to gels containing normal embryo protein patterns of a similar developmental stage.

Protein patterns of mutant embryos at an abnormal late transition stage at 11 dap were most similar to patterns of normal transition stage embryos at 9 dap (Figure 30). A

careful comparison of these two protein profiles reveals that mutant profiles at this stage carried a similar number of reproducible spots (about 88) as the normal transition stage embryos (71 spots). Two of the landmark spots, numbers 7 and 10 in Figure 30 were greatly diminished in the mutant profiles. The remaining landmark spots are present in both profiles at approximately the same intensity and in the same relative position. The normal transition stage profile contains two prominent spots in zone C3 termed early embryonic (EE). These two spots are of the same relative molecular weight (M_r), near 60 kD, but differ in isoelectric point (pI). One of these spots is missing from the mutant abnormal late transition stage profile, the location of the missing spot is labelled ee in Figure 30.

Patterns of mutant embryos at an abnormal coleoptilar stage at 15 dap were most similar to normal coleoptilar stage patterns of embryos at 10 dap in the number and density of their spots (Figure 31). The two EE spots are both present in the normal profile; the mutant profile contains one of these spots (labelled EE in Figure 31) and may contain a very faint spot at the other location (labelled ee in Figure 31). No darkening of the ee spot was

detected in profiles of mutant embryos at later stages.

Landmark spot 10, which was greatly diminished in profiles of abnormal late transition stage mutant embryos, appears to be present at the same level in both abnormal and normal coleoptilar stage profiles in Figure 31. Landmark spot 7 is present at a greatly reduced level in the mutant profile as compared to the normal profile. Landmark spots 13 and 14 in zone D3 both stain a yellow/orange color, which indicates a modification of the protein with sugars or lipids (Sammons et al. 1981). This characteristic coloring of these spots is seen in both the mutant and normal coleoptilar stage profiles, and these spots appear to have the same intensity in the two patterns. Their position relative to other spots on the gel displays some difference between the profiles; spots 13 and 14 have a lower M_r in the mutant abnormal coleoptilar stage profile than in the normal coleoptilar stage profile. It is possible that the spots identified as 13 and 14 in the mutant profile are new proteins that are present, due to the presence of the *dek23* mutant allele. These proteins may be produced from gene loci that are different than the loci that produced spots 13 and 14 in the normal profile. This difference persisted at

subsequent stages of mutant embryo development and is described below. Spots (labelled A and M) in zone E3, exhibit differences between mutant and normal coleoptilar stage profiles. Spot A is actually a pair of closely associated spots near 30 kD. In the mutant profile the two spots are very close together at this location, almost overlapping; in the normal profile the two spots at the same location as A are separated by a greater distance and they stain less intensely than the proteins in the mutant profile. The spot labelled M in Figure 31 is very prominent in the normal coleoptilar stage profile, but is almost undetectable in the mutant abnormal coleoptilar stage profile. This spot does become apparent in the profiles of subsequent stages of mutant embryo development (see Figure 32).

Patterns of abnormal stage 1 mutant embryos at 18 dap were comparable with stage 2 normal embryos at 19 dap. All of the protein profiles of normal stage 2 embryos were produced using 100 µg of total protein to facilitate comparisons between profiles of normal embryo stages. None of the profiles of mutant embryos at an abnormal stage 1

that contained 100 µg of total protein were of acceptable quality. Therefore, Figure 32 is a comparison of a profile containing 200 µg of total protein from abnormal stage 1 mutant embryos with a profile containing 100 µg of total protein from normal stage 2 embryos.

Landmark spot 7 is present at a lower level in the mutant profile as compared to the normal profile (Figure 32). This difference is highlighted by the two-fold difference in total protein content of these profiles; spot 7 appears more abundant in the profile containing less protein.

Some other spots exhibit a similar pattern of lower abundance in the abnormal stage 1 mutant profile than in the normal stage 2 profile. Spots C and D in zone D3 are much less prominent in the mutant profile, as are the group of spots at G. The spots at G are of the appropriate size to be precursors or members of the globulin family of storage proteins. The double spot labelled A is more prominent in the mutant profile than in the normal, but this may be due to the difference in the amount of total protein used. A qualitative difference in this double spot is apparent; the

two components of the double spot are partially overlapping in the mutant profile and are distinctly separated in the normal profile. Again, this might reflect two novel proteins in the mutant profile as compared to the normal profile.

The spots at I stain a bright yellow color in mutant abnormal stage 1 gels, indicating a high degree of posttranslational modification of these proteins with sugars or lipids (Sammons et al. 1981). This yellow staining was not very apparent in normal stage 2 protein profiles. Since light yellow spots are quite prominent in the normal profiles, I believe that the difference in yellow staining is not entirely due to the difference in total protein between the mutant and normal profiles.

The spot labelled M is prominent in the abnormal stage 1 mutant profile. This spot was not detectable in the abnormal coleoptilar stage mutant profile, but it was present in the normal coleoptilar stage profile (Figure 31) at about the same intensity as in the abnormal stage 1 mutant profile (Figure 32). The latter profiles can be compared qualitatively and quantitatively as both contained

200 µg of total protein. Spot M is prominent in the normal stage 2 profile, but its intensity cannot be directly compared to the spots in the coleoptilar stage profiles.

Landmark spots 13 and 14 in zone D3 and spot B in zone C3 all appear to have a slightly lower M_r in the mutant profile as compared to the normal profile.

Profiles of mutant embryos at the flattened scutellum stage at 29 dap were comparable to profiles of normal stage 3 embryos at 23 dap (Figure 33). The spots labelled I are highly modified by sugars or lipids in both mutant and normal profiles at this stage, as indicated by their bright yellow staining. These profiles contained 100 µg of total protein, so approximately equal amounts of these proteins are present in both profiles.

A group of spots at P are prominent in the mutant flattened scutellum stage profile. These spots are not detectable in the normal stage 3 profile, but are present in the normal stage 4 profile (Figure 34). They may be precursors or components of the globulin storage protein family. Landmark spot 7 is present in both mutant and normal profiles at the same relative position and

approximate intensity. A nearby spot labelled W appears to be altered in charge between the mutant flattened scutellum stage profile and the normal stage 3 profile. Alternatively, a new protein with a slightly different pI than W is present in the mutant profile. In the mutant profile, spot W has virtually the same pI as spot 7 and is visible directly above it. In the normal profile, the spot labelled W has a slightly more basic pI than the spot labelled W in the mutant profile and can be observed just to the right of spot 7 (Figure 33).

Landmark spots 13 and 14 have a lower M_r in the mutant profile, a characteristic observed in the previous figures. Another spot that displays a lower M_r in the mutant profile than in the normal profile is spot S. This spot also stains yellow, but appears to have the same staining and intensity in both the mutant and normal profiles. The group of spots labelled G stain at the same intensity in both mutant flattened scutellum stage profiles and normal stage 3 profiles. These spots continue to accumulate in normal profiles and are very abundant in normal stage 4 profiles (Figure 34), but they do not appear at an increased level in later stage mutant profiles (Figure 34).

Three spots exhibit similar behavior between the mutant and normal profiles. Spots H, K, and L are all much more abundant in the normal stage 3 profile than in the mutant flattened scutellum stage profile. Two double spots provide a distinguishing feature between mutant and normal profiles. Spots A and J each appear as a double spot in the mutant profile with both components having the same pI. In the normal profile, the double spots exhibit some charge heterogeneity, the two components are no longer positioned one above the other (Figure 33). It is possible that one or both of the proteins in the mutant profile are novel products and do not correspond directly to spots A and J in the normal profile. Spot M is very prominent in the mutant flattened scutellum stage profile and in the normal stage 3 profile and it appears at approximately equal intensity in both profiles. This spot diminishes in subsequent profiles of mutant and normal embryos (see Figure 34).

The protein profile of mutant embryos at the degenerative stage at 40 dap is comparable to the profile of normal stage 4 embryos at 29 dap (Figure 34). The most striking feature in both of these profiles is the decrease in intensity of most of the spots as compared to the

preceding stage profiles. The normal stage 4 profile does contain some spots that increase in intensity significantly (spots P, G, and X), but most of the other spots in the profile are lower in intensity than in the normal stage 3 profile (Figure 33). A very small group of spots are detectable at P and G in the mutant degenerative stage profile, and no detectable spots are present at position X.

The spots labelled I in these profiles are much less intense than in previous stage profiles and exhibit much less yellow staining than before. Two of these group I spots are not detectable in the mutant degenerative stage or normal stage 4 profile.

Landmark spot 7 is present in both profiles, and spot W, which is closely associated with spot 7, displays a shift to a more basic pI in the normal profile. This shift was observed in profiles of the previous developmental stage (Figure 33). Landmark spots 13 and 14 also exhibit the same pattern of change as in previous profiles. Each spot has a lower M_r in the mutant profile as compared to the normal profile. Spot J is not well resolved in the mutant degenerative stage profile, but it is present at a low level, and it does appear as a double spot in the normal

stage 4 profile. This double spot was present at a higher intensity in the mutant flattened scutellum stage profile and normal stage 3 profile (Figure 33) and appears to follow the trend of reduced intensity in the later developmental stage.

A group of spots at Y provide a distinguishing feature between the mutant degenerative stage and normal stage 4 profiles. Whereas several prominent dark spots are present in the normal profile only a few weak reddish staining spots are present in the mutant profile. Spot Z is also much more prominent in the normal profile than in the mutant profile, but is not as abundant as the putative storage proteins at P, G, and X. Spot M is present in both profiles, but shows a reduction in intensity from the previous developmental stage (Figure 33).

The diagram in Figure 35 summarizes the comparisons of mutant and normal embryo protein profiles in a single pattern. All of the landmark spots are shown, as well as the specific spots which differ between mutant and normal profiles at any given developmental stage. At least twenty individual spots or groups of spots were observed that differ in relative molecular weight, isoelectric point,

amount of posttranslational modification, or relative abundance. These differences were detected at the abnormal late transition stage and at every other stage up through the degenerative stage of mutant embryo development.

Figure 30. Comparison of the protein profile of mutant embryos at an abnormal late transition stage at 11 dap (left) with that of normal transition stage embryos at 9 dap (right). Each profile contains 200 µg of total protein. The mutant embryo profile contains 88 spots which can be reliably detected. The normal profile contains 71 spots. A group of sixteen landmark spots (numbered 1-16 and described in the preceding chapter) were found at all stages of mutant and normal embryogenesis and were used to establish grid lines to aid gel comparisons. Two of those landmark spots, numbers 7 and 10, appear to be present at a lower level in this mutant profile as compared to the normal transition stage embryo profile. The remaining landmark spots appear to be present at approximately the same level and are located at the same relative positions in both profiles. The normal transition stage profile contains two prominent spots labelled EE (early embryonic). The mutant abnormal transition stage profile contains only one of these spots, the location of the missing spot is labelled ee.

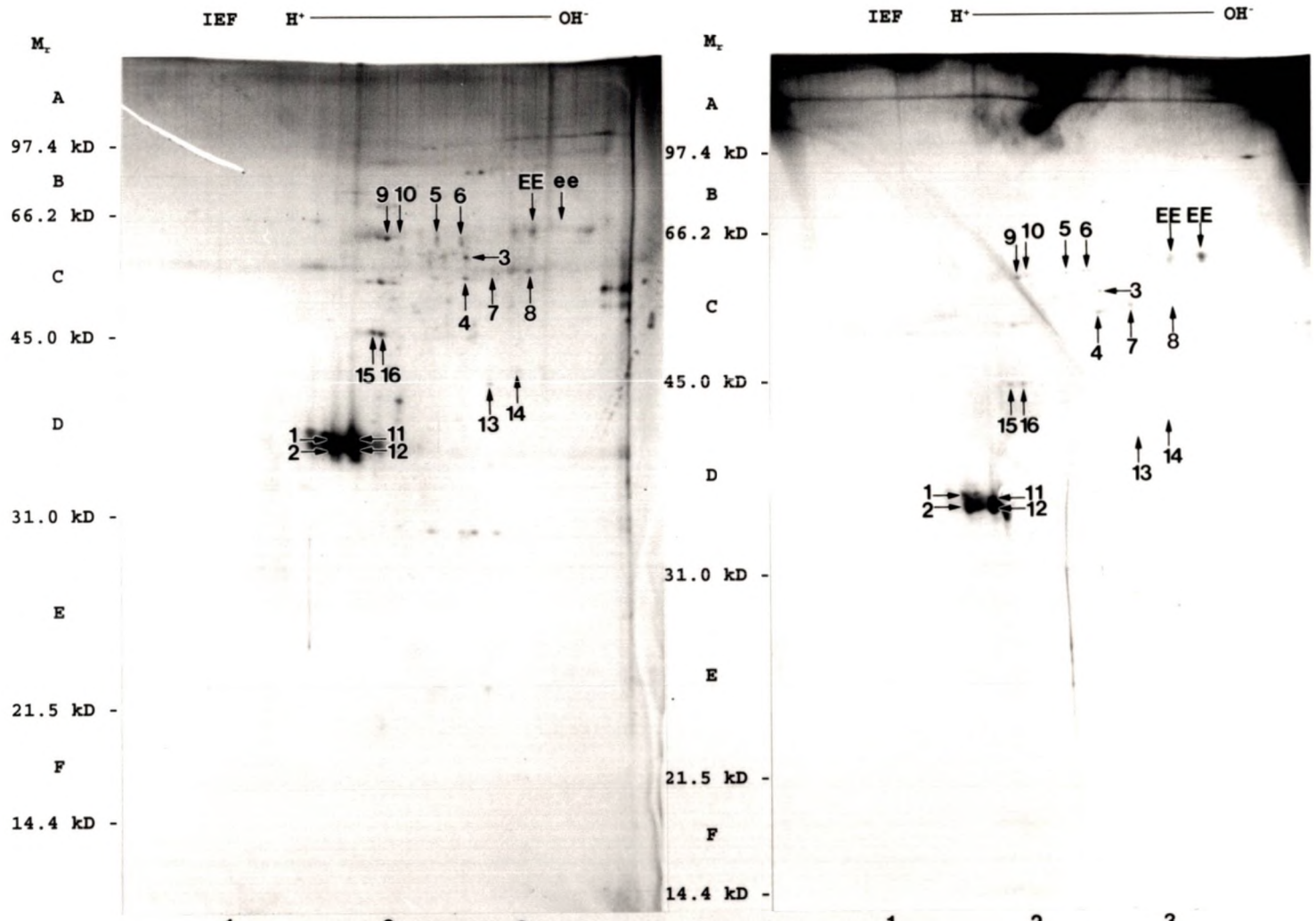

Mutant embryos at an abnormal late transition stage 11 dap

Normal embryos at a normal transition stage 9 dap

Figure 31. Comparison of the protein profile of mutant embryos at an abnormal coleoptilar stage at 15 dap (left) with that of normal embryos at a normal coleoptilar stage at 10 dap (right). Each profile contains 200 µg of total protein. The mutant profile contains one of the early embryonic (EE) spots, and may contain the second (ee) spot, but at a much lower level than in the normal coleoptilar stage profile. Both EE spots are prominent in the normal profile. The landmark spot 10 appears to be present at the same level in both profiles, but spot 7 is greatly reduced in the mutant profile as compared to the normal coleoptilar stage profile. Landmark spots 13 and 14 stain at the same intensity and characteristic color in these two profiles, but exhibit a shift in relative molecular weight (M_r); both spots migrate slightly further in relation to other spots in the mutant profile. Two prominent 30 kD spots, labelled A, are very close together in the mutant profile. In the normal profile these spots are less prominent and are slightly separated in both M_r and isoelectric point (pI). The spot labelled M is prominent in the normal profile, but it is almost undetectable in the mutant profile.

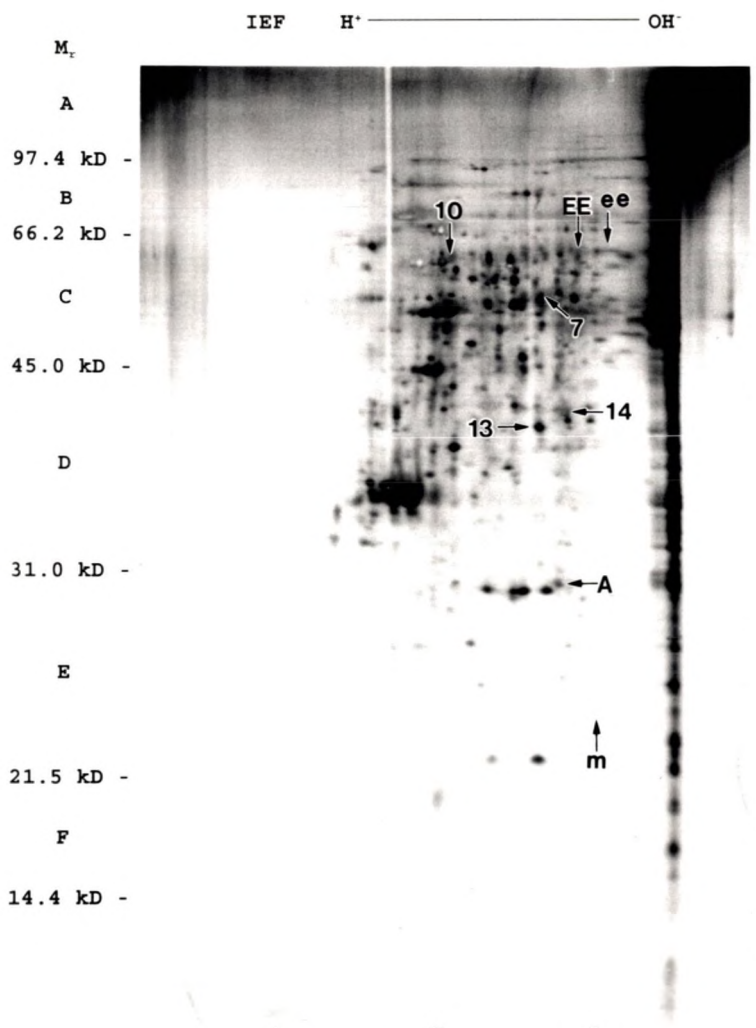

Mutant embryos at an abnormal coleoptilar stage 15 dap

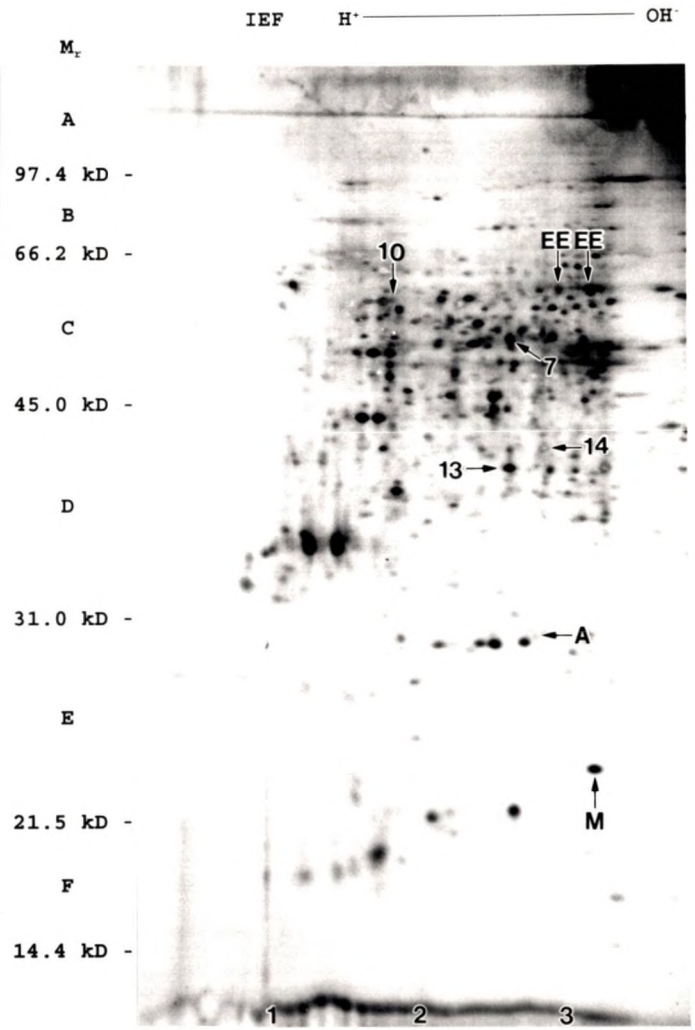

Normal embryos at a normal coleoptilar stage 10 dap

Figure 32. Comparison of the protein profile of mutant embryos at an abnormal stage 1 at 18 dap (left) with that of normal embryos at stage 2 at 19 dap (right). The mutant profile contains 200 µg of total protein, the normal profile contains 100 µg of total protein. Landmark spot 7 continues to be present at a lower level in the mutant profile as compared to the normal profile, despite the fact that the mutant profile contains twice the amount of total protein as does the normal profile. Spots 13 and 14 exhibit the same M_r shift as seen in Figure 31; they appear to have a slightly lower M_r in the mutant profile as compared to the normal profile. Spot B also appears to have a lower M_r in the mutant abnormal stage 1 profile as compared to the normal stage 2 profile. The double spot at A is prominent in the mutant profile and the two components are partially overlapping; in the normal profile the two spots are less prominent and are separated by M_r and pI. The spots labelled G (which may be precursors or members of the globulin storage protein family) and C and D are present at very low levels in the mutant profile. These spots are much more prominent in the normal profile, which contains one-

half the amount of total protein as compared to the mutant profile. The spot labelled M is prominent in the mutant abnormal stage 1 profile, it was undetectable in the mutant abnormal coleoptilar stage profile (see Figure 31). Spot M is also prominent in the normal stage 2 profile. The spots labelled I stain bright yellow in the mutant profile, indicating the proteins are complexed with sugars or lipids. This yellow staining was not very apparent in the normal profile.

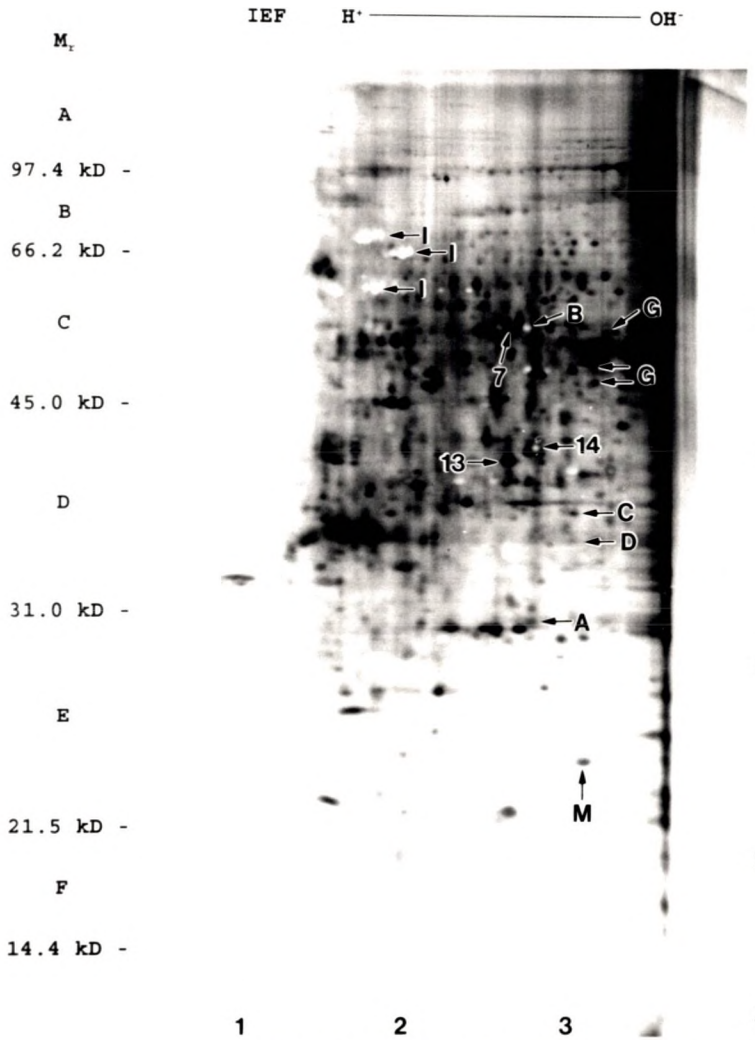

Mutant embryos at an abnormal stage 1 18 dap

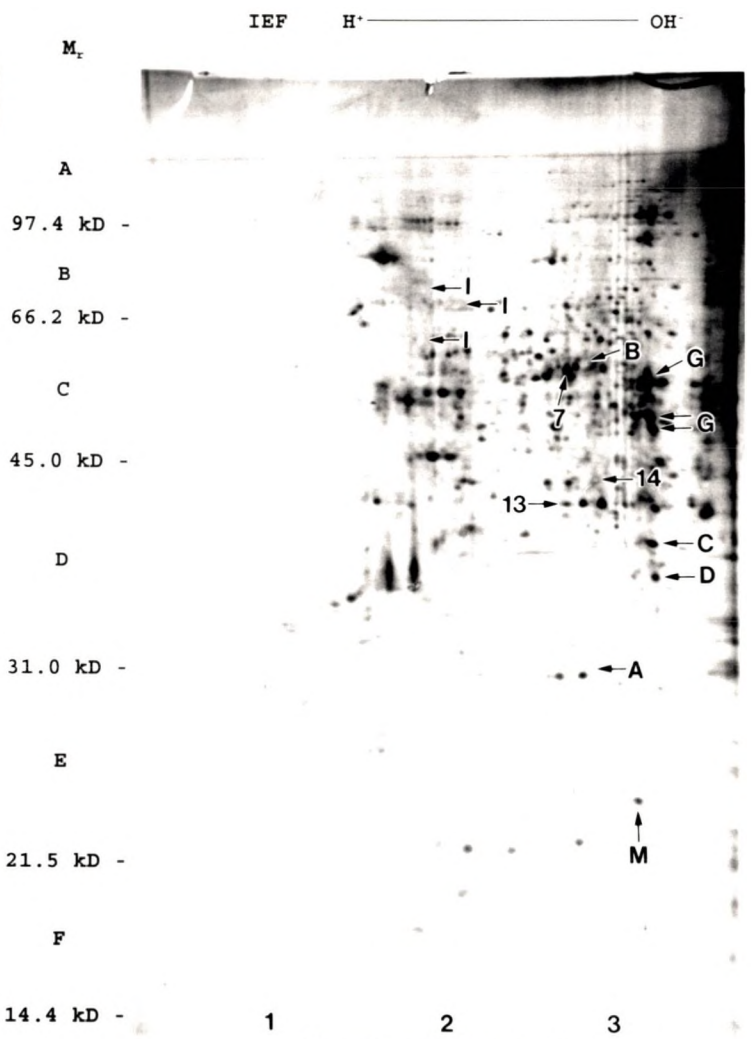

Normal embryos at a normal stage 2 19 dap

Figure 33. Comparison of the protein profile of mutant embryos at an abnormal flattened scutellum stage at 29 dap (left) with that of normal embryos at stage 3 at 23 dap (right). Each profile contains 100 µg of total protein. Spots labelled I in both profiles stained bright yellow, indicating the proteins were highly modified with sugars or lipids. A group of spots at P are prominent in the mutant profile, but not detectable in the normal stage 3 profile at 23 dap. These spots are present in the normal stage 4 profile at 29 dap shown in Figure 34. Landmark spot 7 is prominent in both the mutant profile and the normal stage 3 profile, and its position relative to spot W is noteworthy. Spot W appears to have the same pI as spot 7 in the mutant profile, but it shifts to a slightly more basic pI position in the normal profile. Spots 13 and 14 appear to have a slightly lower M_r in the mutant profile than in the normal profile, as noted in previous figures. Spot S, another yellow staining spot, also appears to have a lower M_r in the mutant profile as compared to the normal profile. The group of spots labelled G are present in approximately equal amounts in both profiles. These may be storage proteins

(possibly globulins) which continue to accumulate in normal embryo profiles but not in subsequent mutant profiles (see Figure 34). Three spots, labelled H, K, and L are much more prominent in the normal profile than in the mutant profile. Spots A and J also exhibit similar patterns; each spot appears as a stacked double-spot in the mutant profile, and as two distinct spots with slightly different pI's in the normal profile. Spot M is very prominent in both profiles, this spot diminishes in subsequent profiles of both mutant and normal embryos (see Figure 34).

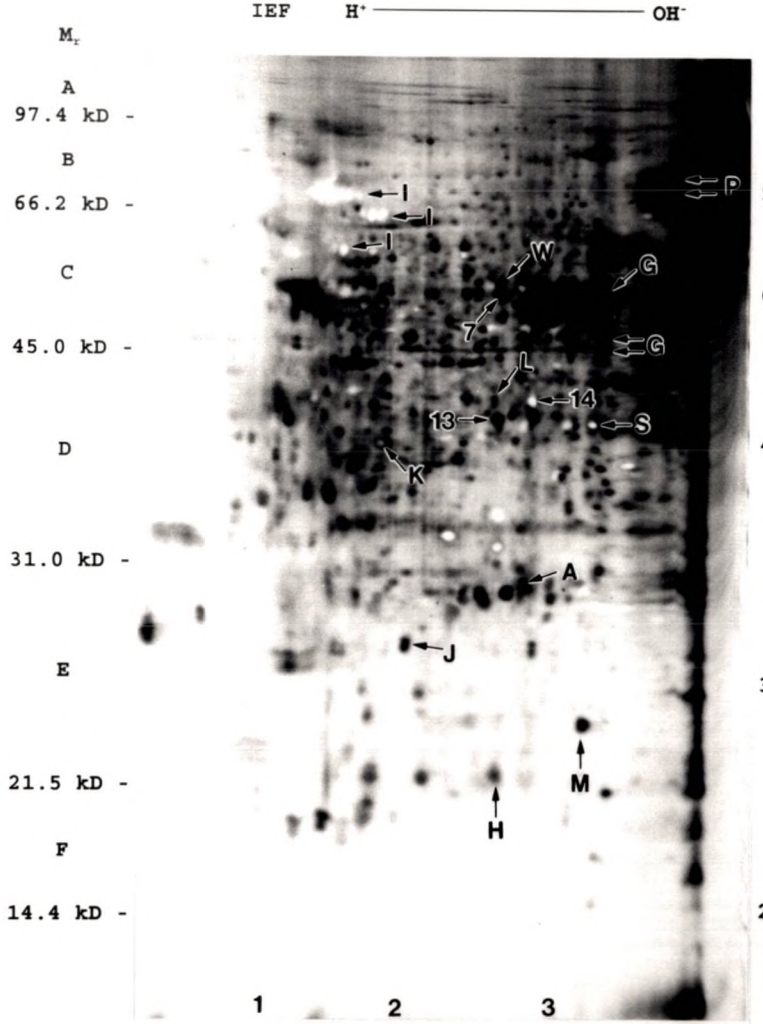

Mutant embryos at an
abnormal flattened scutellum stage
29 dap

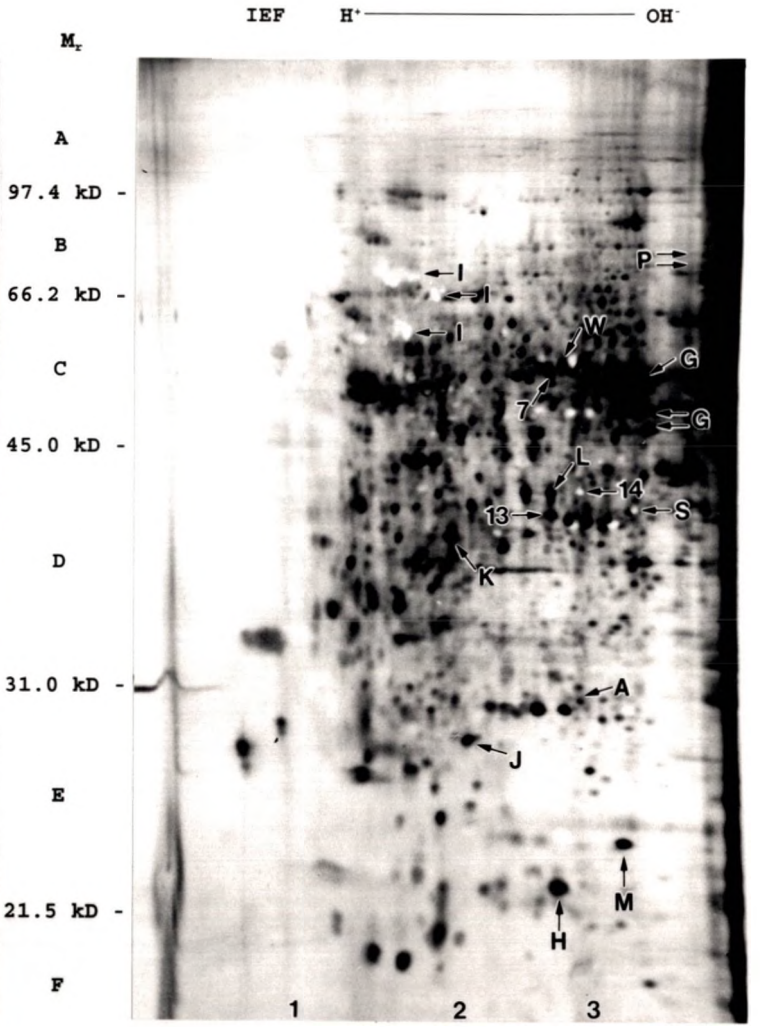

Normal embryos at a
normal stage 3
23 dap

Figure 34. Comparison of the protein profile of mutant embryos at a degenerative stage at 40 dap (left) with that of normal stage 4 embryos at 29 dap (right). Each profile contains 100 µg of total protein. The spot labelled I in both profiles stained slightly yellow and is much less prominent than in profiles of the preceding stage of mutant and normal embryos (see Figure 33). Two previously observed groups of yellow-staining spots could not be detected in the mutant degenerative stage profile or in the normal stage 4 profile. Three groups of putative storage proteins, spots P, G, and X are the most prominent feature in the normal profile. A very small amount of the P and G spots and no detectable X spots are visible in the mutant profile. Landmark spot 7 is present in both profiles, and spot W appears to shift to a slightly more basic pI position in the normal profile, as was seen in Figure 33. Landmark spots 13 and 14 exhibit the same shift to a lower M_r in the mutant profile as was seen in the profiles of preceding stages of mutant embryo development. Spot J appeared as a double-spot in profiles of flattened scutellum stage mutant embryos (Figure 33) but it has diminished significantly in

degenerative stage mutant embryo profiles. It is not clear whether a single- or double-spot is present in the mutant profile, but it does appear as a double-spot in the normal profile. Spots at Y are prominent in the normal profile but are mostly undetectable in the mutant profile. The few detectable spots appear to be somewhat modified as indicated by their reddish staining. Spot Z is much more prominent in the normal profile than in the mutant profile. Spot M is present in both profiles, but is greatly reduced from its intensity in the preceding stage of mutant and normal embryo profiles (Figure 33).

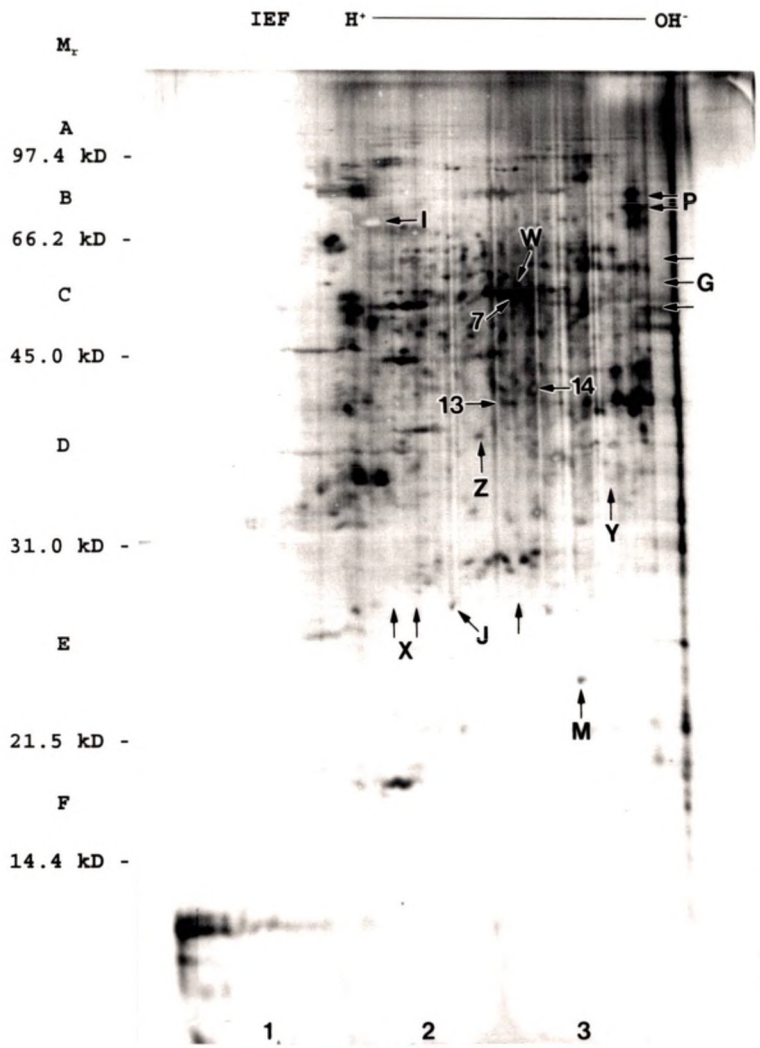

Mutant embryos at an abnormal degenerative stage 40 dap

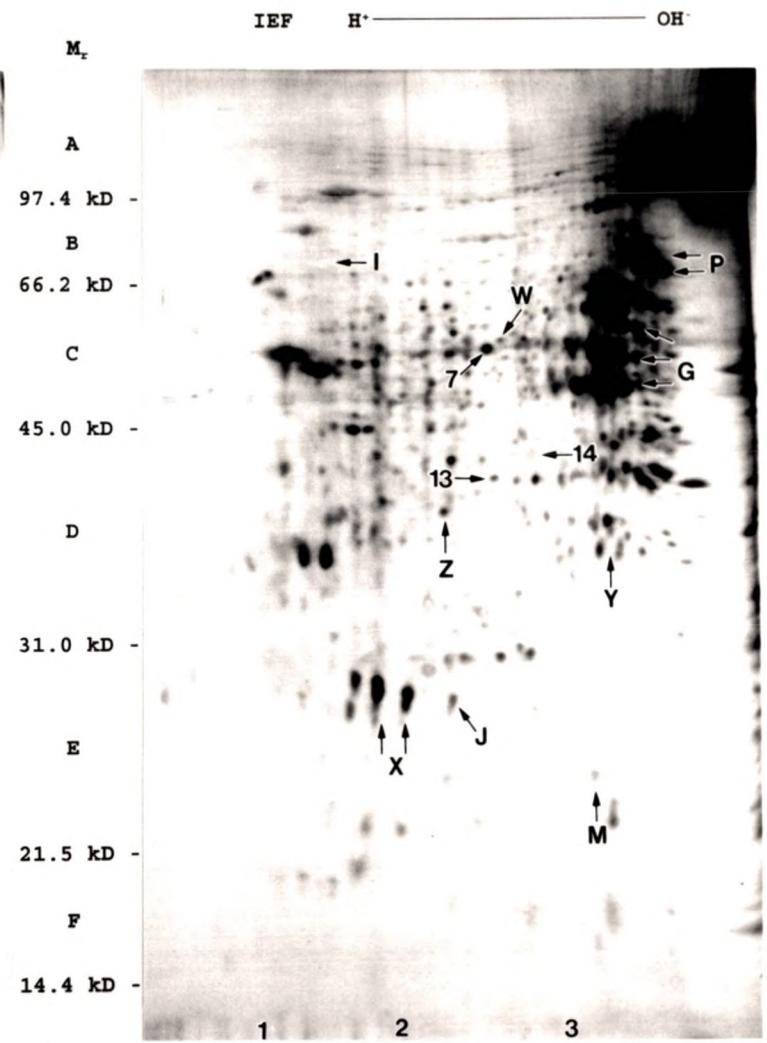

Normal embryos at a normal stage 4 29 dap

Figure 35. Diagram of a 2-D gel containing the sixteen numbered landmark spots (black circles) and the spots which differed between protein profiles of mutant and normal embryos (open circles). The stippled circles at I differed in their degree of yellow staining. Spot ee was absent from all mutant profiles but present in normal profiles up to stage 1. Spots A, J, and W displayed isoelectric point changes between mutant and normal profiles of a similar stage. Spots 7, 10, C, D, H, K, L, M, Y, and Z were present at lower levels in mutant profiles than in normal profiles; spots G, P, and X were present at low levels in mutant profiles and high levels in normal stage 4 profiles. Spots 13, 14, and B appeared to have a lower M_r in mutant profiles than in normal profiles of a similar stage.

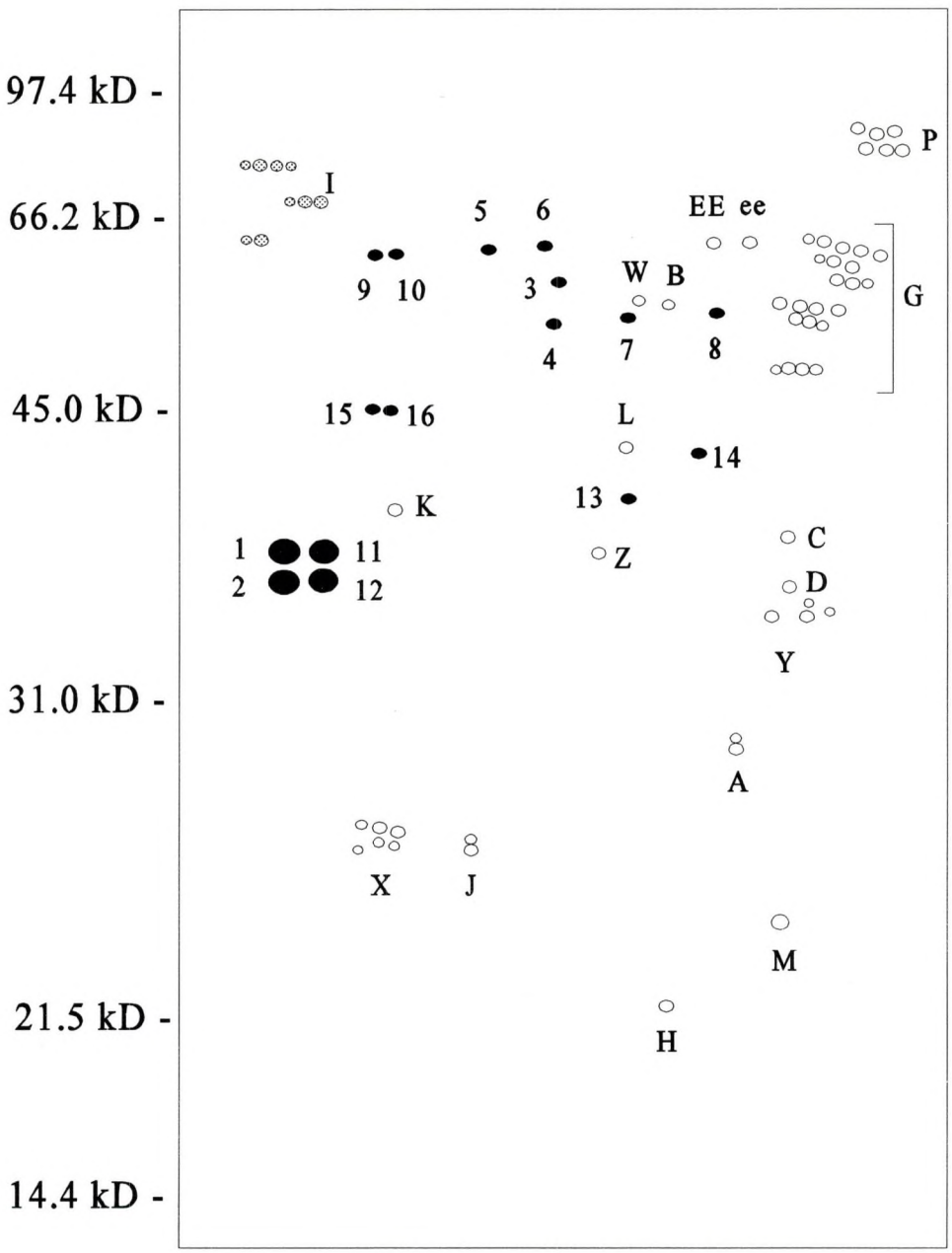
97.4 kD -
66.2 kD -
45.0 kD -
31.0 kD -
21.5 kD -
14.4 kD -
P
I
5
6
EE
ee
9
10
3
W
B
G
4
7
8
15
16
L
14
13
K
1
2
11
12
Z
C
D
Y
A
X
J
M
H

Discussion

The maize embryo-lethal mutation *dek23* has significant effects on embryogenesis, retarding embryo development, preventing formation of a coleoptilar ring, a shoot apical meristem and all leaf primordia (Clark and Sheridan 1986). These effects first become apparent at the transition stage at 9 or 10 dap. Mutant embryos on a self-pollinated ear segregating for *dek23* are developmentally delayed as compared to the normal embryos on the ear at this age. This developmental delay is the first detectable morphological difference; prior to this divergence mutant and normal embryos are indistinguishable. The *dek23* mutation also has a significant effect on the protein profile of developing mutant embryos, although embryos have many proteins in common.

The observation that differences do exist between mutant and normal profiles at a given stage of embryo development is significant. Gottlieb and de Vienne (1988) reported in pea (*Pisum sativum*) that two near-isogenic lines, differing only at the *r*-gene (*RR* round vs. *rr* wrinkled), showed no differences in protein patterns of several different organs and tissues tested, including young

embryos. They observed differences between the two lines only in later stage embryos, and at seed maturity when they reported 62 specific spot differences, along with some additional alterations of spot clusters. They contrast this with their unpublished data on pea leaf mutations which cause conversion between leaflets and tendrils. Identical protein patterns were produced by mutant and wildtype leaflets and mutant and wildtype tendrils, indicating that the loci affecting leaf shape have no detectable effect on the majority of proteins produced.

Comparison of mutant *dek23* and normal embryo protein profiles of a similar developmental stage revealed some specific quantitative and qualitative spot differences. One of two early embryonic (EE) proteins present in normal transition stage embryos was missing from mutant abnormal late transition stage embryo patterns. This single difference, detectable at the transition stage, may help to distinguish mutant from normal embryos before morphological differences become apparent one or two days later. The EE proteins were not observable in later stage profiles.

The reduced intensity of landmark spots 7 and 10 in mutant patterns was detectable at the abnormal late

transition stage and could aid in the identification of embryo genotype before phenotypic differences are apparent. Although it is possible that one of these spots represents the normal gene product of the *dek23* locus, it is more probable that these reduced spots are the result of failure of the normal *dek23* product to exert some effect on other loci in the genome. This effect may involve a cascade of interactions and thus result in several missing or altered spots. All other specific spot differences were observed after the developmental delay allowed mutant and normal embryos to be distinguished on the basis of morphological differences.

Many proteins appeared to have lower relative molecular weights in mutant profiles as compared to the same proteins in normal profiles at the same developmental stage. Landmark spots 13 and 14 first displayed this apparent change in M_r when mutant embryos were at the abnormal coleoptilar stage, and this condition persisted through all stages of mutant embryo development. Spot B displayed similar characteristics when mutant embryos were at an abnormal stage 1. The reduced size of these polypeptides

may be the result of posttranslational modifications that do not occur without the action of the normal *dek23* allele.

Many spots appeared on both mutant and normal gels in the same locations, but the overall protein pattern of spot number and intensity in mutant embryos was delayed chronologically as compared to normal embryos. That is, patterns of 11 dap mutant embryos resembled 9 dap normal patterns; 15 dap mutant patterns resembled 10 dap normal patterns etc. This reflects a developmental sequence of expression of most gene products in the embryo, in contrast to a chronological control of protein patterns. Similar protein patterns were produced by mutant abnormal coleoptilar stage embryos and normal coleoptilar stage embryos, but the normal embryos reached this stage five days before mutant embryos entered this stage. This suggests a model of regulation of embryo development similar to the checkpoints involved in cell cycle control in yeast (Jacobs 1992). Embryos may have to reach a minimum size or complete a specific developmental event before progressing to the next stage. Embryos that have not passed that threshold may continue to produce the proteins of the earlier stage until they do pass it.

The developmental delay was first seen morphologically during the transition and coleoptilar stages when mutant and normal embryos became distinguishable on a segregating ear. After normal embryos began producing leaf primordia, the gap between mutant and normal embryos widened as mutant embryos failed to continue differentiation of their shoot apical meristem. Some development of the scutellum continued and some changes in the protein profile continued to occur; the pattern of mutant embryos at an abnormal flattened scutellum stage at 29 dap showed a strong similarity to normal stage 3 embryos at 23 dap. A few specific spots emphasized this time lag; one prominent 24 kD spot labelled M was present in normal coleoptilar stage embryos at 10 dap (Figure 31) but did not appear until 18 dap in mutant embryos when they had reached an abnormal stage 1 (Figure 32). This same spot almost completely disappeared in 29 dap normal embryos at stage 4, but was at its peak intensity in 29 dap flattened scutellum stage mutant embryos and did not diminish until 40 dap during the degenerative stage.

Some exceptions to this time lag were present. The yellow staining spots that are prominent in normal stage 3 embryos at 23 dap had become quite prominent in mutant

abnormal stage 1 embryos at 18 dap. The yellow staining of these spots is due to addition of sugars or lipids to polypeptides (Sammons et al. 1981) and this modification may be the result of genetic regulation by multiple loci.

Mutant *dek23* embryos don't produce normal amounts of storage proteins. The globulins, thought to provide a nitrogen source for embryos during the first few days of germination (Khavkin et al. 1978), were produced in large quantities in normal embryos beginning at stage 3. Mutant embryos appear to begin production of globulin precursors and other similar proteins at the abnormal flattened scutellum stage (spots at P and G in Figure 33), but these spots have decreased by the degenerative stage.

Kriz et al. (1990) and Rivin and Grudt (1991) demonstrated that the normal gene product of *viviparous1* (*vp1*) is also required for accumulation of storage globulins, as are products of some other *vp* loci. The normal *dek23* gene product may also be required for subsequent accumulation of globulins, although its other effects suggest this is not its primary role in embryo development.

Abscisic acid (ABA) has been shown to be required for initiation of globulin synthesis, suppression of degradation of globulins, and inhibition of precocious germination (Rivin and Grudt 1991). While no measurement of ABA levels nor addition of ABA was done during this study, the ability of *dek23* mutant embryos to produce ABA may be suppressed due to the lack of a normal shoot apical meristem, which may be important for hormone synthesis by the embryo. Alternatively the ability of mutant scutellum cells to detect or respond to ABA may be affected since the scutellum is flattening and degenerating at the stage when globulin synthesis begins in normal embryos. Future investigations may distinguish these possibilities by culturing mutant embryos with varying levels of ABA added to the media, followed by 2-D protein analysis.

The effects of the *dek23* gene product are apparent morphologically and biochemically, as demonstrated by the different protein profiles of mutant and normal embryos of the same developmental stage. At least 20 individual protein spots are altered on 2-D gels of mutant embryos when compared to pattern of normal embryos at the same developmental stage. This is undoubtedly an underestimate

of the effects of the mutant *dek23* allele, since silver staining and analysis of patterns by eye are not sensitive enough to detect subtle changes in protein mobility or spot intensity (Dunbar 1987). This suggests that the *dek23* locus has an effect on production of several different polypeptides and is, therefore, a good candidate as a regulatory locus (Sheridan and Neuffer 1982; Sheridan and Clark 1987; Aeschbacher and Benfey 1992).

Genes regulating plant development have been cloned and characterized in recent years and many encode proteins containing homeodomains (reviewed by Aeschbacher and Benfey 1992 and by Katagiri and Chua 1992). Homeodomains are capable of binding specific DNA sequences and acting as transcription factors, regulating the timing and amount of transcription of one or more genes (Schwarz-Sommer et al. 1990). Some of these homeobox genes (coding for homeodomain proteins) and other types of DNA binding proteins have been cloned from maize, including the *Knotted1* (*Kn1*) gene (Hake et al. 1989), *Viviparous1* (*Vp1*, McCarty et al. 1991), and *Zmhox1a* (Bellmann and Werr 1992). Levels of the KN1 protein in wildtype cells have been found to be very low in most tissues (Smith et al. 1992). Transcription factors have

been shown to activate promoters in *in vivo* assays at a concentration of 10,000 molecules per cell (Katagiri and Chua 1992). At this concentration a transcription factor with an M_r of 60 kD would be below the limit of resolution of a silver stained gel.

Given an embryo of 1000 cells: 6×10^4 gm/mol ÷ 6×10^{23} molecules/mol = 1×10^{-19} gm/molecule x 1×10^4 molecules/cell x 1×10^4 cells/embryo = 1×10^{-12} gm/embryo or 1 picogram/embryo. The detection limit of silver staining is reported to be 100 to 500 picograms (Ochs et al. 1981; Gottlieb and de Vienne 1988) therefore all of the protein from at least 100 embryos (about 500 µg) of this size would have to be loaded on a gel, assuming the protein is present at this level in all cells. This amount of protein exceeds the practical loading limit by several orders of magnitude, and the spot of interest would likely be overwhelmed by proteins that are present in much greater abundance.

Results from this investigation suggest that the *dek23* locus may have a regulatory function in normal embryogenesis. The normal protein product of this locus may

be present in very small amount and may not be readily detectable on silver stained gels. If this is the case then isolation and peptide sequencing of individual spots on gels that are altered by the mutant *dek23* allele could provide the information necessary to produce oligonucleotide probes that could be used to screen a cDNA library in search of the target sequences of the *dek23* protein. These sequences could then be used to extrapolate the possible configuration of that protein and search for homologous sequences in the genome (Janice K. Clark pers. comm.) Many of the plant transcription factors in *Arabidopsis* and *Antirrhinum* have been isolated by homology to other known transcription factors (Katagiri and Chua 1992). A search for the *dek23* locus might be conducted in this way by screening a cDNA library of chromosome *2L* sequences for homology to homeobox or other DNA binding motif sequences.

A strategy of targeted mutagenesis with a transposable element (Walbot 1992) is another method of tagging and cloning the *dek23* locus. Auger and Sheridan (1994) have developed genetic stocks carrying the *Ac* transposable element at a known location in translocation stocks, bringing it into close proximity to most portions of the

maize genome. The *Ac* element transposes into nearby sites at a higher frequency than to more distant or unlinked sites. Putting it in proximity to chromosome arm *2L* increases the likelihood that it will insert in the *dek23* locus. By crossing the appropriate translocation stock onto or by heterozygous *dek23* plants, new alleles of *dek23* created by the insertion of the *Ac* element into that locus. A new allele would carry a molecular tag and could be cloned by using the already cloned *Ac* element as a probe. Ideally, several different alleles should be isolated, and many thousands of plants would have to be screened in order to find even one insertion of the *Ac* element into the *dek23* locus.

Two-dimensional analysis may speed up the identification of new potential alleles of *dek23*, since protein extraction and 2-D separation can be completed in a few days on field samples as soon as putative mutant kernels can be recognized (12-14 dap). Promising candidates can thus be selected for allelism testing in the next generation from the large populations needed for this type of targeted mutagenesis experiment (Walbot 1992).

It has already been shown that the normal *dek23* gene product is required for normal maize embryogenesis (Clark and Sheridan 1986). This study has elucidated the effect of the *dek23* gene product on the protein profile of developing embryos. The mutant profile is altered very early in development, when mutant embryos are at an abnormal late transition stage and first become distinguishable from normal embryos on the same ear. The mutant allele has a significant effect on the protein profile throughout development, altering more than 20 specific spots.

The *dek23* mutation results in alteration of individual spots in several ways, by changing their relative molecular weight, their isoelectric point, their degree of posttranslational modification, and their relative abundance in the profile. It also causes a developmental delay in the pattern of protein expression that coincides with the morphological delay in development (Clark and Sheridan 1986). Several possible functions for the normal *dek23* gene product could explain the mutant embryo phenotype and alteration in protein pattern observed. The *dek23* gene could code for a cell surface receptor, or a structural element specific to certain region in the embryo (the shoot

apex region). Another possible explanation is that the normal gene product of *dek23* plays a regulatory role in controlling embryogenesis, and might possibly act by binding specific DNA sequences and altering transcription of other genetic loci. Molecular analysis of the *dek23* locus is necessary to determine the actual mode of action of the *dek23* normal gene product during embryo development.

References

Abbe, E.C., and O.L. Stein, 1954 The growth of the shoot apex in maize: embryogeny. Am. J. Bot. 41:285-293.

Aeschbacher, R.A. and P.N. Benfey, 1992 Genes that regulate plant development. Plant Science 83:115-126.

Auger, D.A., and W.F. Sheridan, 1994 Using cytogenetics to enhance transposon tagging with *Ac* throughout the maize genome. Pp. 234-239. In: *The Maize Handbook*. Edited by M. Freeling and V. Walbot. Springer-Verlag, New York.

Bellmann, R. and W. Werr, 1992 *Zmhox1a*, the product of a novel maize homeobox gene, interacts with the *Shrunken* 26 bp *feedback* control element. EMBO J. 11:3367-3374.

Boothe, J.G. and D.B. Walden, 1989 Multivariate analyses of polypeptide synthesis in developing maize embryos. Theor. Appl. Genet. 77:495-500.

Clark, J.K., and W.F. Sheridan, 1986 Developmental profiles of the maize embryo-lethal mutants *dek22* and *dek23*. J. Hered. 77:83-92.

Clark, J.K., and W.F. Sheridan, 1988 Characterization of the two maize embryo-lethal defective kernel mutants *rgh*-1210* and *fl*-1253B*: effects on embryo and gametophyte development. Genetics 120:279-290.

Clark, J.K. and W.F. Sheridan, 1991 Isolation and characterization of 51 embryo-specific mutations of maize. The Plant Cell 3:935-951.

Dunbar, B.S., 1987 *Two-dimensional electrophoresis and immunological techniques*. Plenum Press, New York.

Gottlieb, L.D. and D. de Vienne, 1988 Assessment of pleiotropic effects of a gene substitution in pea by two-dimensional polyacrylamide gel electrophoresis. Genetics 119:705-710.

Hake, S., E. Vollbrecht and M. Freeling, 1989 Cloning *Knotted*, the dominant morphological mutant in maize using *Ds2* as a transposon tag. EMBO J. 8:15-22.

Jacobs, T., 1992 Reviews. Control of the cell cycle. Dev. Biol. 153:1-15.

Katagiri, F. and N.-H. Chua, 1992 Plant transcription factors: present knowledge and future challenges. Trends Genet. 8:22-27.

Khavkin, E.E., S.I. Misharin, Y.Y Markov and A.A. Peshkova, 1978 Identification of embryonal antigens of maize: globulins as primary reserve proteins of the embryo. Planta 143:11-20.

Kriz, A.L., M.S. Wallace and R. Paiva, 1990 Globulin gene expression in embryos of maize viviparous mutants. Plant Physiol. 92:538-542.

McCarty, D.R., T. Hattori, C.B. Carson, V. Vasil, M. Lazar and I.K Vasil, 1991 The *Viviparous-1* gene of maize encodes a novel transcriptional activator. Cell 66:895-905.

Meinke, D.W., 1991 Genetic analysis of plant development. Pp. 437-490. In: *Plant Physiology, A Treatise*. Volume 10 Growth and development. Academic Press, New York.

Neuffer, M.G., and W.F. Sheridan, 1980 Defective kernel mutants of maize. I. Genetic and lethality studies. Genetics 95:929-944.

Ochs, D.C., E.H. McConkey and D.W. Sammons, 1981 Silver stains for proteins in polyacrylamide gels: A comparison of six methods. Electrophoresis 2:304-307.

Rivin, C.J. and T. Grudt, 1991 Abscisic acid and the developmental regulation of embryo storage proteins in maize. Plant Physiol. 95:358-365.

Sanchez de Jimenez, E. and R. Aguilar, 1984 Protein synthesis patterns. Relevance of old and new messenger

RNA in germinating maize embryos. Plant Physiol. 75:231-234.

Sanchez-Martinez, D., P. Puigdomenech and M. Pages, 1986 Regulation of gene expression in developing *Zea mays* embryos. Protein synthesis during embryogenesis and early germination of maize. Plant Physiol. 82:543-549.

Scanlon, M.J., P.S. Stinard, M.G. James, A.M. Myers, and D.S. Robertson, 1994 Genetic analysis of sixty-three mutations affecting maize kernel development isolated from *Mutator* stocks. Genetics .

Schwarz-Sommer, Z., P. Huijser, W. Nacken, H. Saedler and H. Sommer, 1990 Genetic control of flower development by homeotic genes in *Antirrhinum majus*. Science 250:931-936.

Sheridan, W.F., 1988 Maize developmental genetics: genes of morphogenesis. Ann. Rev. Genet. 22:353-385.

Sheridan, W.F., and J.K. Clark, 1987 Maize embryogeny: a promising experimental system. Trends Genet. 3:3-6.

Sheridan, W.F. and J.K Clark, 1993 Mutational analysis of morphogenesis of the maize embryo. The Plant Journal 3:347-358.

Sheridan, W.F., and J.K. Clark, 1994 Fertilization and embryogeny in maize. Pp. 3-10. In: *The Maize Handbook*. Edited by M. Freeling and V. Walbot. Springer-Verlag, New York.

Sheridan, W.F. and M.G. Neuffer, 1982 Maize developmental mutants, embryos unable to form leaf primordia. J. Hered. 73:318-329.

Sheridan, W.F., and Y.R. Thorstenson, 1986 Developmental profiles of three embryo-lethal maize mutants lacking leaf primordia: *ptd*-1130, cp*-1418,* and *bno*-747B*. Dev. Genet. 7:35-49.

Smith, L.G., B. Greene, B. Veit and S. Hake, 1992 A dominant mutation in the maize homeobox gene, *Knotted-1*, causes its ectopic expression in leaf cells with altered fates. Development 116:21-30.

Walbot, V., 1992 Strategies for mutagenesis and gene cloning using transposon tagging and T-DNA insertional mutagenesis. Annu. Rev. Plant Physiol. Plant Mol. Biol. 43:49-82.

CHAPTER VI. SUMMARY

The detailed analysis of the embryo-lethal mutation *dek23* has revealed much about the role of the normal *dek23* gene in maize embryogenesis. Characterization of normal embryo morphogenesis, fine structure, and protein complement provided baseline data for comparison to mutant embryo properties.

Genetic mapping of the *dek23* locus on chromosome arm *2L* places it in a relatively open region with few known gene loci nearby. It is located 22 map units distal to *w3* and 39 map units proximal to *Ch*. This provides a valuable marker for investigators seeking to map new loci in this region. It also opens up the possibility for targeted mutagenesis of the locus using translocation stocks bearing a transposable element. The use of translocations that bring the transposable element into closer proximity to the chromosomal region bearing the gene of interest significantly increases the chances of producing an

insertion mutation, which would facilitate cloning and sequencing of *dek23*. Fine scale mapping using RFLP loci is also made easier by precise genetic mapping and might assist in molecular characterization of the locus.

Transmission analyses revealed an interesting and important feature of the *dek23* locus. Its normal gene product is involved in male gametophyte function as well as embryo and endosperm development. Transmission of the mutant allele was found to be reduced through the pollen, possibly due to aberrant or slowed pollen tube growth. This accounted for the lower than expected overall frequency of mutant kernels with more mutant kernels near the tip than the base of a selfed ear. This pleiotropy provides further evidence that *dek* loci can play different roles in different tissues, and in different life stages of an organism.

Mutant *dek23* embryos showed no obvious difference in phenotype attributable to the number of copies of the mutant allele (dosage effect). Furthermore, as was first reported by Clark and Sheridan (1986), no rescue of mutant embryos by normal endosperm was observed, suggesting the *dek23* gene product is non-diffusible and the locus is cell autonomous in its expression.

Fresh dissection of kernels confirmed earlier observations (Clark and Sheridan 1986) that mutant embryos are developmentally delayed as compared to normal embryos on the same ear, before any endosperm or kernel phenotype is recognizable. This developmental delay is not accompanied by any abnormality at 9-10 dap, but an abnormal coleoptilar ring is formed in mutant embryos by 20 dap. In contrast to the earlier study, a significant finding is that the shoot apex and possibly one leaf primordium were formed by 25 dap in many of the mutant embryos examined, but subsequent maintenance of these structures fails and necrosis often sets in at this site.

Light microscopy of embryos embedded in plastic reveals a slightly earlier onset of abnormality than was revealed by fresh dissection. Onset of degeneration or necrosis in cells at the shoot apical meristem region occurs by 14 dap. Persistence of the root apical meristem reveals the specificity of gene action, since shoot and root meristems are not affected equally by the mutation. Transmission electron microscopy uncovers abnormalities earlier than light microscopy in mutant shoot apical meristem cells. Abundant vacuoles, lobed nuclei, and

aberrant plastids in mutant shoot apical meristem cells were apparent as early as 10 dap and may foreshadow genetically controlled death of those cells, that normally would participate in shoot apical meristem formation. Mutant shoot apical meristem cells failed to accumulate starch and lipid droplets to the same extent as normal shoot apical meristem cells, further emphasizing the developmental delay.

Analyses of the proteins present in normal embryos revealed several trends. First, the number and intensity of protein spots in the profile was low at the transition and coleoptilar stages, they both increased to a peak at stage 3, and tapered off by embryo maturity. Storage proteins were produced in large amounts in maturing embryos and made up a significant portion of total protein on two-dimensional gels at later stages. Several landmark spots were identified that were present on gels of all stages and a few stage specific spots were also identified. These protein profiles of normal embryogenesis provide the baseline against which mutant profiles can be compared and provide insight into the changes in gene expression during the different stages of embryo development.

Mutant embryo protein profiles displayed several significant departures from normal profiles. Mutant embryos at the abnormal late transition stage were missing one early embryonic protein found in normal embryos at the transition stage. They also were deficient in two landmark spots found in all normal embryo patterns. Three proteins had lower relative molecular weights, possibly due to altered post-translational modification, and several proteins were present at lower intensities in mutant profiles than in normal profiles of the same developmental stage.

Protein profiles of mutant embryos displayed patterns that resembled the profiles of normal embryos at a younger chronological age. This delay approximated the morphological delay apparent in fresh and sectioned material. One exception to this delay was the modification of some protein spots by sugars or lipids. This modification of three specific groups of spots appeared earlier on mutant profiles than on normals.

Lastly, no accumulation of storage proteins was detected in mutant protein profiles. Some proteins thought to be precursors of globulin storage proteins were observed,

albeit somewhat late, but no globulins or similar proteins were deposited in large amounts as occurs in normal embryos.

In conclusion, it is apparent that the normal *dek23* gene product is essential for normal embryo development. It is required for endosperm development and is involved in male gametophyte function as well. In the homozygous mutant condition, *dek23* causes an initial developmental delay, observable at the morphological and biochemical level, and to some extent at the ultrastructural level. Specific protein products are missing from mutant embryos, and large classes of missing proteins, such as globulins, are probably due to a secondary effect of the mutant condition. The fine structural differences observed likely indicate that genetically "programmed" cell death is occurring, due to failure of these cells at the shoot apex region to differentiate at the appropriate time. Determination of cells to become the shoot apical meristem may have limited their totipotency and when the appropriate signals were not received, a default program of cell death may have resulted in their degeneration.

These findings support the contention that *dek23* may be a regulatory locus, and that it warrants molecular

characterization in the effort to further elucidate the genetic control of development.

References

Clark, J.K., and W.F. Sheridan, 1986 Developmental profiles of the maize embryo-lethal mutants *dek22* and *dek23*. J. Hered. 77:83-92.